BUFFER GAS MODIFIERS IN ION MOBILITY SPECTROMETRY

By

ROBERTO FERNANDEZ-MAESTRE

A dissertation submitted in partial fulfillment of

the requirements for the degree of

DOCTOR OF PHILOSOPHY

WASHINGTON STATE UNIVERSITY

Department of Chemistry

AUGUST 2009

To the Faculty of Washington State University:

The members of the Committee appointed to examine the dissertation of ROBERTO FERNANDEZ-MAESTRE find it satisfactory and recommend that it be accepted

_____
Herbert H. Hill, Ph.D., Chair

_____
William Siems, Ph.D.

_____
Kenneth Nash, Ph.D.

Acknowledgement

I thank Dr. Herbert H. Hill, Jr. for his permanent inspiration, support, and teachings during my doctorate studies.

I thank my committee members, Dr Kenneth Nash, and especially Dr. William F. Siems for their directions and thoughtful recommendations.

I acknowledge the help from Hill Research Group members, especially Kim Kaplan and Christina Crawford and from Dr. Brad Bendiak (University of Colorado) for his kind donation of reagents.

I thank past and present WSU Chemistry Department staff for their assistance: Paula Broemmeling, Erin Collins, Debbie Arrasmith, Carrie Giovannini, Roger Crawford, Trent Amonett, Gary Johnson, and Rebecca Dodd.

I acknowledge the professional support from past and present WSU Technical Services staff members as George Henry, Lauren Frei, Steve Watson, John Rutherford, Dave Savage, Duke Beattie, and Steve Barner. I am especially grateful to Fred Schuetze for his unconditional and timely help.

I thankfully appreciate the opportunity that WSU and the department of chemistry gave me to come to USA to achieve a doctorate and enjoy so many different experiences for me and my family, master a new language and know a different culture.

I gratefully acknowledge financial support from Dr Ching Wu (Excellims Corporation), NIH grant R33DK0702740351, Universidad de Cartagena, and the Fulbright scholarship (LASPAU).

Special thanks to the Universidad de Cartagena faculty Dr Rafael Galeano, Dr. Ricardo Vivas, and other faculty that made possible my doctorate. I also want to thank to my university staff for all their logistic support. Thanks to my friends in Pullman to make my stay enjoyable: los Pollos Rigo and Dalis, los Mañes Manuel and Jinna, Vicky and Roberto, los Franceses Felipe and Angelica, Edith and Gordo, Rosa, los Rolos Pacho and Katy, and many more.

Very special thanks to my family: my wife Margarita, who was always an emotional support and motivation and my daughters Maria Jose and Luisa Fernanda for making my stay in Pullman sweeter.

BUFFER GAS MODIFIERS IN ION MOBILITY SPECTROMETRY

Abstract

by Roberto Fernandez-Maestre, PhD.

Washington State University

August 2009

Chair: Herbert H. Hill, Jr.

Liquid dopants (modifiers) were vaporized into the buffer gas of an ion mobility spectrometer to change ion mobilities. In this investigation, ion mobilities varied to different extent depending on the structure and size of ions, and the concentration of the buffer gas modifier. Steric hindrance and intramolecular bridges produced low responsiveness of ions to modifiers by inhibiting clustering.

The mobilities of several chemical standards for ion mobility spectrometry (IMS) decreased when modifiers were introduced into the buffer gas to simulate contamination. The order of reduction in mobility with contamination in the buffer gas was: tetraalkylammonium ions < DTBP < 2,4-lutidine ≈ analytes. These different responses of analytes and chemical standards would make the calculation of reduced mobilities, K_0, using chemical standards inaccurate when contamination is present in the buffer gas. Therefore, a new calibration procedure is recommended for IMS that uses two classes of chemical standards, an "instrument standard" and a "mobility standard". Instrument standards calibrate the instrumental parameters. Mobility standards determine the degree of contamination in the buffer gas. An instrument standard should be

insensitive to contamination in the buffer gas and a mobility standard should be sensitive to this contamination. DTBP was confirmed as a good instrument standard and 2,4-lutidine as a good mobility standard. Tetraalkylammonium ions are recommended over DTBP as instrument standards for electrospray ionization (ESI) IMS.

Finally, ESI-IMS was used for the analysis of a set of beverages and over-the-counter drugs. Analysis times below one minute were obtained for IMS after a simple dissolution step, and 12 new reduced mobilities values were reported. Fast analysis times, sensitivity, high resolution, easy operation, inexpensive maintenance, and low cost of IMS instruments make IMS an attractive alternative to slow and expensive methods, such as chromatography, for the qualitative analysis of over-the-counter drugs and beverages.

Table of Contents

List of Tables

Appendix: Tables

List of Figures

Chapter One: Figures

Chapter Two: Figures

Chapter Three: Figures

Chapter four: Figures

Chapter five: Figures

Appendix : Figures

Dedication

Esta disertacion esta dedicada a mi amada y nunca bien ponderada esposa, Margarita, que proveyo todo el soporte emocional y logistico necesario para que ambos pudieramos soportar toda una carrera continua sin vacaciones, y trabajando de sol a sol, sin quejarse, siempre con una sonrisa, un chiste, y de buen humor.

Chapter One

Introduction

Ion Mobility Spectrometry

IMS is an analytical technique that separates gas-phase ions moving under an applied electric field based on their size to charge ratios. The ***ion mobility spectrometer*** (Figures 1 and 2) consists of two basic units: an ionization source and an ion drift tube maintained at either a positive or negative uniform electric field gradient. Ions produced in the ionization source are accelerated down the drift tube by the electric field where they are separated according to their mobilities.

Ceramic insulator tube

***Drift tube*.** In the drift tube, ions are separated by an electric field before entering the detector. The drift tube comprises a reaction and a drift region separated by an ion gate. The drift tube (Figures 1 and 2) is constructed of a series of stainless-steel guard rings alternating with insulating quartz, glass or ceramic rings (Figure 3). A counterbore into each metallic ring supplies a support to hold the neighboring ceramic insulator. Insulating spacers and steel rings are stacked one after the other, in a horizontally interlocking design, to form a completely closed tube. All rings are kept in an alumina tube placed in an aluminum heating case. Each guard ring is connected to the next one in series through resistors (Figure 2). A high electrical potential is placed on the first guard ring to produce a fixed field of 200-500 V cm^{-1} throughout the drift tube.[1] Alteration of the drift region length is possible by addition or removal of stainless steel rings. An ESI target screen, placed at the first ring of the reaction region, is made out of 2-mm stainless steel mesh with an orifice in the center (Figure 3).

Buffer gas. To help desolvate the ions, a countercurrent of preheated inert buffer gas is introduced through a stainless-steel tube at the low voltage end of the tube at a flow rate on the order of 0.5-1.5 L min^{-1}. The buffer gas that enters the IMS tube must be pre-heated to the tube temperature to avoid cooling the drift tube; to heat the buffer gas, it is passed through a stainless-steel tube coiled inside a heated aluminum block (Figure 4). The gas passes through the drift tube and exits through the ionization region. Nitrogen or air is usually used, but He, CO_2, and Ar also have been utilized. [2]

Ion gate. Once the gas-phase ions are formed in the ionization source, they are directed by the electric field down the drift tube towards the detector. On their way, the ions encounter sets of parallel wires at the beginning of the drift region that prevent them from continuing their migration through the spectrometer. These sets of parallel wires are called ion gates (Figure 4). The Bradbury-Nielsen gate is made of a pair of interdigitated electrodes or wire grids held between two insulating rings. A typical gate has 20-80 parallel 75-μm stainless steel wires approximately 0.6 mm apart. Electronically, the entrance ion gate is opened for a few tenths of a millisecond to permit a pulse of analyte ions to enter this region. Typical pulses are 0.2 ms; longer pulses increase broadening of the IMS peaks, and shorter pulses may decrease sensitivity.

The gate is open (all ions pass) when each gate wire is at the potential of the drift field at that point in the drift tube; in this case, the ions travel through the spaces between the wires under the influence of the drift field. The gate is closed (ions are stopped) when a potential higher than the drift voltage is placed between each wire. When a potential difference, typically about 30-50 V, is applied between the two sets of wires, the field is greater than the drift field. This field difference makes the ions migrate to one of the set of wires where they are

annihilated. The resolving power of the system can never be greater than that permitted by the entrance-gate pulse; a short pulse is desired. The detector response, however, is a function of the sampling fraction, entrance pulse divided by the scan time; for a 20 ms scan time and 0.20 ms pulse, the current available is $1/100^{th}$ of the total available.[3] The use of ion gates decreases the sensitivity since the gates are open only a fraction of the analysis time. To increase sensitivity, FTIMS and pulsed sources are used.[4]

Aperture grid. After passing the gate, the ions drift with the electric field, some faster and some slower, according to their individual ion mobilities, and arrive at the detector at different times. Ions can find a second gate, located approximately 1 mm before the detector, when Faraday cups are used. The purpose of this aperture grid is to shield the Faraday cup detector from the inductive effects of the incoming ion cloud. Without an aperture grid, the collector electrode begins to respond to the ion cloud before it reaches the electrode, which results in a broadened ion peak.[1] The aperture grid can either be opened at progressively increasing intervals after the first gate to produce an ion mobility spectrum, or it can be opened at some fixed intervals, after the entrance gate is opened, to monitor only ions of certain mobility.[5]

Ionization sources. There are several ionization methods to convert molecules into ions in IMS in order to be separated in the drift tube. These methods include ^{63}Ni β ionization,[6] photoionization,[7] laser ionization,[8] resonance enhanced two-photon ionization,[9] corona spray ionization,[10-11] and electrospray ionization.[10,12] The most used ionization sources for IMS are ^{63}Ni β and electrospray ionization.

Radioactive sources. The ^{63}Ni foil is a secondary ionization source, analogous to that found in an electron capture detector (ECD). Ionization in this source is produced by the emission of electrons from the radioactive source with average energies of 19 keV. These electrons collide with neutral molecules of analyte or buffer gas, and ionize them by a series of charge transfer reactions. When dry nitrogen (5–10 ppm of moisture) is used as the buffer gas, $(H_2O)_nH^+$ and thermal electrons provide the background current, where n = 1–4 depending on the moisture and temperature. When air is used as the buffer gas, $(H_2O)_nH^+$ and $(H_2O)_nO_2^-$ or $(H_2O)_n(CO_2)_mO_2^-$ are the reactant ions for positive and negative ion detection, respectively.[22] Vapors of organic compounds present in the ionization region are ionized by the reactant ions through a series of charge transfer reactions.[1] An advantage of radioactive sources is that they do not require a power supply, and, consequently, are suitable for portable instruments. Disadvantages are potential radioactive contamination and the bureaucratic complications due to governmental regulation of radioactive materials.

Electrospray ionization. In the ESI process using IMS, high electric potentials are applied between a liquid sample in a capillary and a target electrode in the drift tube to create positive charges (Figure 5). Electrospray occurs when the positive liquid is attracted by coulombic forces from the capillary toward the target electrode, which is held at lower voltages. As droplets travel toward the target electrode, solvent evaporates, which leaves increasingly smaller charged drops that 'explode' due to coulombic repulsion. This process produces droplets of increasingly smaller radius, ideally culminating in molecular ions.[22]

Mobility constant. Analytes ions are desolvated in the reaction region, and pulsed by the ion gate into the drift region. The electric field accelerates the ions in the drift region, and

separates them according to their velocities. The ions collide repeatedly with the buffer gas, but are accelerated continuously by the field. This combination of collisions and accelerations rapidly thermalizes the ions, and averages their velocities to a value that depends on their collision cross sections; these velocities can be used to calculate the mobility constant, *K*, a characteristic property of ions drifting under the influence of an electric field:[13,14]

$$K = \frac{v}{E} = \frac{L^2}{V.t_d} \quad (1)$$

where *v* is the velocity of the ion in cm s^{-1}, *E* the electric field in the drift region in V cm^{-1}, *L* the distance in centimeters the ion travels from the ion gate to reach the detector, *V* the total voltage drop in volts in the drift region, and t_d the time the ion takes traveling the distance *L* in seconds. If the electric field is less than approximately 500 V cm^{-1} at atmospheric pressure, *v* should be a linear function of the potential.[2] In order to compare *K* values in different experimental conditions, ion mobilities must be normalized to standard conditions to obtain reduced mobilities (in cm^2V^{-1} s^{-1}). Reduced mobilities are characteristic of every ion in a given buffer gas:

$$K_0 = K \frac{P}{760} \frac{273}{T} \quad (2)$$

where *P* is the pressure in Torr, and *T* the temperature of the buffer gas in Kelvin.[14] Gas-phase ions traveling in an ion mobility spectrometer are governed by the Mason–Shamp equation:[13]

$$K_0 = \frac{3q}{16N_0}\sqrt{\frac{2\pi}{\mu kT}}\frac{1+\alpha}{\Omega}\frac{P}{760}\frac{273.16}{T} \quad (3)$$

where q is the charge of the ion, N_0 the gas number density at STP (2.69 x10^{19} cm^{-3}, $N_0 = P/kT$), μ the reduced mass of an ion-buffer gas molecule pair, k the Boltzmann constant, Ω the ion-neutral collision cross section, P the pressure in Torr, T the temperature in Kelvin, and α a small correction term with a magnitude of less than 0.02, when the ion mass is larger than the mass of the buffer gas molecule; μ is defined as [mM/(m + M)], where m and M are the molecular mass of the analyte and the buffer gas, respectively.

IMS coupled to mass spectrometers (IMS-MS). IMS-MS advantages are fast separations in 40 ms or less, high resolving powers, increased signal to noise ratio, and interfacing with multiple atmospheric pressure ionization sources, such as MALDI, ESI, corona discharge, radioactive, and photoionization. IMS-MS provides two dimensions of separation: the mass/charge ratio dimension of mass spectrometry and the size/charge ratio of ion mobility. The latter allows isomer separation, and provides structural information. Additionally, fragmentation pattern information is given by collision induced dissociation at the IMS-MS interface. When used with electrospray ionization, mobility spectrometers permit better solvent evaporation for mass spectrometers and allow higher flow rates to be used with the same sensitivity.[15]

Modes of operation of IMS-MS. Spectra in ion mobility spectrometers coupled to quadrupole mass spectrometers can be acquired in IMS (total ion monitoring) or SIM-IMS (single ion monitoring) modes. In the IMS mode, the IMS gate continually opens and closes, and the mass spectrometer lets all the ions reach the detector; in this mode, the ion mobility spectrum of all ions is obtained with a large sensitivity. In SIM-IMS, the IMS gate continually opens and closes, and the DC and RF voltages are set to allow only ions with a specific mass,

or a selection of specific masses, to reach the detector. SIM allows IMS analysis of specific compounds without interference of others of different masses. In IMS and SIM-IMS modes, the mass spectrometer serves as a detector for IMS, and no mass scan is performed. Mass spectra are obtained by keeping the IMS gate open, while the amplitudes of the quadrupole DC and RF voltages are ramped, though keeping the RF/DC ratio constant; in this mode, all ions pass continuously through the mobility spectrometer directly to the mass spectrometer, where they are mass analyzed.

Resolving power. Resolving power is an indication of separation efficiency in IMS and can be calculated by:

$$R = t_d / w \qquad (4)$$

where t_d is the drift time of the ion of interest, and w is the temporal peak width measured at half-height.[16] Regardless of its resolving power, an instrument cannot separate two compounds with identical drift times.

Separation factor, α: The separation factor describes the degree of separation of two compounds. When this value is large, separation is easy:

$$\alpha = \frac{t_{d2}}{t_{d1}} \qquad (5)$$

where t_{d1} and t_{d2} are the drift times of the faster and slower ions, respectively. An α value of 1 indicates that two compounds cannot be separated with the current resolution of the IMS instrument.

Resolution. Resolving power is a measure of separation efficiency. To specify the extent to which two different peaks are resolved (Rs) it is necessary to use the resolution equation:

$$Rs = \frac{\Delta t_d}{W_{base}} \quad (6)$$

where Δt_d is the drift time difference between the center of the two peaks and w_{base} is the average peak width at the baseline. This expression is equivalent to that in chromatographic techniques where an *Rs* value of 1.5 is considered baseline resolution.

History of ion mobility spectrometry

Ion mobility spectrometry (IMS) is an analytical technique that separates ions according to their size to charge ratio in an electric field. By the end of the 19th century, Ernest Rutherford measured the mobility of ions formed by x-ray ionization,[17] and characterized the ions using ion mobilities.[18] During the first three decades of the 20th century, there was a strong interest in mobility studies, and a large body of theory on ion kinetics and experimental data was compiled. In that period, the effect of collisions, attractive forces, temperature, pressure, accelerating voltage, and contamination on mobilities were recognized.[19,20] Ion gates were introduced in 1929[21] to simplify the analysis of spectra because they allowed the sampling of small pulses of ions. In the 30's and 40's, the interest for ion mobility declined due the introduction of mass spectrometry, which was free of the complicated reactions present at the lower vacuum used for mobility studies.

The period 1948-1970 was called as a phase of ***foundational studies*** by Eiceman and Karpas.[22] A number of theoretical studies in ion mobility from Mason and Schamp,[13] McDaniel, [14] and Kebarle,[23] were conducted in this period, creating the base of modern IMS. In this period, there was a renewed interest in mobility studies revealed by: a) primitive ion detectors used by military during and after world word II for the detection of chemical warfare agents, fuel from submarines, and other applications;[22] b) an ionization anemometer, invented by Lovelock in 1948, that was sensitive to organic vapors, which opened the possibility of using mobility instruments for chemical analysis;[24] and c) the construction of suitable drift tubes, such as that of Albritton and McDaniel, similar to modern drift tubes.[25]

The ***plasma chromatography period*** of IMS starts by the end of the 60's with the first analytical applications of IMS by Cohen,[6] and the introduction of the first commercial IMS instrument in 1970.[23] In those times, IMS was called plasma chromatography because a swarm of positive and negative ions in the gas-phase is called plasma, and the separation capabilities of IMS resembled those of chromatography. The first publications on IMS were authored by Karasek and Cohen in 1970.[2,26] The first application of IMS to the detection of illicit drugs and explosives appeared in 1976,[27] and, soon, IMS became the method of choice for the determination of chemical warfare agents and their degradation products, drugs, and explosives. IMS devices were soon used in most airports for the detection of explosives and chemical and biological threats, and are the most common portable chemical instrument used by military and security forces, which reflects the success of these applications to the point that governments around the world trust the lives of military personnel and civilians to the capabilities of IMS instruments.

The ***modern era of IMS*** starts in 1982 with the introduction of the unidirectional flow design by Baim and Hill.[5] Previous IMS instruments were not sealed, and there was a complex flow of neutrals into the mobility instrument, which caused numerous undesired secondary reactions, clustering, and memory effects. Baim and Hill designed a sealed tube and introduced the buffer gas from the end of the instrument, keeping most neutrals out of the drift region, which simplified the IMS spectra. Later, IMS was used as a detector for liquid,[12] supercritical fluid,[26] and gas chromatography,[29] and its applications were extended to the detection of microorganisms,[30] food contaminants,[31] and illegal drugs using portable instrument,[32] resolution of isomers,[33] identification of wood types in the logging industry,[34] screening of phosphopeptides,[35] on-line monitoring,[15] and monitoring of hazardous inorganic vapors in industrial plants.[36] When IMS was coupled to mass spectrometers, a second dimension of analysis was added that allowed the application of this technique to profiling and imaging of tissues[37] and proteomics;[38] separation of biological mixtures,[39] sodium adducts of isomeric oligosaccharides,[40] metal-adducted isomeric flavonoid diglycosides,[41] and peptides and negative charged carbohydrates;[42] and study of peptide folding,[43] protein structure,[44] and gas-phase molecular interactions.[45]

Neutrals in the drift tube

In 1910 and 1912, Lattey demonstrated that neutrals, such as water molecules, air, and carbon dioxide, in the drift region affected ion mobility.[46] Since the introduction of IMS in the 70s, neutrals were injected intentionally in mobility spectrometers, and were called reagent gases. Reagent gases are used mainly to simplify spectra by allowing a preferential ionization of

compounds with higher proton affinity than the reagent gas. Ammonia was used as a reagent gas by Kim et al. to selectively ionize amines[47] and acetone was utilized by Blyth (1983) to eliminate interferences in the determination of chemical warfare agents;[48] Proctor and Todd (1984) found better results for the selective detection of explosives doping the buffer gas with dichloromethane than doping with dibromomethane, methyl iodide, acetic acid, dimethyl sulfide, or acetonitrile[49] and Spangler et al. (1985) doped the carrier gas with carbon tetrachloride to selectively detect explosives.[50] In 1995, Eiceman et al. used acetone and dimethylsulfoxide as dopants in the buffer gas to selectively analyze mixtures of organophosphorus and organic compounds[51] and Meng et al. doped the buffer gas with water, acetone, and dimethylsulfoxide to avoid interferences in the detection of volatile organic compounds.[52]

Other types of reagent gases, called buffer gas modifiers, are introduced into the carrier or buffer gas to form clusters with the analytes, and selectively change their mobilities. Eiceman et al. (1993) found interferences of ammonia in the determination of alkanolamines when using acetone as a reagent gas; they found that this interference was avoided by replacing acetone with 5-nonanone.[53] In this work, $[5\text{-nonanone}\cdot H]^+$ reactant ions were produced, which reacted with alkanolamines forming analyte-5-nonanone complexes with different mobilities from the analyte-acetone complexes. In 2000, Gan and Corino doped the carrier gas with 4-heptanone reagent gas to monitor monoethanolamine, 3-amino-1-propanol, 4-amino-1-butanol, and 5-amino-1-pentanol in air to avoid the interference of ammonia, Freon 22, and fuel vapors. The interferences overlapped the alkanolamines when acetone was used as the doping gas, but the interferences were shifted to different drift times doping with 4-heptanone.[54] In 2006, Dwivedi et

al. separated enantiomers of amino acids, drugs, and sugars by injecting a chiral modifier, (S)-2-butanol, into the buffer gas of a IMS-MS instrument. The drift times of these compounds showed increases from 0.5 to 5 ms when (S)-2-butanol was injected into the buffer gas, and the changes in drift times were different for different compounds.[55] In 2007, Bollan et al. used ketones to dope the buffer gas of an ion mobility spectrometer to avoid the interference of ammonia on the determination of hydrazines. They concluded that ions with comparable mobility may be separated when gas atmospheres are modified with a reagent gas, where the core ion is not chemically altered but the overall ion mobility is changed. Bollan et al. found that the reagent gas giving the best separation and detection of ammonia and hydrazines under laboratory conditions was 5-nonanone.[56] A comprehensive review on the use of reagent gases and modifiers in IMS in negative and positive modes was published by Puton et al. in 2008.[57] The application of these selective changes in mobilities for various analytes as a result of the addition of a buffer gas modifier to separate analytes with similar K_0 values in IMS has not been achieved, and is investigated in this study. In this work, 2-butanol was used as buffer gas modifier in an ion mobility spectrometer to investigate the separation selectivity of this modifier on mixtures of selected compounds, such as amino acids and drugs.

Calibration in IMS

In IMS, the measurement of accurate mobilities is important because they are used to characterize ions, but this measurement is complicated by some issues. The mobility of ions is known to be affected by clustering with water[56] and other neutrals.[53-56] This susceptibility of mobility to contamination in the buffer gas makes the use of some standards inaccurate to correct the mobility scale. The calculation of the mobility of ions is also affected by imprecise measurement of the drift time and drift tube length,[58] as well as other instrumental parameters such as temperature, pressure, and voltages.[59] To account for these errors, in 1929, Dusault and Loeb expressed the necessity of calibrating mobility values with chemical standards.[60] In 1930, air ions were proposed as a calibration gas.[61] In 1989, Karpas used 2,4-lutidine as a chemical standard to correct the mobility scale in IMS.[59,62] Protonated dimethyl methylphosphonate $(DMMP)H^+$, its proton-bound dimer, $(DMMP)_2H^+$,[63] and the reactant ion peaks[64] were suggested as standards for IMS, but their mobilities significantly changed with temperature. 2,4-lutidine also has been considered unsuitable as an IMS standard for the same reason.[58] $(2,4\text{-lutidine})_2H^+$,[65,58] and $(DMMP)_2H^+$ [58] were considered as chemical standards for IMS, but high concentrations of 2,4-lutidine and DMMP were required to see these dimers, which has a negative effect on the signal of analytes. DTBP was suggested as a chemical standard for IMS in 2002[66] because its mobility was independent of buffer gas temperature and moisture in the buffer gas.[58] Tetraalkylammonium ions were proposed as chemical standards for ESI-IMS in 2005 because they are inherently ionic, which guarantees high sensitivity, produce only a single ion mobility peak, and are insensitive to temperature, moisture in the buffer gas, and solvent composition.[58] In this work, the effect of contamination with moisture and organic compounds on the mobility of chemical standards was investigated to determine their suitability as chemical standards.

Rapid and low cost qualitative analysis by IMS

Modified foods, as well as food, drugs, and cosmetic additives, were introduced to the market over the past three decades. Additives are used to make products appealing, conceal damaged products, or retard food spoilage. The health risks of food additives have been a subject of controversy. Some authors claim that food additives do not pose health threats,[67] but others hold different opinions.[68-72] On the other hand, in these times of economic crisis more people is relying in low-cost generic over-the-counter drugs for treatment of simple adverse health conditions, such as flues and pains. These issues together with the importance of the drug and food market are increasing the demand for fast, low-cost, and sensitive analytical methods for routine screening and cleaning verification in the pharmaceutical and food industry.[73-75] Current techniques used for quality control in these industries, such as HPLC and total organic carbon (TOC), are slow, expensive, unselective, or relatively inaccurate.[73,76] In contrast, IMS have analysis run times of about 10–45 ms, and not only can lab-assembled IMS instruments be put together and maintained at low cost, but they are also easy to use.[73] In the pharmaceutical industry, IMS has been applied to the analysis of over-the-counter drugs by IMS-MS,[77] detection of trace level impurities in drugs by HPLC-IMS-MS[78] and pharmaceutical formulations using LC-ESI-IMS,[79] and validation of cleaning verification.[80] ESI-IMS represents an attractive alternative to current methods for the rapid, low cost, and sensitive qualitative analysis of beverages and over-the-counter drugs. In this work, ESI-IMS is applied to the determination of active ingredients in over-the-counter drugs and food additives in beverages.

GENERAL AIM

The primary goal of this project was to determine the effects of introducing polar modifiers into the buffer gas of an ion mobility spectrometer on the mobilities of selected compounds. Reagents gases (dopants or modifiers) have been introduced into the carrier gas of ion mobility spectrometers, parallel to the flow of analytes, but mainly to simplify spectra by allowing a preferential ionization of compounds with higher proton affinity than the reagent gas. Dwivedi et al.[55] and Bollan et al.[56] introduced modifiers into the buffer gas of an ion mobility spectrometer, in countercurrent of the flow of analytes, and found that the ion mobilities decreased to different extents. This investigation is a follow-up to Dwivedi's et al. work. Here, we introduced new modifiers into the buffer gas to selectively change the mobilities of compounds overlapping in the ion mobility spectrum to separate them, and to investigate the origin of the changes in mobilities.

SPECIFIC AIMS

1. Separate analytes overlapping in IMS through the selective formation of clusters with polar modifiers that exhibit different selectivities towards the analytes.

2. Investigate the effects of the buffer gas temperature and concentration of buffer gas modifiers, parameters that are related to changes in cluster formation, in the mobilities of ions.

3. Test compounds of different molecular weights and steric properties for IMS separation to establish the effect of steric hindrance and size on the changes in ion mobility occurring when modifiers are injected into the buffer gas.

4. Investigate the effect of contamination in the buffer gas on (a) the reduced mobility values for selected chemical standards and (b) their competence as chemical standards.

5. Establish the capabilities of ESI-IMS for the qualitative analysis of complex over-the-counter drugs formulations and beverages.

ATTRIBUTION

The instrument used in this investigation was built by Dr. Ching Wu.[81] All experiments were designed by Roberto Fernandez and Dr Herbert Hill and conducted by Roberto Fernandez with the supervision of Dr Herbert Hill. Chapter Two was written in the format required by the *International Journal of Mass Spectrometry*. Chapter Three was written in the format required by *Rapid Communications in Mass Spectrometry*. Chapter Four was written in the format required by *Analytical Chemistry.* Charles S. Harden suggested the study of chemical standards in IMS and together with Robert Ewing and Christina L. Crawford helped with the experimental design for this part of the research, analysis of data, and writing of the chapter. Chapter Five was written in the format required by the *International Journal of Ion Mobility Spectrometry*. Figure captions are below the figures and not in a separate list for a better reading. The software for data acquisition is based in LabView, and, together with an IGOR-based data input program, was written by Brian H. Clowers.[82]

REFERENCES

1. Hill, H. H. Jr.; Simpson, G. *J. Field Anal. Chem. Technol.* **1997,** *1*, 3, 119-134.

2. Cohen, M. J.; Karasek, F. W. ***J.*** *Chromatogr. Sci.* **1970,** *8,* 330-337.

3. Siems, W. F.; Wu, C.; Asbury, G. R.; Tarver, E. E.; Hill, H. H. Larsen, P. R.; McMinn, D. *Anal. Chem.* **1994**, *66*, 4195-4201.

4. Chen, Y. H.; Siems, W. F.; Hill, Jr., H. H. *Anal. Chim. Acta* **1996,** 334, 75-84.

5. Baim, M. A.; Hill, H. H. Jr., *Anal. Chem.,* **1982**, *54*, 38-43.

6. Cohen, M.J. Plasma Chromatography: a new dimension for gas chromatography and mass spectrometry; Pittsburgh Conference on Analytical Chemistry and Applied Spectroscopy, March **1969**.

7. Baim, M. A.; Eatherton, R. L.; Hill, Jr., H. H. *Anal. Chem.* **1983**, 55, 1761-1766,.

8. Lubman, D. M.; Kronick, M. N. *Anal. Chem.* **1982**, *54*, 1546-1551.

9. Lubman, D. M.; Kronick, M. N. *Anal. Chem*. **1983**, *55*, 1486–1492.

10. Shumate, C. B.; Hill, H. H. *Anal. Chem.* **1989,** *61*, 601 – 606.

11. Tabrizchi, M.; Rouholahnejad, F. *Rev. Sci. Instr.* **2004**, *75*, 11, 4656- 4662.

12. McMinn, D. G.; Kinzer, J. A.; Shumate, C. B.; Siems, W. F.; Hill, H. H. Jr. J. *Microcol. Sep*. **1990**, *2*, 4, 188-192.

13. Mason, E. A.; Schamp, H. W., Jr. *Annals Phys.* **1958,** *4*, 3, 233-270.

14. McDaniel, E. W. *Collisional Phenomena in Ionized Gases*, Wiley, New York, **1964**.

15. Shumate, C. B.; Hill, H. H. Jr., Electrospray ion mobility spectrometry - Its potential as a liquid - stream process sensor. In Pollution Prevention in Industrial Processes - The Role of Process Analytical Chemistry; Breen, J. J.; Dellarco, M. J., Eds.; American Chemical Society: Washington, DC, 1992; Borsdorf, H.; Raemmler, A. *J. Chromatogr. A* **2005**, *1072,* 1, 45-54.

16. Rokushika, S.; Hatano, H.; Baim, M. A. Hill, H. H., Jr. *Anal. Chem.* **1985**, 57. 1902-1907

17. Rutherford, E. *Phil. Mag.* **1897**, *44*, 422-440.

18. Rutherford, E. *Phil. Mag*. **1899**, *47*, 109-163.

19. Langevin, P. *Ann. de Chim. Phys.***1903,** *28,* 289-384.

20. Langevin, P. *Ann. de Chim. et de Phys.***1905,** *5,* 245-288. Langevin, P. *J. Phys.***1905,** *4,* 322.

21. Cravath, A. M. *Phys. Rev*, **1929**, *33,* 605-613.

22. Eiceman, G. A.; Karpas, Z. **Ion mobility spectrometry**. Taylor & Francis; 2nd ed., Boca Raton, FL, USA, **2005**.

23. Kebarle, P.; Hogg, A.M. *J. Chem. Phys*. **1965**, *42*, 2, 668-674.

24. Lovelock, J.E.; Wasilewska, E.M. *J. Sci. Instr.* **1949**, *26*, 367-370.

25. Albritton, D.L.; Miller, T.M.; Martin, D.W.; McDaniel, E. W. *Phys. Rev.* **1968**, *171*, 94-102.

26. Karasek, F. W. Res. &Develop, **1970,** 21, 3, 34-37.

27. Karasek, F. W.; Hill, H. H. ; Kim, S. H. *J. Chromatogr.,* **1976,** *117*, 327-336.

28. Eatherton, R. L.; Morrissey, M. A.; Siems, W. F.; Hill, Jr. H. H. *J. High Resolut. Chromatogr. Commun.* **1986**, *9*, 1, 154-160.

29. Karasek, F. W.; Hill, Jr., H. H.; Kim, S. H.; Rokushika, S. *J. Chromatogr.,* **1977,** *135,* 2, 329-339.

30. Snyder, A. P.; Shoff, D. B.; Eiceman, G. A.; Blyth, D. A.; Parsons, J. A. *Anal. Chem.* **1991**, *63,* 5, 526-529.

31. Bota, G. M.; Harrington, P. B. Talanta **2006**, 68, 3, 629-635.

32. Chauhan, M.; Harnois, J.; Kovar, J.; Pilon, P. *J. Can. Soc. Forens. Sci*. **1991**, *24*, 1, 43-49.

33. Borsdorf, H.; Nazarov, E. G.; Eiceman, G. A. *Int. J. Mass Spectrom*. **2004**, *232*, 2, 117–126; Tou, J. C.; Boggs, G. U. Anal. Chem. **1976**, 48, 9, 1351-1357;

34. Lawrence, A. H.; Barbour, R. J.; Sutcliffe, R. *Anal. Chem*. **1991**, *63*, 13, 1217-1221.

35. Ruotolo, B. T.; Gillig, K. J.; Woods, A. S.; Egan, T. F.; Ugarov, M. V.; Schultz, J. A.; Russell, D. H. *Anal. Chem*., **2004**, *74,* 22, 6727-6733.

36. Bacon, A. T.; Getz, R.; Reategui, *J. Chem. Eng. Prog.* **1991**, *87,* 6, 61-64.

37. McLean, J. A.; Ridenour, W. B.; Caprioli, R. M. *J. Mass Spectrom*. **2007**, *42*, 8, 1099–1105.

38. McLean, J. A.; Ruotolo, B. T.; Gillig, K. J.; Russell, D. H. *Int. J. Mass Spectrom*. **2005**, *240*, 3, 301–315.

39. Ruotolo, B. T.; Gillig, K. J.; Stone, E. G.; Russell, D. H.; Fuhrer, K.; Goninband, M.; Schultz, J. A. *Int. J. Mass Spectrom*. **2002**, *219*, 1, 253-267.

40. Clowers, B. H.; Dwivedi, P.; Steiner, W. E.; Bendiak, B.; Hill, H. H. Jr. *J. Am. Soc. Mass Spectrom.* **2005**, *16*, 5, 660–669.

41. Clowers, B. H.; Hill, H. H., Jr. *J. Mass Spectrom*. **2006**, *41*, 3, 339-351.

42. Clowers, B. H.; Hill, H. H., Jr. *Anal. Chem.* **2005**, *77*, 18, 5877-5885.

43. Ruotolo, B. T.; Tate, C. C.; Russell, D. H. *J. Am. Soc. Mass Spectrom.* **2004**, *15*, 6, 870-878.

44. Myung, S.; Wiseman, J. M.; Valentine, S. J.; Takats, Z.; Cooks, R. G.; Clemmer, D. E. *J. Phys. Chem. B.* **2006**, *110*, 10, 5045-5051.

45. Levin, D. S.; Vouros, P.; Miller, R. A.; Nazarov, E. G.; Morris, J. C. *Anal. Chem.* **2006**, *78*, 1, 96-106.

46. Lattey, R. T. *Proc. Royal Soc. London (A)* **1910**, *84*, 569, 173-181. Lattey, R. T.; Tizard, H. T. *Proc. Royal Soc. London (A)* **1912**, *86*, 604, 349-357.

47. Kim, S. H.; Karasek, F. W.; Rokushika, S. *Anal. Chem.* **1978**, *50*, 1, 152-155.

48. Blyth, D. A. A vapor monitor for detection and contamination control. In: *Proc. Int. Symp. Against Chem. Warfare Agents,* Stockholm **1983.**

49. Proctor, C. J.; Todd, J. F. J. *Anal. Chem*. **1984**, *56*, 1794-1797.

50. Spangler, G. E.; Carrico, J. P.; Campbell. D. N. *J. Test Eval.* **1985,** *13,* 234.

51. Eiceman, G. A.; Wang, Y. F.; Garcia-Gonzalez, L.; Harden, C. S.; Shoff, D. B. *Anal. Chim. Acta* **1995**, *306*, 1, 21-33.

52. Meng, Q.; Karpas, Z.; Eiceman, G. A. *Int. J. Environ*. *Anal. Chem.* **1995**, *61*, 2, 81-94.

53. Eiceman, G. A.; Salazar, M. R.; Rodriguez, M. R.; Limero, T. F.; Beck, S. W.; Cross, J. H.; Young, R.; James, J. T. *Anal. Chem.* **1993**, *65*, 13, 1696-1702.

54. Gan, H.; Corino, G. T. *Anal. Chem.* **2000**, *72*, 4, 807-815

55. Dwivedi, P.; Wu, C.; Matz, L.M.; Clowers, B.H.; Siems, W.F.; Hill, H.H. Jr. *Anal. Chem.* **2006**, *78*, 24, 8200-8206.

56. Bollan, H. R.; Stone, J. A.; Brokenshire, J. L.; Rodriguez, J. E.; Eiceman, G. A. J. Am. Soc. Mass Spectrom. **2007**, 18, 940–951.

57. Puton, J.; Nousiainen, M.; Sillanpaa, M. *Talanta* **2008**, *76*, 978–987.

58. Eiceman, G. A.; Nazarov, E. G.; Stone, J. A. *Anal. Chim. Acta* **2003**, *493*, 2, 185-194.

59. Berant, Z.; Karpas*, Z. J. Am. Chem. Soc.* **1989**, *111*, 11, 3819–3824.

60. Dusault, L.; Loeb, L. B. *Proc. Natl. Acad. Sci. U.S.A.* **1928,** *14*, 384-393.

61**.** Loeb, L. B. *Phys. Rev.* **1931,** *38*, 549-571.

62. Karpas, *Z. Anal. Chem.* **1989**, *61,* 7, 684-689.

63. Shoff, D. B.; Harden, C. S. in: *Proceedings of the Fourth International Conference on Ion Mobility Spectrom*., Cambridge, **1995**, pp. 6–9.

64. Tabrizchi, M. *Appl. Spectrom.* **2001,** *55,* 1653.

65. Rearden, P.; Harrington, P. B. *Anal. Chim. Acta* **2005,** *545*, 1, 13–20.
66. Eiceman, G. A.; Kelly, K.; Nazarov, E. G. *Int. J. Ion Mobility Spectrom.* **2002**, *5,* 1, 22-30.

67. Weihrauch, M. R.; Diehl, V. *Ann Oncol.* **2004**, *15*, 10, 1460-1465.

68. Huff, J.; LaDou, J. *Int. J. Occup. Environ. Health.* **2007**, *13*, 4, 446-448.

69. Andreatta, M. M.; Munoz, S. E.; Lantieri, M. J.; Eynard, A. R.; Navarro, A. *Argentina Preventive Medicine* **2008** *47*, 1, 136-139.

70. Wüthrich, B. *Ann. Allergy* **1993**, *71*, 4, 379-384.

71. Williamson, C. S. *Nutrition Bulletin* **2008,** *33*, 1, 4-7.

72. McCann, D.; Barrett, A.; Cooper, A. *et al. Lancet* **2007,** *370,* 1560–1567.

73. Tan, Y.; DeBono, R. *Today's Chemist at Work* **2004**, November p. 15.

74. Heydari, R. *Anal. Lett.* **2008***, 41*, 6, 965-976.

75. Wongiel, S.; Hymete, A.; Mohammed, A. I. M. *Ethiopian Pharm. J.* **2008**, *26*, 1, 39-48.

76. Chiarello-Ebner, K. *Pharm. Techn*. *Pharm. Technol.* **2006,** *30*, 3, 52-64.

77. Eiceman, G. A.; Blyth, D. A.; Shoff; D. B.; Snyder, P. A. *Anal. Chem.* **1990,** *62*, 14, 1374-1379.

78. Eckers, C.; Laures, A. M.-F.; Giles, K.; Major, H.; Pringle, S. *Rapid Comm. Mass Spectrom.* **2007**, *21,* 1255–1263.

79. Budimir, N.; Weston, D. J.; Creaser, C. S. *Analyst (Cambridge, U.K.)* **2007,** *132*, 34-40.

80. Payne, K.; Fawber, W.; Faria, J.; Buaron, J.; DeBono, R.; Mahmood, A. *Spectroscopy Magazine Online* **2005**, 24–27**.** In internet: http://www.forumsci.co.il/newsletters/IMS-for-Cleaning-Verification.doc Accessed on February 12, **2009**.

81. Wu C, Siems WF, Asbury GR, Hill HH (1998) Anal Chem 70: 4929-4938

82. Clowers, B. H. Separation of Gas Phase Isomers Using Ion Mobility and Mass Spectrometry, Washington State University, Pullman WA, **2005**.

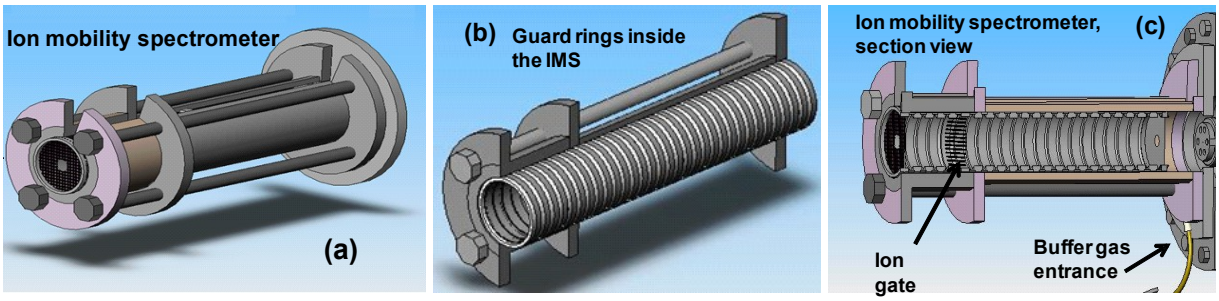

Figure 1. (a) Ion mobility spectrometer. (b) Section view of the ion mobility spectrometer showing the guard and insulator rings. (c) Section view of the ion mobility spectrometer showing the position of the ion gate and the buffer gas entrance.

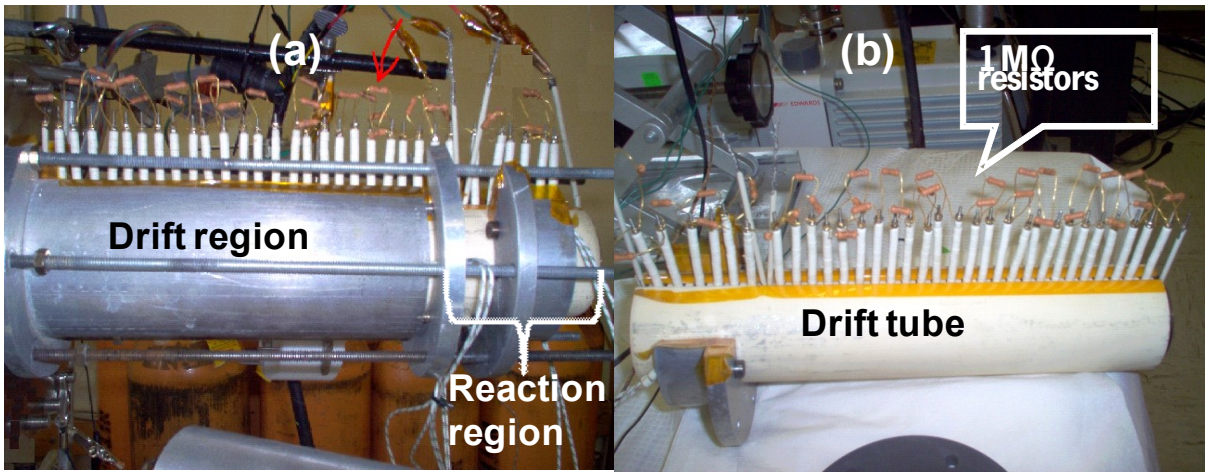

Figure 2. (a) A drift tube inside its metallic aluminum heating block. (b) A drift tube out of the heating block. The arrows show the resistors connecting the guard rings.

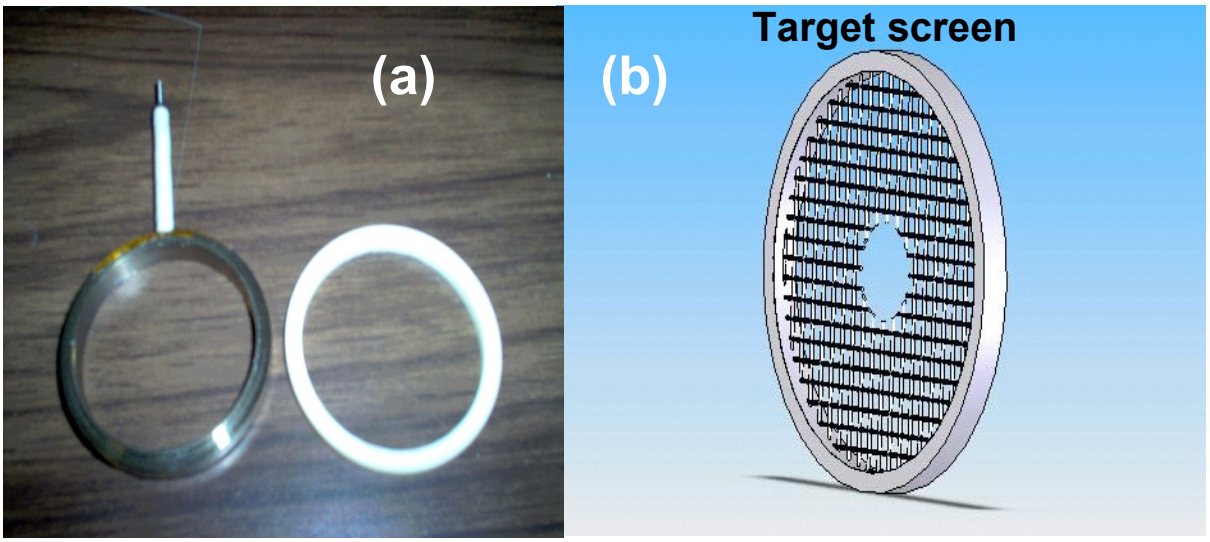

Figure 3. (a) A metallic guard ring (left) and ceramic insulator ring (right). (b) Stainless-steel target screen.

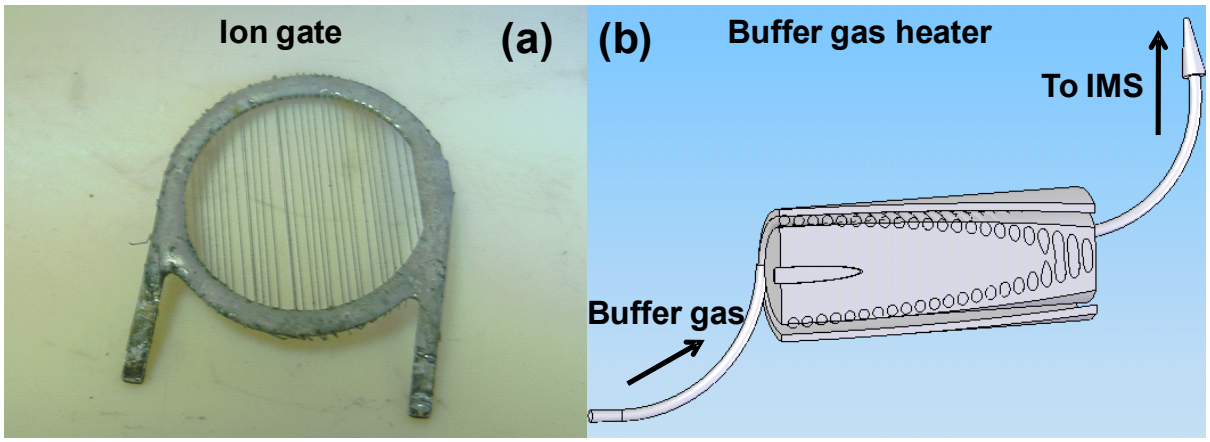

Figure 4. (a) Ion gate. (b) Buffer gas heater showing the tube coiled inside the heated aluminum block.

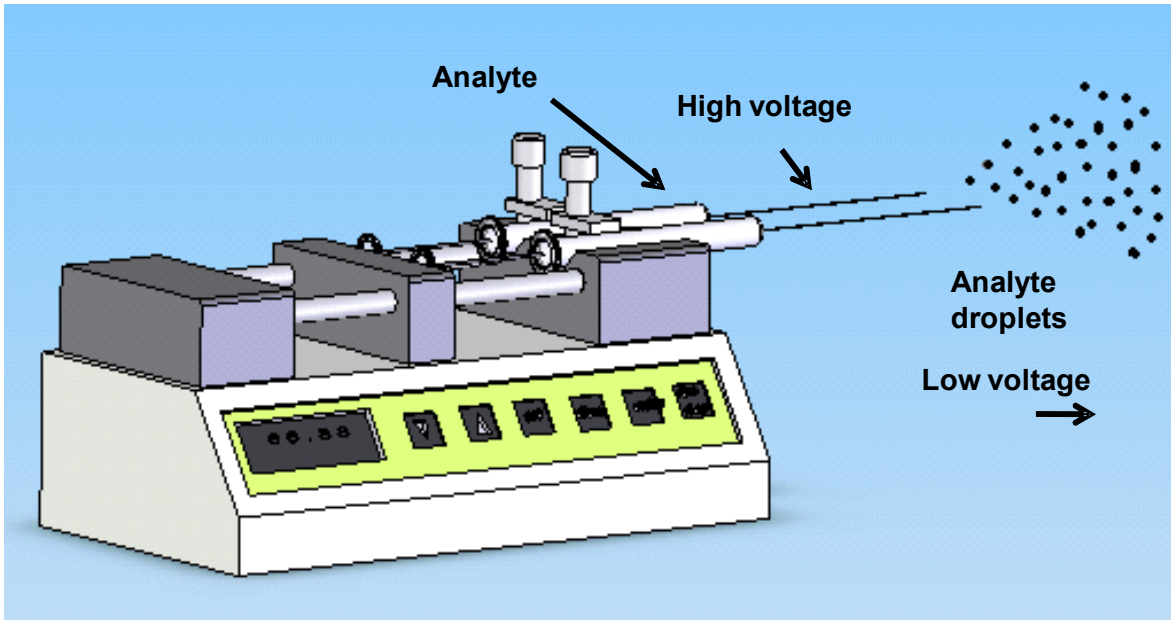

Figure 5. Electrospray ionization source

Chapter Two

Using a Buffer Gas Modifier to Change Separation Selectivity in Ion Mobility Spectrometry

Roberto Fernández-Maestre,[a1] Ching Wu,[b] and Herbert H. Hill Jr.[2]

[a] *Department of Chemistry, Washington State University, Pullman, WA 9914, USA.*

[b] *Excellims Corporation, 20 Main Street, Acton, MA 01720, USA.*

ching.wu@excellims.com. Phone: 1- 978-461-6050

Submitted to

INTERNATIONAL JOURNAL OF MASS SPECTROMETRY

May 2009

[1] Permanent Address: Programa de Quimica, Campus de Zaragocilla, Universidad de Cartagena, Cartagena, Colombia.

[2] Corresponding author. E-mail address: hhhill@wsu.edu. Tel. 1-509-335-5648 Fax 1-509-335-8867

ABBREVIATIONS: 2,4-dimethyl pyridine (2,4-lutidine), 2,6-di-tert-butyl pyridine (DTBP), tetramethylammonium ion (TMA), tetraethylammonium ion (TEA), tetrapropylammonium ion (TPA), tetrabutylammonium ion (TBA), electrospray ionization-ion mobility spectrometry-quadrupole mass spectrometry (ESI-IMS-QMS), hydrazine (HZ), monomethylhydrazine (MMH), single ion monitoring-IMS mode (SIM-IMS). reduced mobility (K_0); drift time (t_d).

ABSTRACT

The mobilities of a set of common α-amino acids, four tetraalkylammonium ions, 2,4-dimethyl pyridine (2,4-lutidine), 2,6-di-tert-butyl pyridine (DTBP), and valinol were determined using electrospray ionization-ion mobility spectrometry-quadrupole mass spectrometry (ESI-IMS-QMS) while introducing 2-butanol into the buffer gas. The mobilities of the test compounds decreased by varying extents with 2-butanol concentration in the mobility spectrometer. When the concentration of 2-butanol increased from 0.0 to 6.8 mmol m^{-3} ($2.5x10^2$ ppmv), percentage reductions in mobilities were: 13.6% (serine), 12.2% (threonine), 10.4% (methionine), 10.3% (tyrosine), 9.8% (valinol), 9.2% (phenylalanine), 7.8% (tryptophan), 5.6% (2,4-lutidine), 2.2% (DTBP), 1.0% (tetramethylammonium ion, TMA, and tetraethylammonium ion, TEA), 0.0% (tetrapropylammonium ion, TPA), and 0.3% (tetrabutylammonium ion, TBA). These variations in mobility depended on the size and steric hindrance on the charge of the ions, and were due to formation of large ion-2-butanol clusters. This selective variation in mobilities was applied to the resolution of a mixture of compounds with similar reduced mobilities such as serine and valinol, which overlapped in N_2-only buffer gas in the IMS spectrum. The relative insensitivity of tetraalkylammonium ions and DTBP to the introduction of 2-butanol into the buffer gas was explained by steric hindrance of the four alkyl substituents in tetraalkylammonium ions and the two tert-butyl groups in DTBP, which shielded the positive charge of the ion from the attachment of 2-butanol molecules. Low buffer gas temperatures (100 °C) produced the largest reductions in mobilities by increasing ion-2-butanol interactions and formation of clusters; high temperatures (250 °C) prevented the formation of clusters, and no reduction in ion mobility was obtained with the introduction of 2-

butanol into the buffer gas. Low temperatures and high concentrations of 2-butanol produced a series of ion clusters with one to three 2-butanol molecules in compounds without steric hindrance. Clusters of two and three molecules of 2-butanol were also visible. Ligand-saturation on the positive ions with 2-butanol molecules occurred at high concentrations of modifier (6.8 mmol m^{-3} at 150°C); when saturated, no further reduction in mobility occurred when 2-butanol was introduced into the buffer gas.

Keywords: Ion mobility spectrometry, gas modifier, 2-butanol, clustering, dopant

Graphical abstract

Using a Buffer Gas Modifier to Change Separation Selectivity in Ion Mobility Spectrometry

Roberto Fernández-Maestre,[a3] Ching Wu,[b] and Herbert H. Hill Jr.[4]

[a] *Department of Chemistry, Washington State University, Pullman, WA 9914, USA.*

[b] *Excellims Corporation, 20 Main Street, Acton, MA 01720, USA.*

ching.wu@excellims.com. Phone: 1- 978-461-6050

ABSTRACT

Ion mobilities were determined using IMS-QMS by injecting 2-butanol into the buffer gas. Ion mobilities decreased to different extents due to clustering with 2-butanol, resolving compounds with similar mobilities.

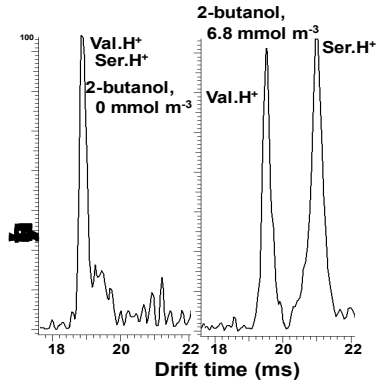

[3] Permanent Address: Programa de Quimica, Campus de Zaragocilla, Universidad de Cartagena, Cartagena, Colombia.

[4] Corresponding author. E-mail address: hhhill@wsu.edu. Tel. 1-509-335-5648 Fax 1-509-335-8867

1. INTRODUCTION

Adding trace quantities of vapors to ion mobility spectrometers to produce specific analytical effects was first utilized by Kim et al. (1978) who added ammonia to the N_2 carrier gas to selectively ionize a series of amines [1]. Later, Blyth (1983) used acetone for the selective detection of chemical warfare agents [2] and Spangler et al. (1985) introduced the use of carbon tetrachloride for the selective detection of explosives [3]. In a comparative study of halogen containing dopants, Proctor and Todd found dichloromethane to be superior to dibromomethane, methyl iodide, acetic acid, dimethyl sulfide, and acetonitrile [4] for the detection of explosives. Eiceman et al. (1995) selectively detected mixtures of volatile organic and organophosphorus compounds using acetone and dimethylsulfoxide reagent gases [5] and Meng et al. (1995) used water, acetone, and dimethylsulfoxide reagent gases to provide specific ionization of indoor ambient atmospheres for volatile organic compounds [6].

Eiceman et al. (1993) used acetone and 5-nonanone to monitor hydrazine (HZ) and monomethylhydrazine (MMH) in air, avoiding the interference of ammonia [7]. They produced $(C_9H_{18}O)H^+$ reactant ions, which reacted with HZ and MMH to form HZ:$(C_9H_{18}O)_nH^+$ and MMH:$(C_9H_{18}O)_nH^+$ complexes; these complexes had different drift times from the original HZ and MMZ ions, and the interference of ammonia was avoided. In a similar work, Gan and Corino (2000) introduced 4-heptanone reagent gas in the carrier gas to detect alkanolamines in the presence of ammonia, Freon 22, and diesel fuel vapors [8]. Puton et al. (2008) reviewed the use of reagent gases and modifiers in IMS in negative and positive modes (66 references) [9].

In most cases, when trace quantities of dopant vapors are added to IMS instruments, the purpose is to reduce ionization interferences and selectively ionize the target analytes of

interest. When doping agents are introduced directly into the drift region of the mobility spectrometer rather than the ionization region, they modify mobilities through dynamic ion-molecule interactions as they drift through the buffer gas. In work similar to Eiceman, Bollan et al. (2007) complexed hydrazines by introducing ketones into the buffer gas of an ion mobility spectrometer to avoid the interference of ammonia on the determination of hydrazines [10]. Dwivedi et al. (2006) demonstrated the separation of enantiomers of sugars, drugs, and amino acids by introducing 10 ppm of (S)-2-butanol modifier into the buffer gas. As the concentration of this modifier was increased, drift times of both enantiomers increased up to 5 ms. Interestingly, shifts in drift times were different for different compounds [11]. It is these differential shifts in drift times for various analytes as a result of the addition of a buffer gas modifier, which is the subject of this investigation. In this study, 2-butanol was introduced into the buffer gas of an ion mobility spectrometer to investigate the analytical potential of modifying the buffer gas for separation selectivity.

2. EXPERIMENTAL SECTION

2.1. Instrumentation

Experiments were performed using an electrospray-ionization atmospheric-pressure ion mobility spectrometer interfaced through a 40-μm pinhole to a quadrupole mass spectrometer (ESI-IMS-QMS) (Figure 1). The operating conditions routinely used for this instrument are shown in Table 1.

2.2. IMS instrument

The IMS instrument was built at Washington State University, and its full description and schematics can be found elsewhere [11,12]. A brief description of the instrument follows. The ESI-APIMS instrument was equipped with an electrospray ionization source and a drift tube. The tube had two parts: a desolvation and a drift region operating in positive mode, and separated by a Bradbury-Nielsen-type ion gate. Both regions had alternating 2.2”-OD, 2.0”-ID alumina insulating spacers (99.6% Al_2O_3, Advalue Tech., Tucson, AZ) and conducting stainless steel rings. A counterbore into each drift ring external face supplied a pocket for the neighboring ceramic insulator. Insulating spacers and steel rings were stacked in a horizontally interlocking design. All rings were kept together in a 2.5”-OD, 2.3”-ID alumina tube housed in an aluminum heating block. Steel rings were connected in series by 1 MΩ (drift region) or 0.5 MΩ (desolvation region) high-temperature resistors (Caddock Electronics Inc., ±1%). When a high electrical potential was applied to the first ring, a 200-500 V cm^{-1} electric field was created throughout the drift tube [13]. To help desolvate ions, a countercurrent of preheated N_2 buffer gas was introduced at the end of the drift tube at a flow rate of 0.93 L min^{-1} through a stainless-steel tube. To heat the buffer gas, it was passed through a 2 meter stainless-steel tube coiled inside a heated aluminum block (Figure 1). The mobility spectrometer was operated at ambient pressure (690-710 Torr in Pullman, WA). Custom LabView software (National Instruments, Austin, TX) collected the IMS data and controlled the ion gate. The electronic controls for IMS gating and data acquisition were built at WSU [14].

2.3 Ion gate

The ion gate was made of eighty 75-μm parallel Alloy 46 wires (California Fine Wire Co., Grove Beach, CA) separated 0.6 mm. When the gate was open, all wires had a voltage with a value equal to the average of the adjacent drift rings. The gate was closed when ±40 V were applied to adjacent wires so that a 320 V cm^{-1} orthogonal field stopped positive or negative ions approaching the gate. These voltages neutralized the ions on the negative or positive wires. This closure voltage was removed for 0.1 ms so that a narrow pulse of ions could enter the drift region to be analyzed.

2.4. MS instrument

An ABB Extrel 150-QC (Pittsburgh, PA) quadrupole mass spectrometer (0-4000 Da) was used in these experiments. A Keithley model 427 amplifier (Keithley Instruments, Cleveland, OH) amplified the output signal from the electron multiplier detector of the mass spectrometer and sent it to the data acquisition systems. The mass spectrometer was controlled with Merlin software (version 3.0 ABB Extrel, Pittsburgh, PA), which collected the mass spectral data. Igor Pro 5.0.3 (WaveMetrics, Portland, OR) was used to process the spectral data text files.

2.5. Modes of operation

When coupling an ion mobility spectrometer to a quadrupole mass spectrometer, there are several possible modes of operation. In radiofrequency-IMS mode (IMS), the DC voltages in the mass spectrometer are off, and all ions reach the detector; in this mode, the IMS spectrum of ions of all masses is obtained. In single ion monitoring-IMS mode (SIM-IMS), the

DC and RF voltages in the mass spectrometer are set to allow only ions with a specific mass or a selection of specific masses to reach the detector. SIM-IMS allows the analysis of specific compounds without the interference of others of different masses. In MS mode, all ions pass continuously, without pulsing, through the mobility spectrometer directly to the mass spectrometer, and are mass analyzed; mass spectra are obtained in this mode.

2.6. Materials and reagents

The amino acids methionine, phenylalanine, serine, threonine, tryptophan, and tyrosine; valinol, 2,4-dimethylpyridine (2,4-lutidine), 2,6-di-tert-butyl pyridine (DTBP), 2-butanol (2B), and tetramethylammonium, tetraethylammonium, tetrapropylammonium, and tetrabutylammonium chlorides (ACS reagent grade, ≥98% purity) were purchased from Sigma Aldrich Chemical Co. (Milwaukee, WI). These compounds were selected as analytes because they provide a series of ions with different molecular weights and steric properties required to test the effects of size and steric hindrance on the change in mobilities with the introduction of 2-butanol into the buffer gas.

2.7. Sample preparation and introduction

Standard solutions of the analytes (50 μM) were prepared in ESI solution (47.5 % methanol: 47.5 % water: 5 % acetic acid). Liquid samples or blank solution (ESI solution) was infused continuously by electrospray ionization using 250 μl syringes (Hamilton, Reno, NV) at a flow rate of 3 μl min^{-1} into 30 cm long, 100 μM ID capillary (Polymicro Technologies, Phoenix, AZ). This capillary was connected, through a stainless steel union (Valco, Houston, TX), to a 50 μm ID silica capillary. The end of this capillary was centered at a target screen, placed at the entrance of the mobility spectrometer. The target screen was made out of 2-mm stainless steel mesh with a 0.5-cm round hole in the center. A high voltage of 15.6 kV (or 3.5 kV bias with respect to the target screen at the first ring) was applied to the stainless steel union to produce positive electrosprayed ions. To prevent cross contamination between the analytes, different syringes and capillaries were used for every compound whenever possible.

2.8. 2-butanol introduction

2-butanol was introduced into the buffer gas at concentrations up to 6.8 mmol m^{-3}. To introduce the modifier, the method used by Dwivedi et al. was modified as follows [11]. 2-butanol was injected with gas tight syringes (pumped by a KD Scientific pump, model 210) to avoid leaking. 2-butanol was introduced through a 10-cm-long, 50-μm ID silica capillary into the buffer gas line using a T-junction, before the buffer gas heater (Figure 1). Introducing 2-butanol before the buffer gas heater provided a longer path to obtain a homogeneous mixture of 2-butanol with the buffer gas. To help vaporize the modifier, the temperature of the T-junction was increased to approximately 150 °C using a heating tape (OMEGA Engineering, Stamford, CT).

2.9. Identification of compounds and calibration

All analytes were detected as $[M+H]^+$ ions or their clusters with 2-butanol. Analytes were identified by comparing their m/z ratio in mass spectrometry to the molecular weight of their protonated molecules or clusters. Also, reduced mobilities of protonated analyte ions were compared with those from literature.

To account for errors in measuring instrumental parameters, Eiceman et al. [15] recommend correcting reduced mobilities by comparing with standards:

$$\frac{K_{o\,(\text{unknown})}}{K_{o\,(\text{standard})}} = \frac{t_{d\,(\text{standard})}}{t_{d\,(\text{unknown})}} \qquad (1)$$

where K_0 is the reduced mobility in $cm^2V^{-1}s^{-1}$ and t_d the drift time in ms. A new IMS calibration method, recently proposed, was used [16]. This method uses DTBP as the chemical standard to calibrate the instrument by replacing its drift time and mobility value in Equation 1. The method also uses 2,4-lutidine to determine the presence of contamination in the buffer gas.

3. RESULTS AND DISCUSSIONS

3.1. 2-butanol and the reactant ions

When no modifier was added to the buffer gas, the ion mobility spectrum of the reactant ions after electrospray ionization is shown in Figure 2a.

In this spectrum, the main reactant ion peak was observed at a drift time of 13.7 ms, which corresponded to a reduced mobility value of 2.65 $cm^2V^{-1}s^{-1}$. When the ion gate was held open, and all of the ions passed into the mass spectrometer, the predominant ions seen in the mass spectrum were $(H_2O)_nH^+$ at m/z 37, 55, 73, and 91 as shown in Figure 2b. These peaks coalesced into a single mobility peak at 13.7 ms in the IMS spectrum due to the equilibria $(H_2O)_nH^+ \leftrightarrow (H_2O)_{n-m}H^+ + mH_2O$. Figures 2c and 2d show the spectra of the solvent when 1.7 mmol m^{-3} of 2-butanol (2B) was added to the buffer gas. At these 2-butanol concentrations the reactant ion was modified by forming proton bound dimers with 2-butanol. The monomer and dimer of 2-butanol occurred at m/z 75 and 149 (Figure 2d); in the IMS spectra in Figure 2c, the major reactant ion occurred at a drift time of 20.3 ms, which corresponded to the monomer and dimer ions of 2-butanol, with a reduced mobility of 1.71 $cm^2V^{-1}s^{-1}$; $(H_2O)_nH^+$ ions were shifted to 16.6 ms, with a reduced mobility of 2.16 $cm^2V^{-1}s^{-1}$.

3.2. Drift region equilibria

When the amino acid serine was electrosprayed at a concentration of 500 μM into the IMS-MS, with no modifier added to the buffer gas, the product ion peak was observed at 18.4 ms, as shown in Figure 3a. When 2-butanol was added to the buffer gas at concentrations of 1.7 mmol m^{-3} (62ppmv), 3.4 mmol m^{-3} (125ppmv), and 6.8 mmol m^{-3} (250 ppmv) the drift time of the

serine product ion peak increased from 18.4 ms with no modifier to 19.3, 20.0, and 20.4 ms. The ion mobility spectra from each of these conditions are shown in Figure 3a. Figure 3b is the mass spectrum of serine at the maximal modifier concentration of 6.8 mmol m^{-3}. Under these conditions, clusters of 2-butanol with serine are formed. Ion peaks at m/z values of 180, 254, and 328 were observed, which corresponded to the ion clusters of $Ser(2B)H^+$, $Ser(2B)_2H^+$, and $Ser(2B)_3H^+$.

Although the mass spectra showed several ion clusters, the ion mobility spectrum contained only one peak for serine. This single peak indicated that the clustering/declustering reactions occurred in equilibrium in the buffer gas at rates sufficiently rapid to produce a single ion mobility peak with a weighted average of the mobilities of the individual ions. The analyte-modifier clusters along with the protonated analyte ion traveled through the drift tube interconverting rapidly among one another. Thus, the following equilibria occurred in the drift region between the protonated molecule of serine, 2-butanol, and serine-2-butanol clusters:

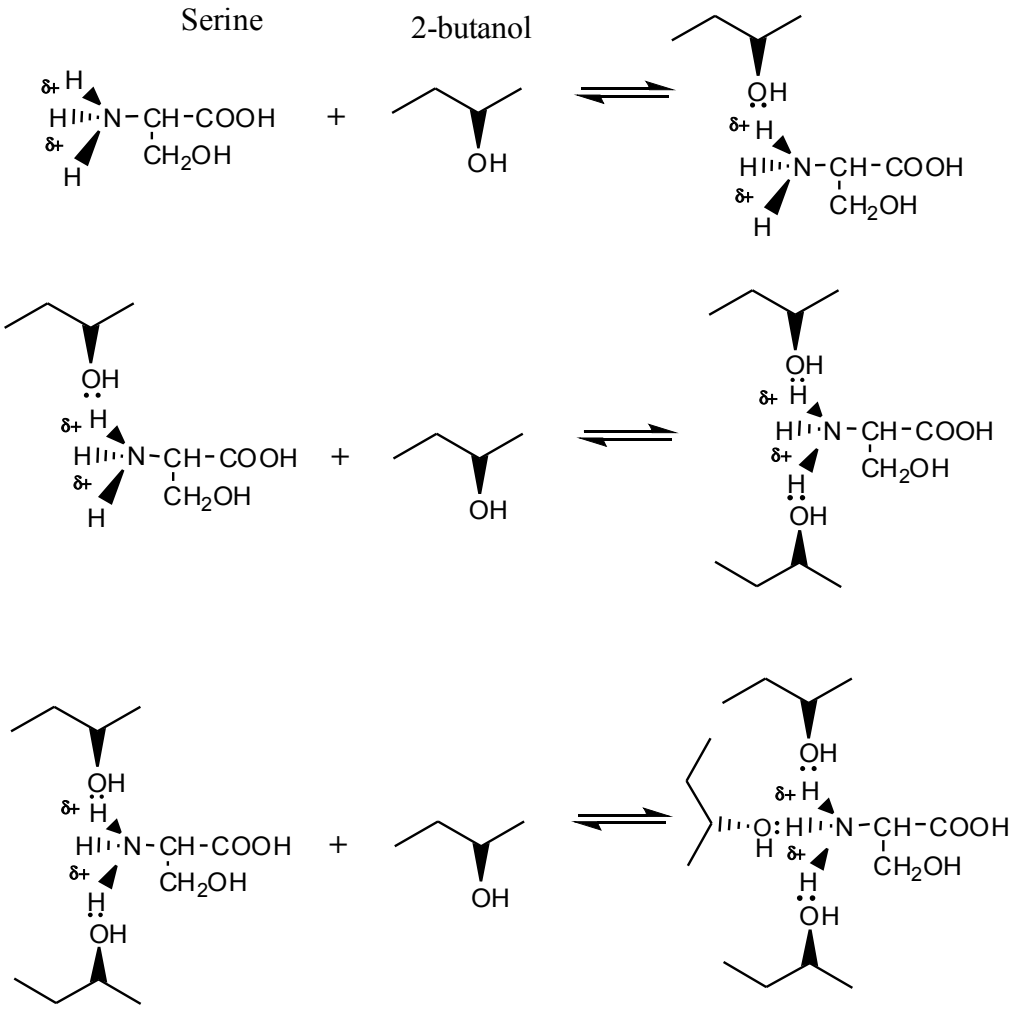

This clustering is possible due to the formation of hydrogen bonds between the electronegative oxygen atom in 2-butanol and the partially positive charge on the amine hydrogen atoms of serine. As a result of these equilibria, the drift time of serine increased with increasing 2-butanol concentration in the buffer gas. Assuming that the clusters do not form or decompose at the atmospheric/vacuum interface, the intensity of each ion species in the mass spectrometer is indicative of the relative concentration of the individual ion species that produced the ion mobility peak. The clusters formed in the source, and were in equilibria with

2-butanol while traveling the drift tube because serine's drift time increased as 2-butanol concentration increased, and the IMS peaks were well defined.

The maximum number of 2-butanol molecules clustering with serine was three, which corresponded to the number of hydrogen atoms on the positive nitrogen. These results agreed with those reported by Bollan et al [10]. They found that the number of ketone molecules binding to hydrazines and ammonia analytes, when the buffer gas was doped with ketones, depended on the number of hydrogen atoms on the protonated nitrogen of the analytes; these were four H atoms for ammonia, three for hydrazine, two for monomethyl hydrazine, and one for 1,1-dimethylhydrazine.

3.3. **Selective clustering with 2-butanol**

Reductions in mobilities for analytes other than serine also were found when 2-butanol was introduced into the buffer gas. Figures 4a and 4b plot the changes in K_0 values for a number of analytes as a function of modifier concentration when 2-butanol was increased in the buffer gas at 150 °C. As the 2-butanol concentration increased, the mobility of threonine, methionine, tyrosine, valinol, phenylalanine, tryptophan, and 2,4-lutidine decreased, but the mobility of tetraalkylammonium ions and DTBP did not change.

Table 2 summarizes the percentage reduction in mobilities ($\%\Delta K_0$) for the test compounds with the introduction of 2-butanol in the drift tube. $\%\Delta K_0$ was defined as the percentage difference between K_0 in N_2-only buffer gas and K_0 when 2-butanol modifier was introduced into the buffer gas at a given concentration. K_0 values in N_2-only buffer gas and literature values are shown in Table 3. When 2-butanol concentration was increased from 0.0 to

6.8 mmol m^{-3} ($2.5x10^2$ ppmv) at 150 °C, $\%\Delta K_0$ values were: 13.6% (serine), 12.2% (threonine), 10.4% (methionine), 10.3% (tyrosine), 9.8% (valinol), 9.2% (phenylalanine), 7.8% (tryptophan), 5.6% (2,4-lutidine), 2.2% (DTBP), 1.0% (TEA and TMA), 0.3% (TBA), and 0.0% (TPA) (Table 2). These $\%\Delta K_0$ values were not statistically different between TBA and TPA. Only differences greater than 0.32% were considered significant. This value was calculated from the maximum relative standard deviation of the drift times, 0.05 ms.

In general, the changes in mobility with the introduction of modifier into the buffer gas were selective and depended on the analyte structure. $\%\Delta K_0$ values decreased with molecular weight of the analytes; this trend may be due to the small effect on ion size when a molecule of 2-butanol clusters to large molecules.

3.4. Effects of ion structure on clustering

$\%\Delta K_0$ values also appeared to depend on the steric hindrance on the ion charge. $\%\Delta K_0$ values were small or negligible for tetraalkylammonium ions and 2,6-di-tert-butyl pyridine (DTBP). The other pyridine, 2,4-lutidine, showed significant changes with the concentration of 2-butanol. When 2-butanol concentration was increased from 0.0 to 6.8 mmol m^{-3} ($2.5x10^2$ ppmv) at 150 °C, $\%\Delta K_0$ values for these compounds were: 5.6% (2,4-lutidine), 2.2% (DTBP), 1.0% (TMA and TEA), 0.3% (TBA), and 0.0% (TPA) (Table 2). This relative insensitivity of tetraalkylammonium ions and DTBP to 2-butanol concentration in the buffer gas was due to the lack of clustering of these ions; the mass spectrum of tetraalkylammonium ions exhibits only single peaks for these compounds up to 6.8 mmol m^{-3} ($2.5x10^2$ ppmv) of 2-butanol in the buffer gas at 150 °C (Figure 5); also, Figure 5b shows only a single peak for DTBP in the mass

spectrum of a mixture of DTBP and 2,4-lutidine when 6.8 mmol m^{-3} ($2.5x10^2$ ppmv) of 2-butanol were introduced into the buffer gas. This lack of clustering of DTBP and tetraalkylammonium ions was probably due to steric hindrance that deterred the attachment of 2-butanol molecules to the positive nitrogen in these compounds, as illustrated in Figure 6; in tetraalkylammonium ions, this steric hindrance was caused by the four alkyl substituents [17]. In DTBP, the hindrance was produced by the two tert-butyl groups. The mobility of 2,4-lutidine was affected by 2-butanol more than that of the other pyridine, DTBP, because 2,4-lutidine formed one cluster at m/z 182 in the mass spectrum in Figure 5b. This clustering in 2,4-lutidine was due to lack of steric hindrance to the charge; the substituents on the ring of 2,4-lutidine are small methyl groups, which are located at positions 2 and 4 on the ring, ineffectively shielding the positive pyridine nitrogen from the attachment of 2-butanol molecules. In contrast, DTBP has two large *tert* butyl groups in positions 2 and 6 on the ring, more effectively shielding the charge. These large substituents in tetraalkylammonium ions and DTBP also delocalized the charge, weakening the ion-modifier interactions, which resulted in less clustering [18,19].

3.5. Effects of buffer gas temperature on clustering

As expected form early work in our laboratory [16], clustering decreased with higher temperatures due to more energetic collisions of the clustered ions with the buffer gas. Figure 4c plot the changes in K_0 values for serine at four different temperatures when 2-butanol concentration was increased from 0.0 to 6.8 mmol m^{-3} ($2.5x10^2$ ppmv) in the buffer gas. For serine $\%\Delta K_0$ values were 1.3% (250°C), 7.0% (200°C), 14% (150°C), and 16% (100 °C). Figure 7a shows the absence of ion-2-butanol clusters at high temperature (250°C) in the mass

spectrum of an amino acid mixture containing serine, threonine, phenylalanine, tyrosine, and tryptophan when 6.8 mmol m^{-3} of 2-butanol were introduced into the buffer gas; these clusters were abundant in the mass spectrum of the mixture at low temperatures (100 °C) at the same 2-butanol concentration (Figure 7b); this figure displays 1:1 clusters of serine, threonine, phenylalanine, tyrosine, and tryptophan with 2-butanol occurring at m/z 180, 195, 240, 256, and 279, respectively. The clusters of serine with one and two molecules of 2-butanol at m/z 180 and 254 may be overlapping with the protonated molecule peak of tyrosine at m/z 182 and its cluster at m/z 256. The cluster of threonine with two molecules of 2-butanol appears as a small peak at m/z 264. These clusters had large collision cross sections, which reduced the mobilities of the analytes.

For compounds that sterically hindered the formation of clusters, temperature did not affect their reduced mobilities even in the presence of modifiers. Figure 4c shows that the reduced mobility of TBA was not affected by temperature between 100 and 250°C. The stability of TBA's mobility is due to its non-clustering behavior (Figure 5a); if TBA had formed clusters with 2-butanol, these clusters would have survived at 100°C, producing changes in mobility of TBA with the increase in 2-butanol concentration.

3.6. **Modifier Saturation**

Locations for ligand binding on an ion are limited. A limit to mobility change as a function of modifier concentration indicates ligand saturation on the analyte's positive charge. Figure 4 demonstrates a flattening of mobility values at a concentration of 6.8 mmol m^{-3} of 2-butanol in the buffer gas, which indicates ligand saturation of the hydrogen atoms, available for binding with modifier molecules, on the positive charge of the analyte [10]; this saturation, due to

overloading of the buffer gas with 2-butanol, deterred the attachment of additional modifier molecules to the analytes, and no further decrease in mobility would be obtained with increasing concentrations of the modifier. This overloading with 2-butanol was evident in the presence of clusters of serine with one, two, and three 2-butanol molecules, and also from the occurrence of the dimer, trimer, and tetramer peaks of 2-butanol in the mass spectrum at high concentrations of the modifier (Figure 3b).

3.7. **Separation Selectivity**

The primary reason why modifiers are useful in IMS is that separations can be affected, which cannot be achieved in the pure buffer gas alone. For example, Figure 4b shows that the product ions of valinol and serine had the same mobility in N_2 buffer gas. When 2-butanol modifier is added to the buffer gas, the mobility of serine changed more than that of valinol. Thus, it should not be possible to separate these two compounds in N_2, but when the modifier is added, they should separate. In Figure 8a, the IMS spectrum of a mixture of valinol and serine in N_2-only buffer gas show the peaks of these amino acids overlapping at 18.9 ms; when introducing 1.7 mmol m^{-3} of 2-butanol modifier into the buffer gas, valinol and serine clustered with 2-butanol, the response ions shifted to 19.5 ms and 21.0 ms (Δt_d = 1.5 ms), respectively, and the mixture was base lined resolved with a resolution 1.5.

4. CONCLUSIONS

The primary objective of this paper was to investigate the addition of modifiers in IMS for the purpose of generating selective ion separations. 2-Butanol was chosen as a model modifier because of its volatility and previous experience in our lab as a buffer gas modifier. The introduction of 2-butanol in the buffer gas of an ion mobility spectrometer decreased the mobilities of several target compounds while other compounds were unaffected. The extent of the reductions in mobility for the compounds that changed was also different; the reductions in mobility were due to the formation of transient ion-2-butanol clusters of large collision cross sections. Clustering depended on the structure and molecular weight of the analyte; steric hindrance deterred formation of clusters with tetraalkylammonium ions and DTBP, and, therefore, the mobility of these compounds were less affected by the presence of a modifier; the mobilities of large compounds, such as tryptophan when compared to smaller amino acids, were less affected by the attachment of 2-butanol molecules because the collision cross section of ions of large size is less affected by formation of clusters; on the contrary, the mobilities of small molecules were largely affected by clustering. These differences in the reductions in ion mobilities were applied towards the separation of compounds with similar K_0 values, such as valinol and serine, which overlapped in the IMS spectra in N_2-only buffer gas. The ion-2-butanol clusters were abundant at low temperatures, due to strong interactions of the ions with 2-butanol. Finally, the change in mobility values as a function of modifier concentration was found to reach a limit at high concentrations of 2-butanol due to ligand saturation of the hydrogen atoms available for binding on the positive nitrogen of the analytes.

ACKNOWLEDGEMENTS

This work was supported by a grant from Excellims Corporation (Acton, MA) and NIH grant R33DK0702740351. The authors thank Dr. Brad Bendiak (University of Colorado) for his kind donation of reagents and the WSU-GPWC for proofreading the manuscript.

REFERENCES

[1] S.H. Kim, F.W. Karasek, S. Rokushika Anal. Chem. (1978) 50:152-155.

[2] D.A. Blyth A vapor monitor for detection and contamination control. In: Proc. Int. Symp, Against Chem, Warfare Agents Stockholm, 1983.

[3] G.E. Spangler, J.P. Carrico, D.N. Campbell J. Test Eval. (1985) 13:234.

[4] C.J. Proctor, Todd J.F.J. (1984) Anal. Chem. 56:1794-1797.

[5] G.A. Eiceman, Y.F. Wang, L. Garcia-Gonzalez, C.S. Harden, D.B. Shoff Anal. Chim. Acta (1995) 306:21-33.

[6] Q. Meng, Z. Karpas, G.A. Eiceman Int. J. Environ. Anal. Chem. (1995) 61:81-94.

[7] G.A. Eiceman, M.R. Salazar, M.R. Rodriguez, T.F. Limero, S.W. Beck, J.H. Cross, R. Young, J.T. James Anal. Chem. (1993) 65:1696-1702.

[8] H. Gan, G.T. Corino Anal. Chem. (2000) 72:807-815.

[9] J. Puton, M. Nousiainen, M. Sillanpaa Talanta (2008) 76:978–987.

[10] H.R. Bollan, J.A. Stone, J.L. Brokenshire, J.E. Rodriguez, G.A. Eiceman J. Am. Soc. Mass Spectrom. (2007) 18:940-951.

[11] P. Dwivedi, C. Wu, L.M. Matz, B.H. Clowers, W.F. Siems, H.H. Hill Jr., Anal. Chem. (2006) 78:8200-8206.

[12] C. Wu, W.F. Siems, G.R., Asbury, H.H. Hill Anal. Chem. (1998) 70:4929-4938.

[13] H.H. Hill Jr., G. J. Simpson Field Anal. Chem. Technol. (1997) 1:119-134.

[14] D. Wittmer, Y.H. Chen, B.K. Luckenbill, H.H. Hill Anal. Chem. (1994) 66:2348-2355.

[15] G.A. Eiceman, E.G. Nazarov, J.A. Stone Anal. Chim. Acta (2003) 493:185-194.

[16] R. Fernandez-Maestre, Buffer Gas Modifiers in Ion Mobility Spectrometry, PhD dissertation, Washington State University, Pullman, WA, 2009.

[17] J. Viidanoja, A. Sysoev, A. Adamov, T. Kotiaho Rapid Commun. Mass. Spectrom. (2005) 19:3051-3055.

[18] G.A. Eiceman, Z. Karpas, Ion mobility spectrometry, second ed., Taylor & Francis, Boca Raton, FL, USA, 2005.

[19] J. Sunner, M.G. Ikonomou, P. Kebarle (1988) Anal. Chem. 60 1308-1313.

[20] L.W. Beegle, I. Kanik, L. Matz, H.H. Hill Anal. Chem. (2001) 73:3028-3034.

[21] G.R. Asbury, J. Klasmeier, H.H. Hill Jr., Talanta 50 (2000) 1291-1298.

Table 1. ESI-APIMS operating conditions summary

Parameter	**Settings**
Reaction region length	7.5 cm
Drift tube length	25.0 cm
ESI voltage	15.6 kV
Voltage at first ring	12.1 kV
ESI flow	3 µl min^{-1}
Voltage at the gate	10.80 kV
Gate closure potential	±40 V
Gate pulse width	200 µs
Scan time	35 ms
Buffer gas	Nitrogen
Buffer gas temperature	150 ± 1 $^{\circ}C$
Buffer gas flow	900 ml min^{-1}
2-butanol flow rate	0.17 to 0.75 µl min^{-1}

Table 2. Percentage decrease in K_0 values, $\%\Delta K_0$, at 6.8 mmol m^{-3} of 2-butanol in the buffer gas for selected compounds. Differences of less than 0.32 units in $\%\Delta K_0$ may arise from the standard deviation of the drift time measurements (0.05 ms). $\%\Delta K_0$ was defined as the percentage difference between K_0 in N_2-only buffer gas and K_0 when a modifier was introduced into the buffer gas at a given concentration.

Class	Compound	$\%\Delta K_0$
Amines	2,4-lutidine	5.6
	DTBP	2.2
	TBA	0.3
	TEA	1.0
	TPA	0.0
	TMA	1.0
Amino acids	Methionine	10.4
	Phenylalanine	9.2
	Serine	13.6
	Threonine	12.2
	Tryptophan	7.8
	Tyrosine	10.3
Amino alcohol	Valinol	9.8

Table 3. Reduced mobility values (K_0) in $cm^2/(V.s)$ for selected compounds and literature values.

Analytes	Literature K_0		This work		
			K_0	RSD	%δK_0
Alanine	1.82 [a] 1.81 [b]		1.92	0.4	5.1 [a] 5.7 [b]
Serine	1.73 [a] 1.82 [b]		1.87	0.3	7.2 [a] 2.7 [b]
Threonine	1.68 [a] 1.76 [b]		1.81	0.2	6.9 [a] 2.8 [b]
Isoleucine	1.58 [a] 1.63 [b]		1.68	0.4	5.8 [a] 3.0 [b]
Methionine	1.55 [a] 1.60 [b]		1.67	0.1	7.4 [a] 4.2 [b]
Phenylalanine	1.45 [a] 1.50 [b]		1.55	0.1	6.7 [a] 3.2 [b]
Tyrosine	1.37 [a] 1.44 [b]		1.48	0.3	8.0 [a] 2.7 [b]
Tryptophan	1.31 [a] 1.35 [b]		1.40	0.2	7.1 [a] 3.6 [b]
Valinol	1.74 [c]		1.85	0.1	6.0 [c]

[a] [20]; [b] [21]; [c] [11]. RSD: Relative standard deviation (repeatability). The repeatability of the reduced mobilities, calculated as the RSD of the K_0 values of one sample analyzed continuously (n≥5), showed an average of less than 0.2%. The reproducibility of the reduced mobilities, calculated as the relative standard deviation of the K_0 values of 5 different samples of different concentrations, prepared independently and analyzed in different days, was <2%. Data were obtained in the SIM-IMS mode. %δK_0: % difference in K_0 values with respect to values of Beegle 2001 [20], Dwivedi 2006 [11], or Asbury 2000 [21].

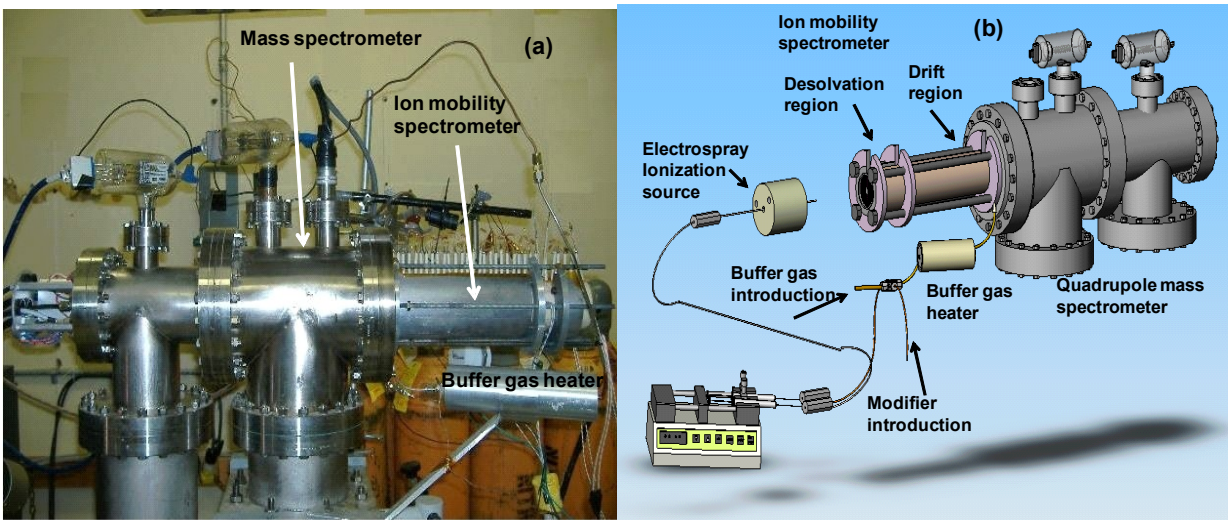

Figure 1. Photograph (a) and sketch (b) of the electrospray ionization-atmospheric pressure ion mobility-mass spectrometer.

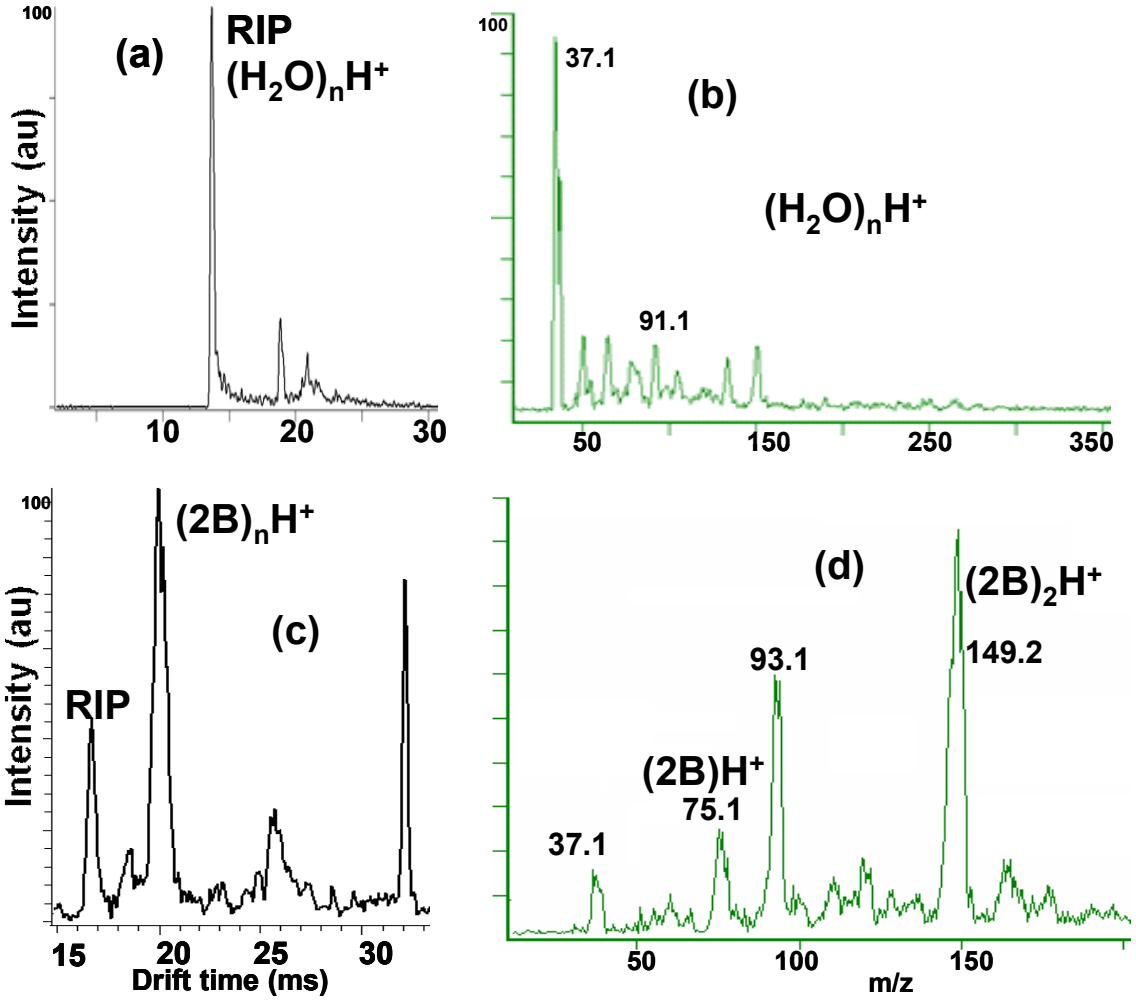

Figure 2. Clustering of the reactant ion peaks with 2-butanol, and clusters of 2-butanol. IMS (a and c) and MS spectra (b and d) of the ESI solvent in pure nitrogen (a and b), and when 1.7 mmol m^{-3} of 2-butanol was injected into the buffer gas (c and d). The reactant ion peak, $(H_2O)_nH^+$, appeared at 13.7 ms in (a). The IMS peaks are broadened and shifted to lower mobilities in (c) due to interactions with the modifier. The peak at 32 ms in (c) is due to a contaminant at m/z 371.

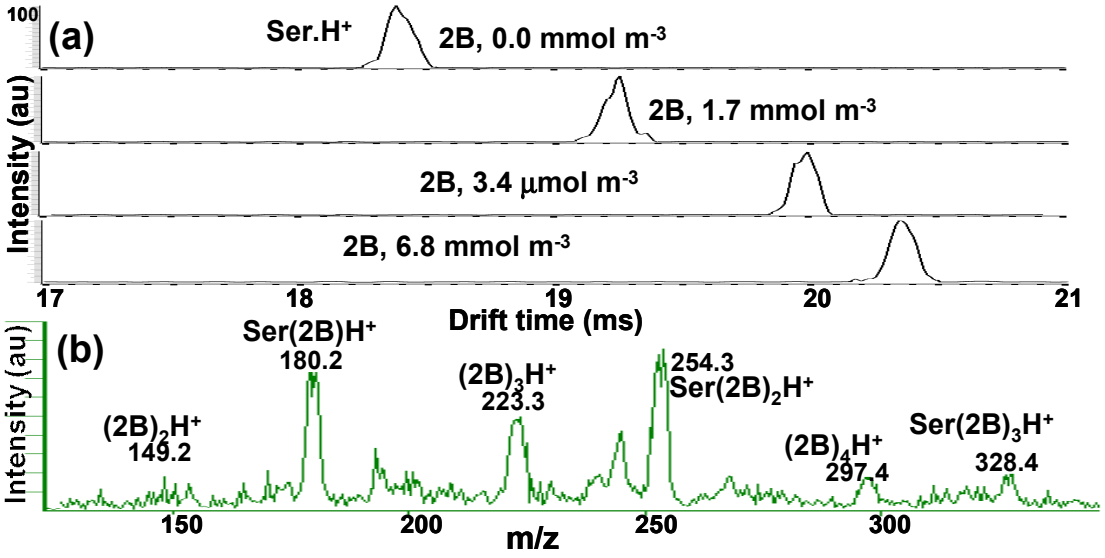

Figure 3. Reduction in mobility with the introduction of 2-butanol into the buffer gas. (a) IMS spectra showing the variation in drift times of a 500-µM solution of serine (Ser) with 2-butanol (2B) concentration in the buffer gas at 150°C. (b) Mass spectrum of a 100-µM solution of serine (500 averages) when 6.8 mmol m^{-3} ($2.5x10^2$ ppmv) of 2-butanol were introduced into the buffer gas at 100°C.

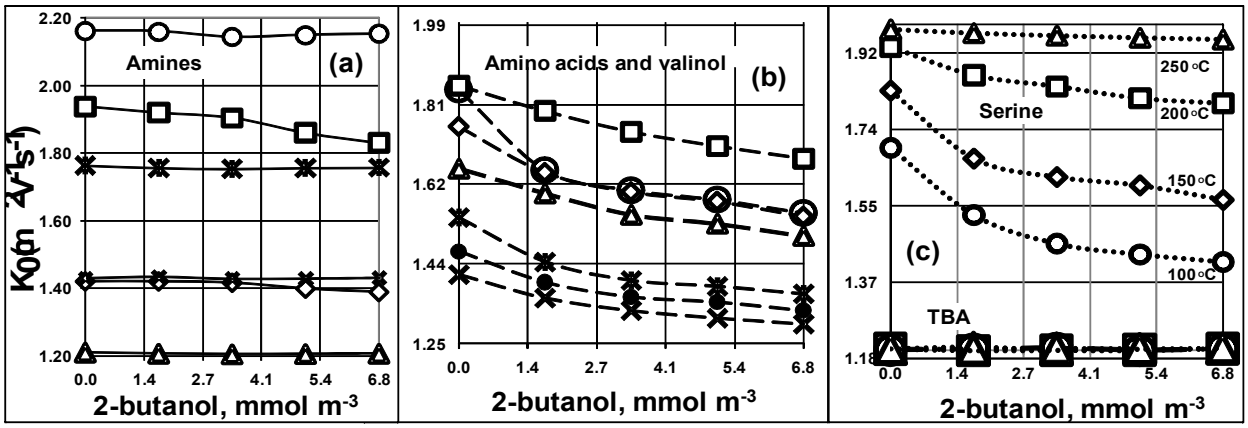

Figure 4. Effect of 2-butanol concentration in the buffer gas and temperature in ion mobility. (a) TMA (–○–), 2,4-lutidine (–□–), TEA (——), TPA (–x–), DTBP (–◊–), TBA (–Δ–); **(b)** valinol (--□--), serine (--○--), threonine (--◊--), methionine (--Δ--), phenylalanine (-- --), tyrosine (--●--), and tryptophan (--x--). **(c)** serine and TBA at 100 (··○··), 150 (··◊··), 200 (··□··), and 250 °C (··Δ··); the mobility of analytes decreased due to the formation of ion-2-butanol clusters as 2-butanol concentration increased at 150 °C (a and b) or as the temperature decreased (c). Figure 4c indicates an increase in the ion-2-butanol interactions at lower temperatures for serine (revealed by a reduction in mobility). TBA was not affected by temperature due to its lack of clustering. The mobilities of serine were lower at lower temperatures in N_2-only buffer gas due to clustering with moisture.

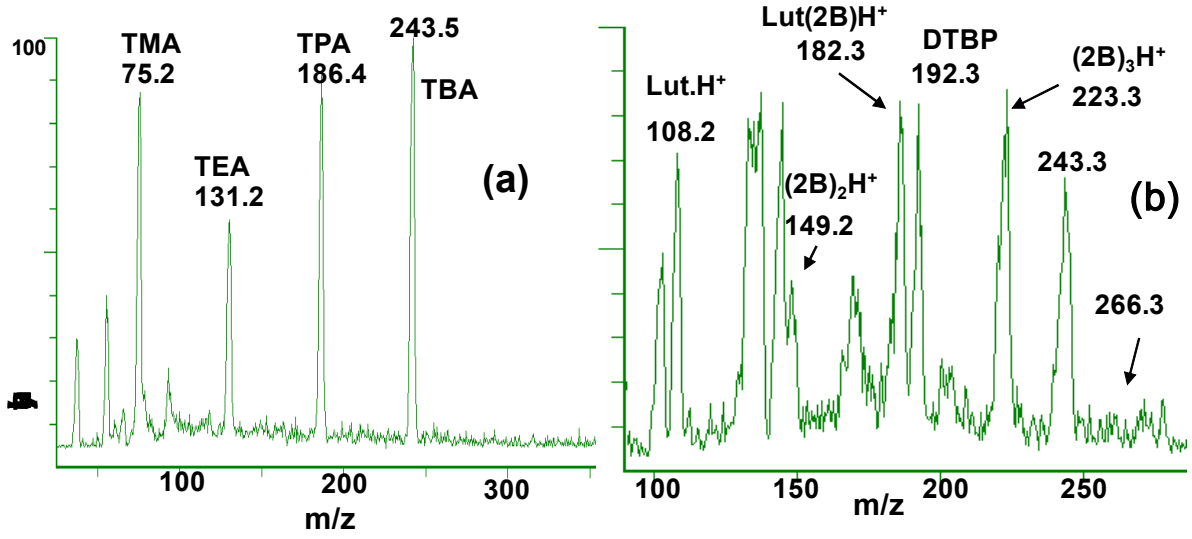

Figure 5. Non-clustering compounds. Mass spectra (500 averages) of selected compounds when 6.8 mmol m^{-3} ($2.5x10^2$ ppmv) of 2-butanol were introduced into the buffer gas at 150°C (a) 100-µM solution of tetraalkylammonium ions showing the lack of clustering of these ions; this lack of clustering was due to steric hindrance produced by the four alkyl substituents on the positive nitrogen that shield the positive charge from 2-butanol molecules. (b) Mixture of DTBP (0.2 µM) and 2,4-lutidine (0.001 ppm) showing the absence of the cluster of DTBP with 2-butanol at m/z 266.3 due to steric hindrance, and the cluster of 2,4-lutidine at m/z 182.3.

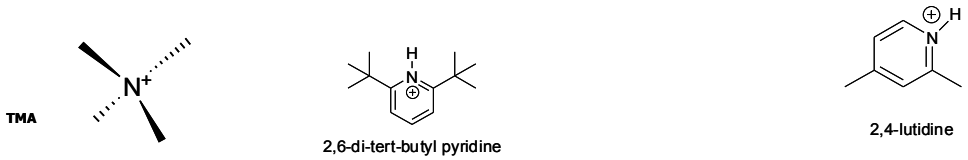

Figure 6. 3D models of TMA, 2,6-di-tert-butyl pyridine (DTBP), and 2,4-lutidine. The arrows signal the positive charge, sterically hindered in TMA and DTBP, but more accessible in 2,4-lutidine.

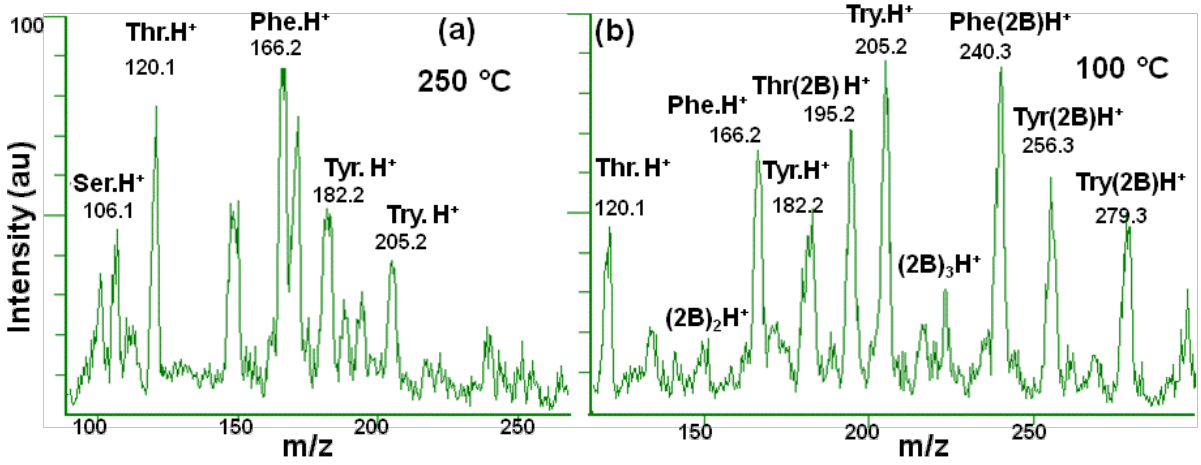

Figure 7. Absence of clusters at high temperature. Mass spectra (500 averages) of 100-μM mixtures of the amino acids serine (Ser), threonine (Thr), phenylalanine (Phe), tyrosine (Tyr), and tryptophan (Try) at 250 °C (a) or 100 °C (b) and 6.8 mmol m^{-3} ($2.5x10^2$ ppmv) of 2-butanol (2B) in the buffer gas. No clusters were present at high temperature; in contrast, at low temperature, there is an extensive formation of clusters. The clusters of serine (m/z 180.2 and 254) may be overlapped with the broad protonated molecule peak of tyrosine (m/z 182) and its cluster at (m/z 256). The cluster of threonine with two molecules of 2-butanol appears as a small peak at m/z 264.3.

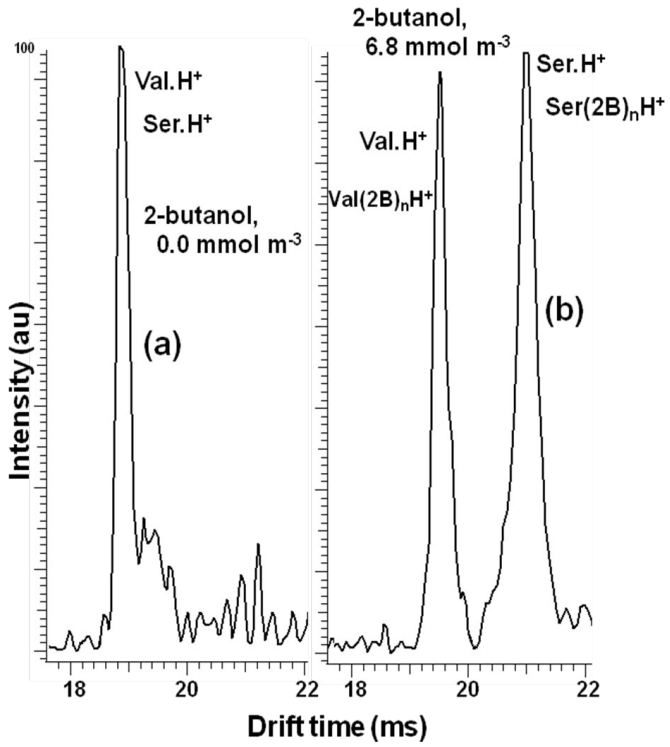

Figure 8. Separation of a mixture of valinol and serine by introducing 2-butanol into the buffer gas. (a) IMS spectra of the mixture in N_2-only buffer gas showing one overlapping peak for both compounds at 18.9 ms. (b) Resolution of the mixture by introducing 1.7 mmol m^{-3} of 2-butanol modifier into the buffer gas.

Chapter Three

Intramolecular Bridges Limited Clustering in an Ion Mobility Spectrometer

Roberto Fernández-Maestre[1,5] and Herbert H. Hill Jr.[16]

[1]*Department of Chemistry, Washington State University, Pullman, WA 99164, USA*

Submitted to

RAPID COMMUNICATIONS IN MASS SPECTROMETRY

June 2009

[5] Permanent address: Programa de Quimica, Campus de Zaragocilla, Universidad de Cartagena, Cartagena, Colombia

[6] Corresponding author. E-mail: hhhill@wsu.edu. Fax 509-335-8867

Abstract

When polar molecules (modifiers) are introduced into the buffer gas of an ion mobility spectrometer, ion mobilities decrease due to formation of ion-modifier clusters. In this investigation, the mobilities of several diamines (the basic amino acids arginine, histidine, and lysine, and the drug atenolol) were not affected or only slightly reduced when modifiers were introduced into the buffer gas of an ion mobility spectrometer. We found evidence indicating that the formation of intramolecular bridges caused this limited change in the mobilities of diamines when modifiers were added to the buffer gas; these bridges hindered the attachment of modifier molecules to the positive charge of ions and delocalized the charge, which deterred clustering. Ethyl lactate, nitrobenzene, 2-butanol, and tetrahydrofuran-2-carbonitrile were used as buffer gas modifiers and electrospray ionization ion mobility spectrometry coupled to quadrupole mass spectrometry was used as the analytical technique. Ethyl lactate, nitrobenzene, and tetrahydrofuran-2-carbonitrile had not been tested as buffer gas modifiers and 2-butanol had not been used with basic amino acids and atenolol. There was a tendency towards large changes in mobility when the mass of the analyte diminished; ethanolamine, the smallest compound tested, had the largest reduction in mobility with the introduction of modifiers into the buffer gas. These differences in mobilities were used to separate compounds that overlapped in IMS, such as isoleucine and lysine, and arginine and phenylalanine, and made possible the prediction of separations of overlapping compounds.

Keywords: Ion mobility spectrometry, clustering, intramolecular bridge, ethyl lactate, 2-butanol

INTRODUCTION

Drift tube ion mobility spectrometry (IMS) is a time-of-flight analytical technique that uses the distinctive mobilities of ions in a gas-phase for separation and identification of analytes. Ion mobility spectrometry has been applied to detection of heroin and cocaine,[1] explosives,[2] halogenated compounds,[3] explosives in hair,[4] veterinary drugs in meat,[5] screening of methamphetamines in human serum,[6] direct analysis of swabs for pharmaceutical equipment cleaning verification,[7] resolution of carbohydrate isomers,[8] analysis of complex peptide mixtures,[9] detection of large noncovalent protein-ligand and protein-protein complexes,[10] metabolic profiling,[11] and mapping of the human plasma proteome.[12] IMS also has been proposed as a potential diagnostic tool for diseases such as cancer.[13] Different reviews of IMS applications are available.[14,15]

In IMS, separation is based on the different velocities ions acquire under the influence of an electric field due to their different size-to-charge ratios. In electrospray ionization ion mobility spectrometry, single stable gas-phase ions are created in an electrospray source. Ion mobility spectrometers have a desolvation region where electrosprayed ions are stripped of solvent molecules by a countercurrent of preheated buffer gas. Ions are pulsed into the drift region, where they are accelerated by an electric field, but are continually decelerated by collisions against the buffer gas. This combination of collisions and accelerations thermalizes the ions and averages their velocities to distinct values that can be used to calculate a characteristic parameter, the mobility constant, K:[16]

$$K = \frac{v}{E} = \frac{L^2}{V t_d} \qquad (1)$$

where v is the velocity of the ion in cm s^{-1}, E the electric field in the drift region in V cm^{-1}, L the length of the drift region in cm, V the total voltage drop in volts across the drift region, and t_d the time the ion spends traveling the distance L in s. Velocity, ν, should be linear with E in an electric field of less than approximately 500 V cm^{-1} (at ambient pressure).[17] In IMS, ion mobilities are normalized to standard pressure and temperature as reduced mobilities (K_0, cm V^{-1} s^{-1}), which are constants useful for identification purposes. This standardization allows comparison of results in different laboratories by correcting for variations in environmental and instrumental conditions:

$$K_0 = K \frac{P}{760} \frac{273}{T} \tag{2}$$

where P is the pressure in the drift tube in Torr and T the buffer gas temperature in Kelvin.[17] However, as noted as early as the beginning of the 20th century, these mobilities can be affected by the presence of neutral contaminants in the buffer gas of an ion mobility drift tube. The reduction in ion mobilities by moisture and other neutral contaminants in the buffer gas was first noted by Lattey in the 1910s.[18,19] Recently, doping the buffer gas intentionally has been

used to vary arrival times of ions. The addition of ketones to the buffer gas allowed the separation of ammonia from hydrazines [20,21] and the addition of 2-butanol enabled the separation of enantiomers.[22]

Dopants mainly have been introduced, however, to preferentially ionize compounds with higher proton affinities (as in the case of drugs) or higher electronegativities (as in the case of explosives).[21] Dopants added include ammonia,[23] chloride ions,[24] dichloromethane, methyl iodide, acetic acid, dimethyl sulfide, acetonitrile,[25] acetone,[26-28] dimethylsulfoxide,[27,29] water,[29] 5-nonanone,[28] 4-heptanone,[20] and ketones.[21] A comprehensive review on the introduction of dopants in IMS was published by Puton in 2008.[30]

In this work, we evaluate three modifiers, ethyl lactate, nitrobenzene, and tetrahydrofuran-2-carbonitrile, to test changes in mobility of selected compounds, especially basic amino acids and the drug atenolol, when these modifiers were introduced into the buffer gas of an ion mobility spectrometer; also, we investigate how the introduction of ethyl lactate in the buffer gas affects the IMS separation of compounds with similar mobilities.

EXPERIMENTAL SECTION

Instrument. An electrospray-ionization atmospheric-pressure ion mobility spectrometer (ESI-IMS) coupled to a quadrupole mass spectrometer through a 40-µm pinhole was used in this investigation.[31] The mass spectrometer was an ABB Extrel (Pittsburgh, PA) 150-QC quadrupole (0-4000 Da), and was equipped with a Keithley amplifier (Model 427, Keithley Instruments, Cleveland, OH) that amplified data from the electron multiplier detector

and sent it to the acquisition systems. Merlin software (version 3.0, ABB Extrel, Pittsburgh, PA) controlled the mass spectrometer and collected the mass spectral data.

The ion mobility spectrometer was built at Washington State University, and has been described in detail elsewhere.[32] Briefly, the drift tube consisted of a desolvation and a drift region separated by a Bradbury-Nielsen ion gate. Both regions comprised 2.2"-OD, 2.0"-ID stainless steel rings, insulated from each other by alumina rings of the same size (99.6% Al_2O_3, Advalue Tech., Tucson, AZ). A counterbore into each metallic ring supplied a support to hold the neighboring ceramic insulator. Insulating spacers and steel rings were horizontally stacked in an interlocking design. All rings were kept together in a 2.5"-OD, 2.3"-ID alumina tube placed in an aluminum heating case. Steel rings were connected in series by high temperature resistors. Resistors were 1-MΩ (drift region) or 0.5 MΩ (desolvation region) (Caddock Electronics Inc., Riverside, CA, ±1%). When an electrical potential was applied to the first ring, a 432 V cm^{-1} developed in the drift tube.[33] A target screen was placed at the first ring of the desolvation region. This screen helped to electrospray the samples, and was made out of 2-mm stainless steel mesh with a 0.5-cm round hole in the center. A countercurrent of preheated N_2 buffer gas was introduced by the low voltage end of the drift tube through a stainless-steel tube. The buffer gas was heated by passing it through a 2-m long stainless-steel tube coiled inside an aluminum heating block.

The gate had approximately 80 parallel 75-μm Alloy 46 wires (California Fine Wire Co., Grove Beach, CA) separated 0.6 mm from each other. Ions were prevented from passing to the drift region by applying a closure potential that was 40 V higher for a set of wires and 40 V lower for the other set than the voltage of the gate when it was open. In the current

experimental conditions, these voltages were 10840 V and 10760 V. The open-gate voltage was that of a steel ring in the position of the gate in the tube, 10800 V. This closure voltage was disconnected for 0.1 ms so that a narrow pulse of ions entered the drift region. The mobility spectrometer was run at ambient pressure (685-710 Torr in Pullman, WA). LabView software (National Instruments, Austin, TX), modified in lab, collected the IMS data and controlled the ion gate. Igor Pro 5.0.3 (WaveMetrics, Portland, OR) was used to process spectral data text files. The electronics for IMS data acquisition were built at WSU.[34]

Typical operating parameters used with this instrument were: ESI flow, 3 μl min^{-1}; reaction region length, 7.5 cm; drift tube length, 25.0 cm; ESI voltage, 15.6 kV; voltage at first ring, 12.12 kV; voltage at the gate, 10.80 ± 0.01 kV; gate closure potential, ±40 V; gate pulse width, 0.1 ms; scan time, 35 ms; pressure, 680-710 torr; buffer gas, nitrogen; buffer gas temperature, 150 ± 2 °C; buffer gas flow, 1 liter min^{-1}; modifier flow rates, 1 to 50 μl hr^{-1} (Table 1).

Modes of operation. In ion mobility spectrometry-quadrupole mass spectrometry, mobility spectra can be obtained in two modes. In IMS mode, the DC voltages in the mass spectrometer are removed, no mass spectral scan is performed, and all ions reach the detector. Total ion mobility spectra are obtained in this mode. In SIM-IMS mode (single ion monitoring), the DC and RF voltages in the mass spectrometer are set to allow only ions with a specific mass or a selection of specific masses to reach the detector; ions are pulsed into the mass spectrometer, but only those with a given mass to charge ratio or a range of ions are detected, avoiding interference of other ions. To obtain mass spectra, ions are injected without pulsing into the mass spectrometer and are mass analyzed.

Materials and Reagents. 2,4-dimethylpyridine (2,4-lutidine), 2,6-di-tert-butyl pyridine (DTBP), 2-butanol, arginine, atenolol, desipramine, ethanolamine, ethyl lactate, histidine, lysine, nitrobenzene, serine, tetrahydrofuran-2-carbonitrile, valinol, and tetrabutylammonium (TBA), tetraethylammonium (TEA), tetramethylammonium (TMA), and tetrapropylammonium (TPA) chlorides (ACS reagent grade, ≥98% purity) were purchased from Sigma Aldrich Chemical Co. (Milwaukee, WI). Nitrobenzene was selected as a modifier because it has no affinity for protons, and does not charge through proton transfer reactions with analytes. Ethyl lactate, tetrahydrofuran-2-carbonitrile, and 2-butanol were selected as modifiers because they have different functionalities and steric impediments. Analytes were chosen to have a wide range of sizes and steric effects to test the effects of these parameters on the extent of modifier attachment and changes in mobilities.

Sample preparation and introduction. 100 μM standard solutions of the analytes were prepared in ESI solution (47.5 % methanol: 47.5 % water: 5 % acetic acid). Acetic acid was used to increase protonation of analytes. Liquid samples or blank solution (ESI solution) was continuously infused by electrospray ionization using 250-μl syringes (Hamilton, Reno, NV) at a flow rate of 3 μl min^{-1} into a 30-cm-long, 100-μM ID capillary (Polymicro Technologies, Phoenix, AZ). This capillary was connected, through a stainless steel union (Valco, Houston, TX) to a 50-μm ID silica capillary. The end of this capillary was centered at the target screen placed at the entrance of the mobility spectrometer. A voltage of 15.6 kV (or 3.5 kV bias with respect to the target screen) was applied to the stainless steel union to produce positive electrosprayed ions. To prevent cross contamination between analytes, different syringes and capillaries were used for every compound whenever possible.

Modifier introduction. The liquid modifiers were injected into the buffer gas line (pumped by a KD Scientific pump, model 210) before the buffer gas heater using gas tight syringes to avoid leaking. Modifiers were introduced through a 10-cm-long, 50-μm ID silica capillary into the buffer gas line using a cross-junction. The purpose of introducing the modifier before the buffer gas heater was to provide a longer path to obtain a homogeneous mixture of the modifier with the buffer gas. A heating tape (OMEGA Engineering, Stamford, CT) was wrapped around the buffer gas tube and cross to help vaporize the modifier.

When the flow rate of 2-butanol modifier was 10 μL hr^{-1}, the concentration of 2-butanol in the buffer gas was 1.4 mmol m^{-3} (51 ppmv), assuming a complete vaporization of the modifier. The concentration of modifier in ppmv was obtained by multiplying the flow rate of 2-butanol by its density and dividing by its molecular weight to obtain the flow rate of modifier in moles per minute, which was replaced in the equation of state of ideal gases to obtain the modifier flow rate in liters per minute. The ratio of this flow rate of modifier to the flow rate of buffer gas, multiplied by 10^6 and corrected to account for the expansion of the buffer gas from room temperature to the drift tube temperature, yields the concentration in ppmv. The concentration in mmol m^{-3} was obtained by multiplying the flow rate of 2-butanol by its density and dividing by its molecular weight and the flow rate of buffer gas, again corrected for the thermal expansion. The concentration of other modifiers was obtained in a similar way. The concentration of modifier in the drift tube was much larger than that of the analyte. Typical IMS pulses consist of 10^4 to 10^6 ions traveling in a volume of approximately 0.25 cm^{-3},[34] which correspond to analyte concentrations of approx. $4x10^{-12}$ to $4x10^{-10}$ mmol m^{-3}.

Calibration. To account for errors produced by inaccurate measurement of drift tube

length, temperature, voltages, and pressure, reduced mobilities were corrected by comparing with standards:[35]

$$\frac{K_{o\,(\text{unknown})}}{K_{o\,(\text{standard})}} = \frac{t_{d\,(\text{standard})}}{t_{d\,(\text{unknown})}} \qquad (3)$$

where K_0 is the reduced mobility in $cm^2V^{-1}s^{-1}$ and t_d the drift time in ms. 2,4-lutidine and DTBP were used as chemical standards to calibrate the reduced mobility scale applying a newly recommended procedure: an instrument constant, C_i, is calculated using a standard insensitive to contamination such as DTBP, $C_i = K_{0,standard}\ x\ t_{d,standard}$. Then, the mobility of a standard sensitive to contamination such as 2,4-lutidine is calculated using C_i, $C_i = K_{0,unknown}\ x\ t_{d,unknown}$; if the reduced mobility value of 2,4-lutidine match the literature value, then the instrument is free of contamination, and reduced mobility values of analytes can be calculated using C_i.

Identification of compounds. All analytes were detected as $[M{\cdot}H]^+$ or as cluster ions. Analytes were identified in the mass spectra by the molecular weight of their protonated molecules or clusters. Analyte peaks in the mobility spectrum were identified using SIM-IMS and by comparing their reduced mobilities with literature values.

RESULTS AND DISCUSSIONS

1. *Effect of modifiers on ion mobility*

Figure 1 illustrates the reduction in the ion mobility of ethanolamine when ethyl lactate was introduced as the modifier into the buffer gas of the ion mobility spectrometer. The drift

time of ethanolamine increased more than 10 ms as ethyl lactate concentration increased from 0.0 to 2.8 mmol m^{-3} (104 ppmv), which corresponded to a 41% reduction in mobility. Figure 1 shows clusters of ethanolamine (EA) with ethyl lactate (Lac), sodium ions, and reactant ions in the buffer gas in the IMS and mass spectra; the clusters occurred at ~25 ms, $[EA{\cdot}Lac_nH]^+$, ~26 ms, $[EA{\cdot}Lac_nH_3O]^+$, and ~29 ms, $[EA{\cdot}Lac_nNa]^+$ in the IMS spectra. Clusters of ethanolamine with one to three ethyl lactate molecules occurred at m/z 180 and 298 (Figures 1.2b, 1.3b, 1.4b, and 1.5b), and m/z 416 (Figures 1.4b and 1.5b) in the mass spectra. The mass spectra show that the ratio $[EA{\cdot}Lac_2H]^+$ to $[EA{\cdot}Lac{\cdot}H]^+$ increased with the concentration of ethyl lactate in the buffer gas and that $[EA{\cdot}Lac_3H]^+$ only appeared at high concentrations of modifier, which indicates an increasing clustering when the concentration of ethyl lactate increased. This clustering between ethanolamine and ethyl lactate modifier decreased the mobility of ethanolamine. Clustering with ethyl lactate was evident also in the IMS and mass spectra of the ESI solvent (Figure 2) with ethyl lactate in the buffer gas. Clusters of ethyl lactate occurred at 25.0 ms, $[Lac_nH]^+$, 25.5 ms, $[Lac_nH_3O]^+$, and 29.1 ms, $[Lac_nNa]^+$, in the IMS spectrum (Figure 2a); in the mass spectrum (Figure 2b), the clusters occurred at m/z 119 $[Lac{\cdot}H]^+$, 136 $[Lac{\cdot}H_3O]^+$, 237 $[Lac_2H]^+$, 255 $[Lac_2H_3O]^+$, 259 $[Lac_2Na]^+$, 355 $[Lac_3H]^+$, 373 $[Lac_3H_3O]^+$, and 377 $[Lac_3Na]^+$. $[EA{\cdot}Lac_nH]^+$ were formed in the reaction region and not at the atmospheric/vacuum interface of the IMS-QMS because the drift time of ethanolamine increased with the concentration of ethyl lactate in the buffer gas, which indicates the formation of slow ethanolamine-clusters in the drift region.

Ethanolamine, $[EA{\cdot}H]^+$, and $[EA{\cdot}Lac_nH]^+$ had the same drift times as verified by SIM-IMS measurements on these peaks, and appeared as a single peak in the IMS spectra (Figure 1). This coalescence of the peaks of $[EA{\cdot}H]^+$ and $[EA{\cdot}Lac_nH]^+$ demonstrates that the peaks at m/z

180, 298, and 416 in Figure 1 were $[EA{\cdot}Lac_nH]^+$ clusters, which were in equilibria in the drift region with $[EA{\cdot}H]^+$ and ethyl lactate. These ions traveled the drift tube together, but they were resolved inside the quadrupole according to their masses. Figure 1 shows sharp IMS peaks of $[EA{\cdot}Lac_nH]^+$, which indicates that these equilibria were much faster than the drift time of the ions through the drift tube. However, the peaks were broader than without ethyl lactate in the buffer gas, which also indicates that the equilibria occurred in a finite time. According to these results, the following equilibria occurred in the drift tube:

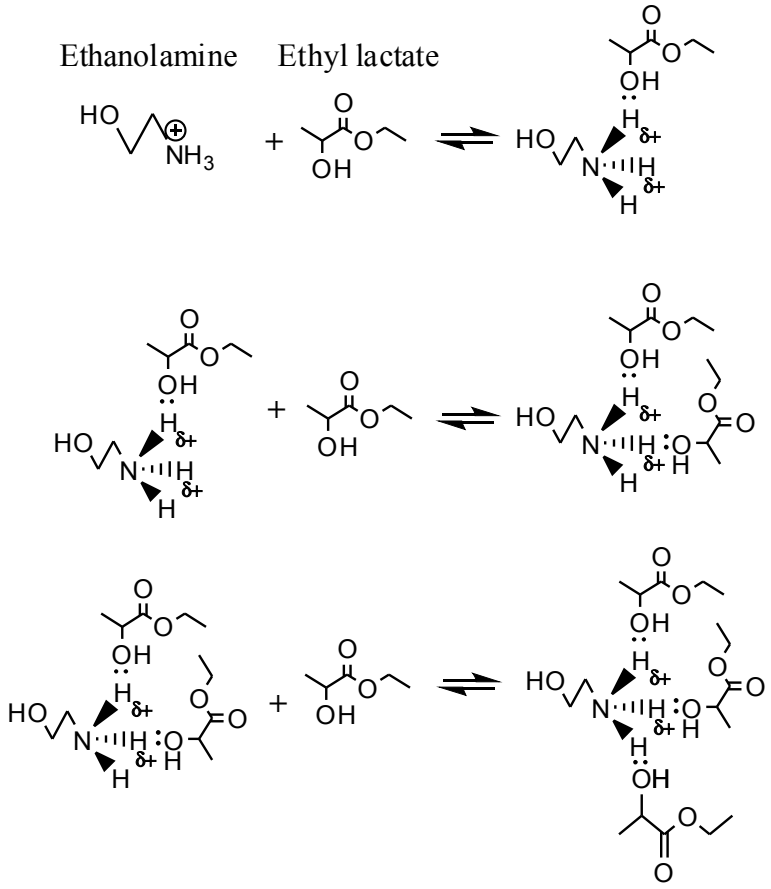

These equilibria must be rapid and occurred many times during the travel of every ion through the drift tube. As a consequence, the drift time of ethanolamine was a weighted average of the drift times of its fast protonated molecule and slow cluster ions. Similar

arguments can be used to demonstrate that peaks in the mass spectra of other analytes corresponded to cluster peaks

A maximum of three molecules of ethyl lactate clustered to ethanolamine; this number corresponds to the number of hydrogens atoms attached to the positive nitrogen of protonated ethanolamine, $[C_2H_5ONH_3]^+$, available for binding modifier molecules. These results agree with the findings of Bollan et al.[21] who reported that the number of ketone molecules binding to hydrazines and ammonia analytes when the buffer gas was doped also depended on the number of hydrogen atoms on the protonated nitrogen of the analytes (four for ammonia, three for hydrazine, two for monomethyl hydrazine, and one for 1,1-dimethylhydrazine).

In summary, the ion mobility of ethanolamine decreased, and ethanolamine-ethyl lactate clusters and clusters of ethyl lactate with sodium ions and the reactant ions occurred in the IMS and MS spectra when ethyl lactate was used as modifier in the analysis of ethanolamine.

2. ***Effect of other modifiers on ion mobility***

Formation of clusters is expected to decrease ion mobilities by increasing the collision cross sections of the ions. 2-butanol, ethyl lactate, nitrobenzene, and tetrahydrofuran-2-carbonitrile were used as modifiers. Ethyl lactate, nitrobenzene, and tetrahydrofuran-2-carbonitrile had not been tested as buffer gas modifiers, and 2-butanol had not been used with basic amino acids and atenolol. Figure 3 plots the changes in mobilities of 2,4-lutidine, arginine, DTBP, ethanolamine, serine, valinol, the drugs atenolol and desipramine, and TBA, TEA, TMA, and TPA ions when the modifiers were introduced into the buffer gas. These

changes are summarized in Table 2 as $\%\Delta K_0$ values. $\%\Delta K_0$ was defined as the percentage difference between K_0 in N_2-only buffer gas and K_0 when a modifier was introduced into the buffer gas at a given concentration.

2.a. ***2-butanol as a buffer gas modifier***

When 2-butanol concentration increased in the buffer gas from 0.0 to 6.8 mmol m^{-3} ($2.5x10^2$ ppmv), $\%\Delta K_0$ values for diamines were: atenolol (0.7%), arginine (0.3%), and histidine and lysine (1.1%) (Table 2). In a previous work,[36] the mobilities of a series of analytes decreased (average $\%\Delta K_0$ value of 10%) when 2-butanol was introduced into the buffer gas at the same experimental conditions used here. In this work, only diamines were tested with 2-butanol, and they showed a low responsiveness to the introduction of this modifier into the buffer gas (average $\%\Delta K_0$ value of 0.8%).

2.b. ***Ethyl lactate as a buffer gas modifier***

Changes in mobilities with the introduction of ethyl lactate in the buffer gas are shown in Figures 3a and 3b. The test compounds showed the following $\%\Delta K_0$ values: 2,4-lutidine (24%), atenolol (7.0%), desipramine (12%), DTBP (1.5%), ethanolamine (41%), serine (30%), TBA (0.3%), TEA (0.5%), TMA (1.0%), TPA (0.1%), and valinol (28%) when ethyl lactate concentration increased in the buffer gas from 0.0 to 1.7 mmol m^{-3}, and $[Lac_nH]^+$ (6.4%), $[Lac_nH_3O]^+$ (10%), and $[Lac_nNa]^+$ (4.3%) as ethyl lactate increased in the buffer gas from 0.33 (12 ppmv) to 2.8 mmol m^{-3} ($1.0x10^2$ ppmv). In general, ion mobilities decreased (average $\%\Delta K_0$ value of 13%, excluding the cluster ions) when ethyl lactate was introduced into the

buffer gas at 1.7 mmol m^{-3}; tetraalkylammonium ions and DTBP showed only small $\%\Delta K_0$ values (≤1.5%) at this ethyl lactate concentration.

2.c. ***Nitrobenzene as a buffer gas modifier***

The changes in mobilities with the introduction of nitrobenzene in the buffer gas are shown in Figure 3c. Test compounds produced the following $\%\Delta K_0$ values when nitrobenzene concentration increased in the buffer gas from 0.0 to 0.96 mmol m^{-3} (36 ppmv): 2,4-lutidine (13%), arginine (2.7%), atenolol (2.0%), DTBP (0.1%), ethanolamine (37%), TBA (0.1%), TEA (0.3%), TMA (1.0%), TPA (0.5%), and valinol (21%) (Table 2). In general, decreases in ion mobility were observed when 0.96 mmol m^{-3} nitrobenzene were introduced into the buffer gas (average $\%\Delta K_0$ value of 7.8%). Only small reductions in mobility were observed for diamines, DTBP, and tetraalkylammonium ions ($\%\Delta K_0$ values ≤ 2.7%).

2.d. ***Tetrahydrofuran-2-carbonitrile as a buffer gas modifier***

When tetrahydrofuran-2-carbonitrile (tHFCN) was used as a modifier, MS peaks were not observed for α-amino acids and valinol at concentrations lower than 3.3 mmol m^{-3} (125 ppmv) of this modifier in the buffer gas. However, peaks of tetraalkylammonium ions and DTBP were observed in the mass spectrum at this concentration. The absence of some analytes peaks from the mass spectrum with tHFCN in the buffer gas may be due to a possible large proton affinity of this modifier (not available in the literature). This large proton affinity of tHFCN stripped off the charge of the test compounds except for those such as DTBP, with steric hindrance that deterred the approach of the modifier to the positive charge (as explained in section 4), and those inherently ionic such as tetraalkylammonium ions.

3. *Effect s of steric hindrance, modifier saturation, and analyte size on changes in ion mobility due to clustering with modifiers*

In Figure 3, several common characteristics of changes in mobility are observed when modifiers were introduced into the buffer gas. The mobilities of the two pyridines changed to different extents when the modifiers were introduced into the buffer gas. The mobilities of DTBP decreased less than those of 2,4-lutidine (average $\%\Delta K_0$ value of 0.8% and 19%, respectively) with ethyl lactate and nitrobenzene modifiers. Figure 4.1 shows the IMS and mass spectra of a DTBP-2,4-lutidine mixture when the buffer gas was spiked with 1.7 mmol m^{-3} of ethyl lactate. No cluster peaks of DTBP were visible, but a 1:1 2,4-lutidine-ethyl lactate cluster occurred at 22 ms in the IMS spectrum and m/z 226 in the mass spectrum. This lack of clustering in DTBP was due to the strong steric hindrance exercised by the large tert-butyl substituents, in positions 2 and 6 on the ring. These substituents shielded the protonated nitrogen atom of DTBP from modifier molecules. The two small methyl groups of 2,4-lutidine, located at positions 2 and 4 on the ring, shielded the nitrogen atom less effectively. This low clustering of DTBP explains the small mobility change observed for this compound with modifiers in the buffer gas.

Table 2 shows that the mobilities of tetraalkylammonium ions decreased ≤1% when the buffer gas was spiked with ethyl lactate or nitrobenzene. When 1.7 mmol m^{-3} of ethyl lactate were introduced into the buffer gas (Figure 4.2a), tetraalkylammonium ions showed single and sharp peaks occurring at 16.7 (TMA), 20.3 (TEA), 24.8 (TPA), and 29.4 ms (TBA) in the IMS spectrum and at m/z 75.2 (TMA), 131.2 (TEA), 186.4 (TPA), and 243.5 (TBA) in the MS spectrum (Figure 4.2b). This lack of clustering was as a consequence of steric hindrance

exerted by the four alkyl substituents in tetraalkylammonium ions that deterred the attachment of ethyl lactate molecules to the nitrogen positive charge and delocalized the charge, which weakened the ion-modifier interactions.[16,37] This low clustering of tetraalkylammonium ions explains the small mobility change observed for these compounds with modifiers in the buffer gas.

Figure 3 shows that the largest reductions in mobility were obtained with the first introduction of modifier, and only small reductions were achieved with further increments of modifier concentration, which caused a plateau in K_0 values at high concentrations of modifier. In Figure 1, the largest increase in the drift time of ethanolamine (60%) was obtained when ethyl lactate concentration increased from 0.0 to 0.33 mmol m^{-3} (12 ppmv), and only a small reduction (8.4%) was obtained for a larger increment of concentration (from 0.33 mmol m^{-3} to 1.7 mmol m^{-3}). Small reductions in mobility with the introduction of ethyl lactate into the buffer gas may indicate modifier saturation of the hydrogen atoms available for ligand binding on the positive charge in ethanolamine, due to overloading of the buffer gas with ethyl lactate. This ligand saturation would deter the attachment of additional molecules of ethyl lactate, and no further decrease in the mobility of ethanolamine would be obtained when the concentrations of ethyl lactate increased.

Table 2 shows that there was a tendency towards large $\%\Delta K_0$ values when the mass of the analyte diminished. For analytes with relatively small steric hindrance to the positive charge such as desipramine, serine, valinol, 2,4-lutidine, and ethanolamine, the correlation coefficient for this trend was -0.91 when ethyl lactate increased from 0.0 to 1.7 mmol m^{-3} in the buffer gas. This trend originated in the large increase of size with the attachment of modifier

molecules to small analytes. Also, increased clustering was expected as size decreased, as a consequence of localization of the positive charge.[16,37] Steric hindrance would obscure this trend by deterring clustering in spite of size as evidenced for TMA that showed $\%\Delta K_0$ values of only 1%, which were small when compared to values of 41 and 37% for ethanolamine, a compound of similar molecular weight.

In summary, ion mobilities decreased, (average $\%\Delta K_0$ value of 9.1% for all the modifiers), probably due to formation of analyte-modifier clusters. The mobilities of DTBP and tetraalkylammonium ions showed only small changes (average $\%\Delta K_0$ value of 0.54% with ethyl lactate and nitrobenzene modifiers) as a consequence of steric hindrance and charge delocalization, which hindered clustering. Also, there was a ligand saturation of binding sites in the analytes at high modifier concentrations, and changes in mobility due to clustering were large for low molecular weight compounds.

4. ***Effect of intramolecular bridges on ion mobility***

When 2-butanol concentration increased from 0.0 to 6.8 mmol m^{-3} ($2.5x10^2$ ppmv) in the buffer gas, a $\%\Delta K_0$ value of 0.7% for atenolol was obtained. This $\%\Delta K_0$ was low compared to an average $\%\Delta K_0$ value of 10% for a series of analytes at the same experimental conditions.[36] A low average $\%\Delta K_0$ value of 0.7% for atenolol also was observed at four different temperatures (100, 150, 200, and 250°C) when 2-butanol concentration increased from 0.0 to 6.8 mmol m^{-3} in the buffer gas. Mixtures of desipramine and atenolol were analyzed by introducing ethyl lactate modifier into the buffer gas to establish if the small change in mobility of atenolol to the introduction of 2-butanol into the buffer gas was determined by the size of

atenolol. Large size of the analytes can cause only small changes in ion mobility with the introduction of modifiers into the buffer gas because the collision cross section of relatively large ions, such as atenolol, is less affected by clustering than that of small ions. Desipramine is an antidepressant and atenolol is a β-blocker drug used to prevent angina and to reduce the risk of heart attacks by reducing heart rate and high blood pressure. The IMS spectra of the mixture of these drugs in Figure 5.1 shows a small separation of the peaks in N_2-only buffer gas (Δt_d = 0.8 ms, α = 1.03); when 0.33 mmol m^{-3} of ethyl lactate were introduced into the buffer gas, the separation increased (Δt_d = 1.6 ms, α = 1.05); and when ethyl lactate concentration increased to 1.7 mmol m^{-3}, the separation increased even more (Δt_d = 3.2 ms, α = 1.11). These drugs have the same nominal molecular weight (266 g mol^{-1}), and, therefore, their mobilities were expected to be affected to the same extent by the attachment of modifier molecules. However, the overall change in mobility of desipramine was more pronounced (12%) than that of atenolol (7.0%) with 1.7 mmol m^{-3} of ethyl lactate in the buffer gas. Figure 5.2 explains why atenolol was less affected than desipramine by the introduction of ethyl lactate in the buffer gas. In this figure, the MS spectra of desipramine and atenolol with ethyl lactate modifier in the buffer gas shows that the intensities of the protonated peak of desipramine (m/z 267) was lower than that of its cluster with ethyl lactate (m/z 385), and that a cluster of desipramine with two ethyl lactate molecules occurred at m/z 503. For atenolol, the peaks of the protonated ion (m/z 267) and its cluster with ethyl lactate (m/z 385) had the same size and the cluster peak at m/z 503 was not observed, which indicates a lower clustering of ethyl lactate with atenolol than with desipramine. The large difference in $\%\Delta K_0$ values between desipramine and atenolol indicates that the small change in mobility for atenolol is not due to size because the size of these two

drugs must be similar. This interaction atenolol-modifier was also small with 0.95 mmol m^{-3} of nitrobenzene in the buffer gas with changes in mobility of 2.0% (Table 2).

The small interaction of atenolol with the modifiers may be related to formation of an intramolecular bridge between its two amine functionalities as illustrated in Figure 5.3. The access of ethyl lactate to the positive charge of atenolol would be restricted by the ring by one side and the propyl group by the opposite side when this bridge was formed. Desipramine clustered more than atenolol because the formation of the intramolecular bridge in desipramine was sterically hindered due to the position of one of the amine moieties between large aromatic rings. This steric hindrance to the formation of the bridge would cause desipramine to adopt an open structure, prone to more collisions and clustering, which explains the larger mobility change observed for this compound compared to atenolol with ethyl lactate in the buffer gas. A steric hindrance to the formation of the bridge, similar to that of desipramine, was observed in the diamine tryptophan, which also has an amine moiety as part of a ring, and its mobility also was affected by modifiers in the buffer gas.[36] Another reason for the higher mobility of atenolol with respect to desipramine would be its compact structure, which originates in the formation of the bridge; this small size would allow atenolol to experience less collisions with the buffer gas.

Evidence of the formation of intramolecular bridges in diamines was reported by Karpas in 1989. Karpas found that the mobilities of α,ω-diamines were higher than those of normal monoamines as a consequence of a cyclization reaction between the two amine moieties.[38] The bridge also would delocalize and stabilize the positive charge on atenolol, weakening ion-ligand interactions. This delocalization was used to illustrate why the mobility

values of tertiary amines (which positive charge is delocalized) changed less than those of primary amines (with a localized charge) when shifting from a low polarizability buffer gas such as helium to a high polarizability buffer gas such as air. Mobilities of tertiary amines changed less due to low clustering with air as a consequence of charge delocalization.[16] Also, ions with delocalized charges hydrate less than those with localized charges, [37] which may translate into a lower formation of clusters with the modifiers. Decreased clustering may be expected as size increase, due to delocalization of the positive charge.[16,37]

Additional evidences of the formation of intramolecular bridges in diamines were obtained studying basic amino acids. The mobilities of arginine, and histidine and lysine only decreased by 0.3 and 1.1%, respectively when 2-butanol concentration increased from 0.0 to 6.8 mmol m^{-3} ($2.5x10^2$ ppmv) in the buffer gas (Table 2). These changes in $\%\Delta K_0$ values of basic amino acids were small when compared to the average value of 10.2% for non-basic amino acids such as methionine, serine, tryptophan, and tyrosine in similar experimental conditions.[36] Also, the mobility of arginine only decreased by 2.7% with 0.95 mmol m^{-3} of nitrobenzene in the buffer gas, which was small compared to $\%\Delta K_0$ values of ethanolamine (37%) and valinol (21%) in the same conditions. Figure 6 shows the mass spectra of arginine, histidine, and lysine when 6.8 mmol m^{-3} ($2.5x10^2$ ppmv) of 2-butanol (2B) were introduced into the buffer gas. These basic amino acids produced large protonated peaks ($[His{\cdot}H]^+$ m/z 156, $[Lys{\cdot}H]^+$ 147, and $[Arg{\cdot}H]^+$ 175) and only small analyte-2-butanol cluster peaks ($[His{\cdot}2B{\cdot}H]^+$ at m/z 230, $[Lys{\cdot}2B{\cdot}H]^+$ at m/z 221, which was overlapped with the modifier trimer at m/z 223, and $[Arg{\cdot}2B{\cdot}H]^+$ at m/z 249). The limited mobility response of basic amino acids to the introduction of modifiers into the buffer gas may be related to this low clustering. Figure 6

compares the high clustering of phenylalanine (Phe) with the low clustering of basic amino acids with 2-butanol (2B) modifier in the mass spectrum. $[Phe{\cdot}2B{\cdot}H]^+$ and $[Phe{\cdot}2B_2{\cdot}H]^+$ clusters occurred at m/z 240 and 314. The lack of clustering of basic amino acids may be due to formation of an intramolecular bridge between the two amine functionalities. This intramolecular bridge would deter the attachment of modifier molecules to the positive charge of basic amino acids by steric hindrance and charge delocalization.

5. ***Separation of IMS overlapping compounds by selective clustering***

The influence of structure (steric hindrance and intramolecular bridges) and size in clustering makes it possible to predict the separation of overlapping compounds in IMS; two compounds overlapping in IMS would be separated if their structures are different in terms of size, steric hindrance, formation of intramolecular bridges, or other structural feature that may produce a difference in clustering. Figure 3 predicts the separation or increased resolution of mixtures of TMA-ethanolamine, 2,4-lutidine-valinol, 2,4-lutidine- serine, TEA-valinol, and TEA-serine using ethyl lactate modifier and TEA-valinol using nitrobenzene modifier. Figure 7 exemplifies the IMS separation of overlapping compounds by introducing 2-butanol into the buffer gas. Figure 7.1a shows the IMS spectra of a mixture of arginine (22.0 ms) and phenylalanine (22.5 ms), which partially overlap in N_2-only buffer gas. Figure 7.1b shows a drift time difference of 3,4 ms between arginine and phenylalanine when 6.8 mmol m^{-3} ($2.5x10^2$ ppmv) of 2-butanol were injected into the buffer gas, which was more than baseline resolution. Figure 6, illustrates the extensive clustering of phenylalanine, which slowed down its product ions, and the low clustering of arginine, causing the separation of the mixture.

Figure 7.2, demonstrates the IMS separation of a mixture of isoleucine and lysine with 2-butanol. Isoleucine and lysine overlapped at 18.8 ms in the IMS spectrum with N_2-only buffer gas. The inset demonstrates the separation of the mixture when 2-butanol concentration increased to 6.8 mmol m^{-3} in the buffer gas; the drift time of isoleucine increased by 1.2 ms but the drift time of lysine increased only by 0.2 ms, producing the separation of these two amino acids with a resolution of 1.4. The shift in drift time of isoleucine probably originated in the clustering allowed by the relatively small steric hindrance in its structure. The limited response of lysine has the same explanation as that for arginine given before: lysine clustered only slightly with 2-butanol (Figure 6c) due to the formation of the intramolecular bridge. The separation of these amino acids could not be obtained at 250 °C (data not shown), perhaps because the decreased isoleucine-2-butanol interactions at high temperature did not allow clustering of isoleucine.

CONCLUSIONS

Formation of ion-modifier clusters was found when liquid modifiers such as ethyl lactate, nitrobenzene, tetrahydrofuran-2-carbonitrile, and 2-butanol were vaporized into the buffer gas of an ion mobility spectrometer. Analytes clustered to different extents with a modifier depending on their size and structure. Intramolecular bridges caused limited clustering in diamines by hindering the attachment of modifier molecules to the positive charge of those analytes, for which diamines only experienced small changes in mobilities with modifiers. Steric hindrance caused by bulky substituents and large size also produced limited changes in mobility with modifiers in the buffer gas. This difference in clustering slowed down the ions with abundant clustering and only slightly affected the mobility of ions with limited clustering. This different clustering behavior was applied to separation of mixtures of compounds that overlapped in IMS by selectively changing their mobilities. Modifiers also produced different changes in mobilities: ethyl lactate had a larger effect than nitrobenzene or 2-butanol on ion mobilities due to larger formation of clusters. Finally, tetrahydrofuran-2-carbonitrile stripped off the charge of the analytes, except for those with steric hindrance that deterred clustering, for which it was considered to be inappropriate as a modifier for shifting drift times of ions. This selective charge stripping suggests a possible use of this modifier as a means to simplify spectra of complex mixtures of analytes.

ACKNOWLEDGEMENTS

This work was supported by NIH grant R33DK0702740351. The authors thank the WSU-GPWC for proofreading the manuscript.

REFERENCES

1. Karasek FW, Hill HH, Kim SH. *J. Chromatogr.* 1976; **117:** 327.

2. Asbury GR, Klasmeier J, Hill Jr. HH. *Talanta* 2000; **50**: 1291.

3. Borsdorf H, Nazarov EG, Miller RA. *Talanta* 2007; **71:** 1804.

4. Oxley JC, Smith JL, Kirschenbaum LJ, Marimganti S, Vadlamannati S. *J. Forensic Sci.* 2008; **53**: 3.

5. Jafari MT, Khayamian T, Shaer V, Zarei N. *Anal. Chim. Acta* 2007; **581:** 147.

6. Alizadeh N, Mohammadi A, Tabrizchi M. *J. Chrom. A,* 2008; **1183:** 21.

7. Strege MA, Kozerski J, Juarbe N, Mahoney P. *Anal. Chem*. 2008; **80**: 3040.

8. Dwivedi P, Bendiak B, Clowers BH, Hill Jr. HH. *J. Am. Soc. Mass Spectrom.* 2007; **18**: 1163.

9. Taraszka JA, Gao X, Valentine SJ, Sowell RA, Koeniger SL, Miller DF, Kaufman TC, Clemmer DE. *J. Proteome Res.* 2005; **4**: 1238.

10. Kaddis CS, Lomeli SH, Yin S, Berhane B, Apostol MI, Kickhoefer VA, Rome LH, Loo JA. *J. Am. Soc. Mass Spectrom.* 2007; **18**: 1206.

11. Dwivedi P, Wu P, Klopsch SJ, Puzon GJ, Xun L, Hill Jr. HH. *Metabolomics* 2008; **4**: 63.

12. Liu X, Valentine SJ, Plasencia MD, Trimpin S, Naylor S, Clemmer DE. *J. Am. Soc. Mass Spectrom.* 2007; **18**: 1249.

13. Isailovic D, Kurulugama RT, Plasencia MD, Stokes ST, Kyselova Z, Goldman R, Mechref Y, Novotny MV, Clemmer DE. *J. Proteome Res.* 2008; **7**: 1109.

14. O'Donnell RM, Sun X, Harrington PB. *Trends Anal. Chem*. 2008; **27**: 1.

15. Kanu AB, Dwivedi P, Tam M, Matz L, Hill Jr. HH. *J. Mass Spectrom.* 2008; **43**: 1.

16. Eiceman GA, Karpas Z. Ion Mobility Spectrometry. Taylor & Francis. Boca Raton, FL, USA, 2005.

17. Revercomb HE, Mason EA. *Anal. Chem.* 1975; **47**: 970.

18. Lattey RT. *Proc. Royal Soc. London (A)* 1910; **84**, 569: 173.

19. Lattey RT, Tizard HT. *Proc. Royal Soc. London (A)* 1912; **86**, 604: 349.

20. Gan H, Corino GT. *Anal. Chem.* 2000; **72**: 807.

21. Bollan HR, Stone JA, Brokenshire JL, Rodriguez JE, Eiceman GA. *J. Am. Soc. Mass Spectrom.* 2007; **18**: 940.

22. Dwivedi P, Wu C, Matz LM, Clowers BH, Siems WF, Hill HH. Jr. *Anal. Chem.* 2006; **78**: 8200.

23. Kim SH, Karasek FW, Rokushika S. *Anal. Chem.* 1978; **50**: 152.

24. Spangler GE, Carrico JP, Campbell DN. *J. Test Eval.* 1985; **13**: 234.

25. Proctor CJ, Todd JF. J. *Anal. Chem*. 1984; **56**: 1794.

26. Blyth DA. A vapor monitor for detection and contamination control. In *Proc. Int. Symp. Against Chem. Warfare Agents,* Stockholm 1983.

27. Eiceman GA, Wang YF, Garcia-Gonzalez L, Harden CS, Shoff DB. *Anal. Chim. Acta* 1995; **306**: 21.

28. Eiceman GA, Salazar MR, Rodriguez MR, Limero TF, Beck SW, Cross JH, Young R, James JT. *Anal. Chem.* 1993; **65**: 1696.

29. Meng Q, Karpas Z, Eiceman GA. *Int. J. Environ*. *Anal. Chem.* 1995; **61**: 81.

30. Puton J, Nousiainen M, Sillanpaa M. *Talanta* 2008; **76**: 978.

31. Fernandez-Maestre R, Hill HH. *Int. J. Ion Mobility Spectrom.* 2009 accepted for publication.

32. Hill HH. Jr, Simpson G. *J. Field Anal. Chem. Technol.* 1997; **1**: 119.

33. Wu C, Siems WF, Asbury GR, Hill HH. *Anal. Chem.* 1998; **70**: 4929.

34. Wittmer D, Chen YH, Luckenbill BK, Hill, HH. *Anal. Chem.* 1994; **66**: 2348–2355.

35. Eiceman GA, Nazarov EG, Stone JA. *Anal. Chim. Acta* 2003; **493**: 185.

36. Fernandez-Maestre R. Buffer Gas Modifiers in Ion Mobility Spectrometry. Ph.D. diss., Washington State University, Pullman, WA, 2009.

37. Sunner J, Ikonomou MG, Kebarle P. *Anal. Chem.* 1988; **60:** 1308.

38. Karpas Z. *Int. J. Mass Spectrom. Ion Proc.* 1989; **93**: 237.

Table 1. ESI-IMS operating conditions summary

Parameter	Settings
Reaction region length	7.5 cm
Drift region length	25.0 cm
ESI voltage	15.6 kV
Voltage at first ring	12.12 kV
ESI flow	3 µl min^{-1}
Voltage at the gate	10.80 ± 0.01 kV
Gate closure potential	±40 V
Gate pulse width	0.1 ms
Scan time	35 ms
Buffer gas	Nitrogen
Buffer gas temperature	150 ± 2 °C
Buffer gas flow	930 ml min^{-1}
Modifier flow rate	1 to 50 µl hr^{-1}

Table 2. Percentage decrease in K_0 values, $\%\Delta K_0$, for selected compounds when modifiers were introduced into the buffer gas. The concentrations of modifier increased in the buffer gas from 0 to 1.7, 0.95, and 6.8 mmol m^{-3} for ethyl lactate, nitrobenzene, and 2-butanol, respectively; for ethyl lactate clusters, ethyl lactate increased in the buffer gas from 0.33 (12 ppmv) to 2.8 mmol m^{-3}. Differences of less than 0.32 units in $\%\Delta K_0$ may arise from the maximum accepted standard deviation of drift time measurements (0.05 ms).

Compound	Ethyl lactate	Nitrobenzene	2-butanol
2,4-lutidine	24	13	
$[Lac_nH]^+$	6.4		
$[Lac_nH_3O]^+$	10		
$[Lac_nNa]^+$	4.3		
Arginine		2.7	0.3
Atenolol	7.0	2.0	0.7[a]
Desipramine	12		
DTBP	1.5	0.1	
Ethanolamine	41	37	
Histidine			1.1
Lysine			1.1
Serine	30		
TBA ions	0.3	0.1	
TEA ions	0.5	0.3	
TMA ions	1.0	1.0	
TPA ions	0.1	0.5	
Valinol	28	21	

[a] Average $\%\Delta K_0$ at 100, 150, 200, and 250°C.

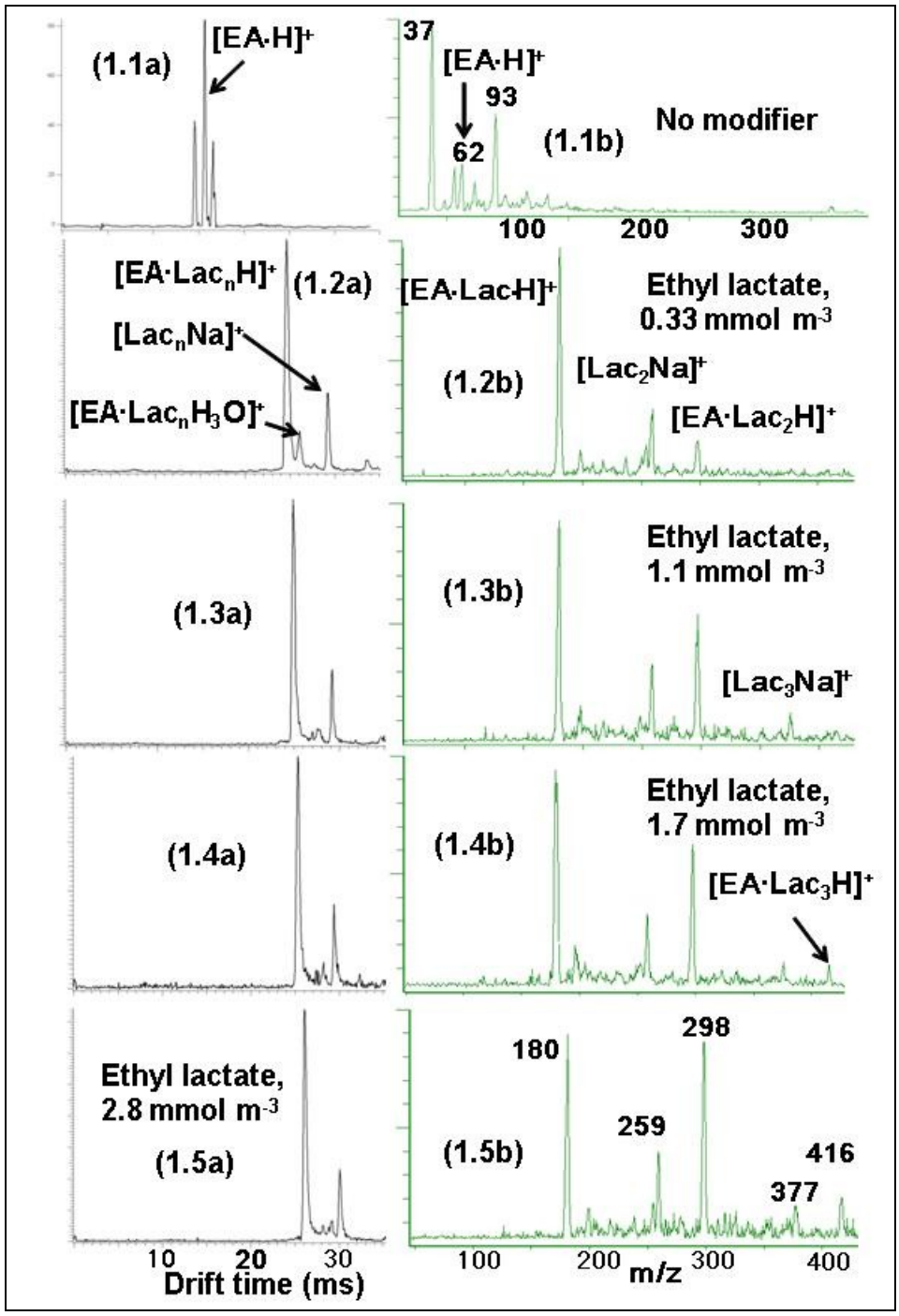
(1.1a)
[EA·H]+
37
[EA·H]+
93
62
(1.1b)
No modifier
100
200
300
[EA·Lac$_n$H]+
(1.2a)
[Lac$_n$Na]+
[EA·Lac$_n$H$_3$O]+
[EA·LacH]+
Ethyl lactate,
0.33 mmol m^{-3}
(1.2b)
[Lac$_2$Na]+
[EA·Lac$_2$H]+
(1.3a)
(1.3b)
Ethyl lactate,
1.1 mmol m^{-3}
[Lac$_3$Na]+
(1.4a)
(1.4b)
Ethyl lactate,
1.7 mmol m^{-3}
[EA·Lac$_3$H]+
Ethyl lactate,
2.8 mmol m^{-3}
(1.5a)
180
298
259
(1.5b)
416
377
10
20
30
Drift time (ms)
100
200
m/z
300
400

Figure 1. Reduction in mobility with ethyl lactate in the buffer gas. The IMS spectra (a) show that the mobility of ethanolamine decreased when the concentration of ethyl lactate increased in the buffer gas. This effect may be due to clustering analyte-modifier. Ethanolamine-ethyl lactate clusters are shown in the MS spectra (b) when ethyl lactate was introduced into the buffer gas. As a consequence of extensive clustering, protonated ethanolamine was not present in the mass spectra when ethyl lactate was injected into the buffer gas.

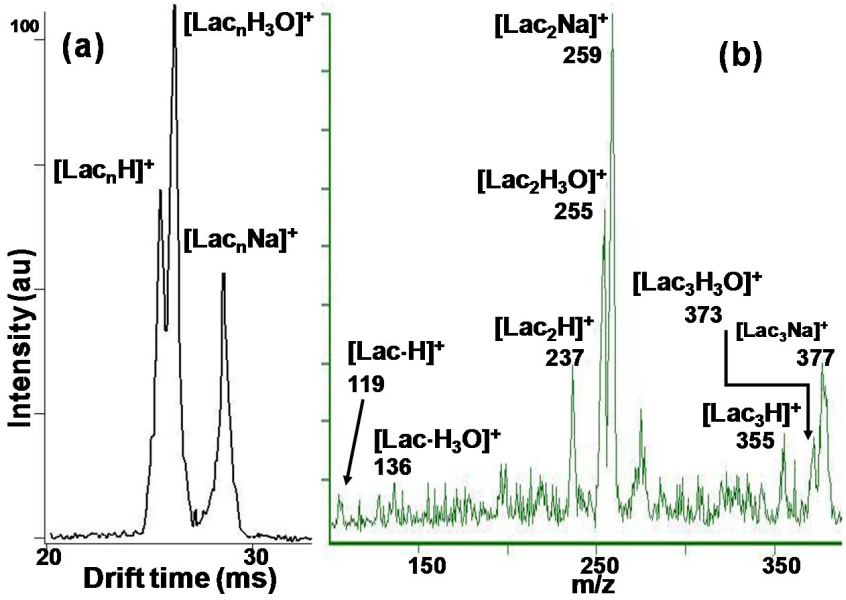

Figure 2. Ethyl lactate clustering with ESI solvent. (a) IMS and (b) mass spectrum of the ESI solvent when ethyl lactate (Lac) modifier was introduced into the buffer gas at a concentration of 1.1 mmol m^{-3} (42 ppmv). The ESI solvent produced extensive clustering due to the relatively small size and low proton affinity of reactant ions.

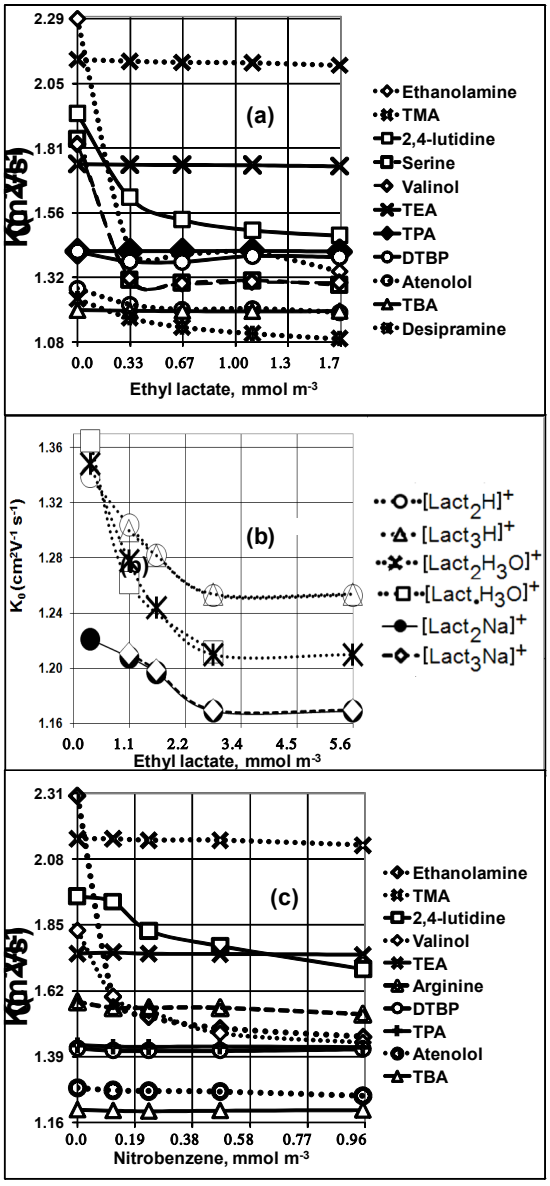

Figure 3. Changes in mobilities of selected compounds with modifiers in the buffer gas. (a) and (c) The mobilities of tetraalkylammonium ions and arginine did not change, and for DTBP and atenolol changed minimally with modifiers in the buffer gas due to steric hindrance, which impeded the attachment of modifier molecules to the positive charge of these ions. Analytes with lower steric hindrance such as 2,4-lutidine, desipramine, ethanolamine, serine, and valinol showed larger changes in mobility. (b) Changes in mobilities of ethyl lactate cluster ions with increasing concentrations of ethyl lactate. The mobilities of all cluster ions coincided within families: protonated, hydrated, and sodiated clusters had the same mobility.

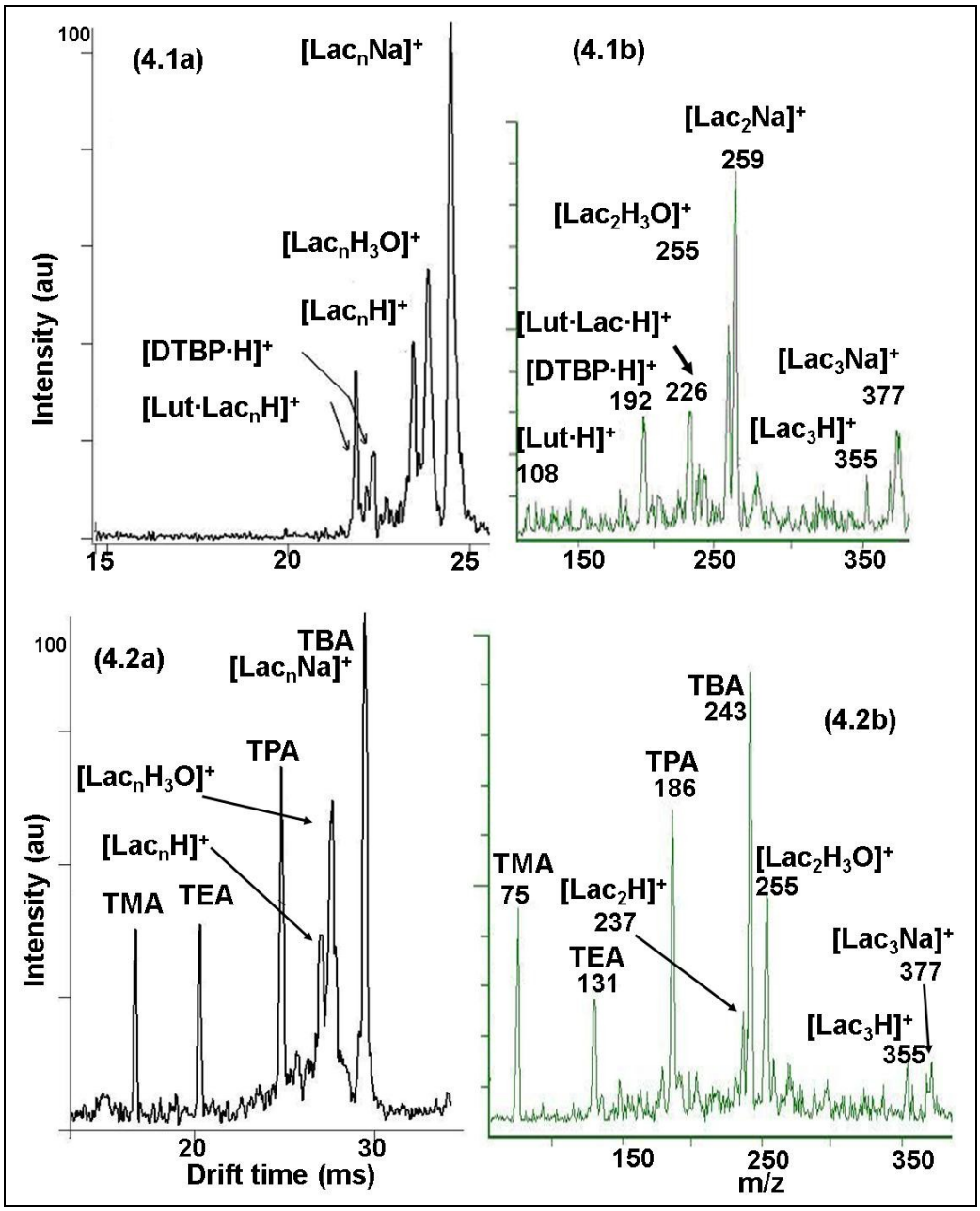

Figure 4. Clustering in DTBP, 2,4-lutidine, and tetraalkylammonium ions. (a) IMS and (b) mass spectra of 2,4-lutidine, DTBP, and tetraalkylammonium ions when 1.1 mmol m^{-3} (42 ppmv) of ethyl lactate (Lac) modifier were introduced into the buffer gas. (4.1a and 4.1b) 2,4-lutidine produced a large MS cluster peak with the modifier and a small protonated peak; In contrast, DTBP did not show clustering with ethyl lactate in the mass spectrum; these features agree with the fact that the mobility of 2,4-lutidine was more affected by the modifier than that of DTBP and results from a previous work with 2-butanol.[36] (4.2a and 4.2b)

Tetraalkylammonium ions did not cluster due to steric hindrance; TBA ions and $[Lac_nNa]^+$ overlapped in the IMS spectrum.

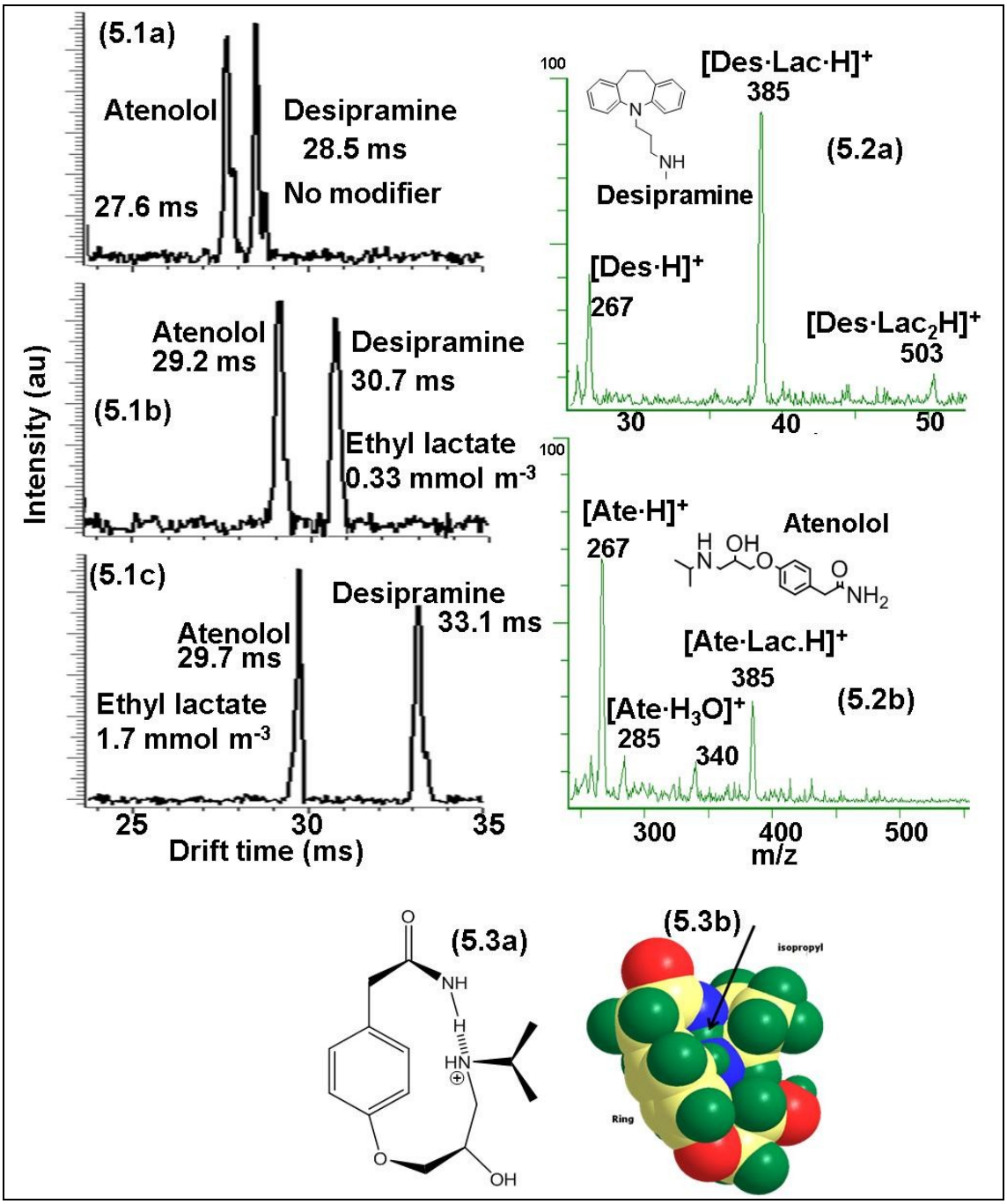

Figure 5. Clustering of desipramine and atenolol and intramolecular bridges. The drift time separation between desipramine and atenolol increased when ethyl lactate modifier was increased from 0 (5.1a), to 0.33 (5.1b), and 1.7 mmol m^{-3} (5.1c). (5.2) MS spectra of desipramine (Des) and atenolol (Ate) at 150 °C when 0.6 mmol m^{-3} of ethyl lactate (Lac) were introduced into the buffer gas. Schematics (5.3a) and 3D model (5.3b) of the formation of the bridge: the arrow signals the hydrogen bridge.

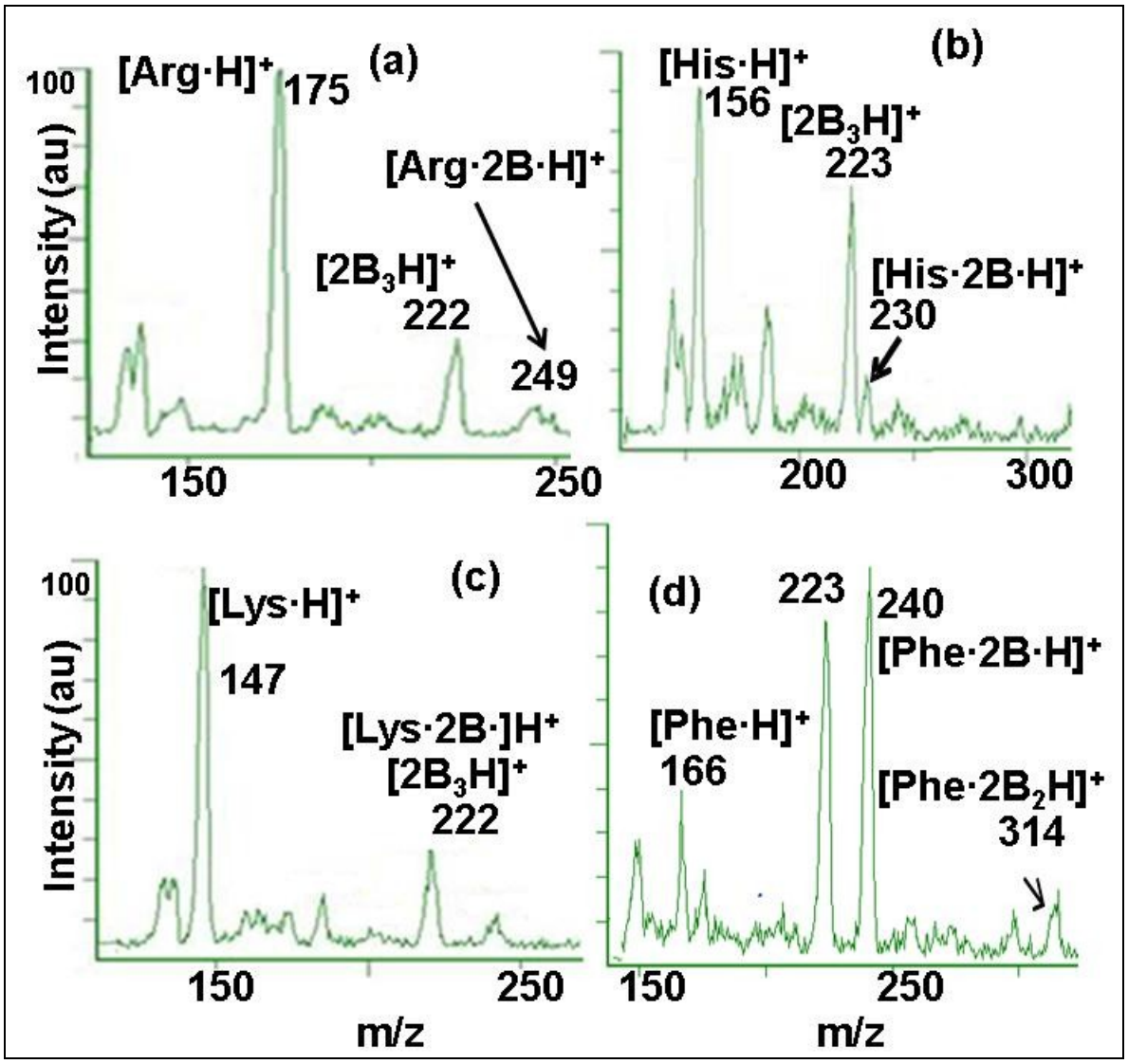

Figure 6. Low clustering in basic amino acids. (a) Mass spectra of arginine, (b) histidine, and (c) lysine with 6.8 mmol m^{-3} ($2.5x10^2$ ppmv) of 2-butanol (2B) in the buffer gas. Basic amino acids showed large protonated MS peaks ($[Arg·H]^+$ m/z 175, $[His·H]^+$ m/z 156, and $[Lys·H]^+$ m/z 147) and only small analyte-modifier peaks ($[His·2B·H]^+$ m/z 230, $[Lys·2B·H]^+$ m/z 221, which was overlapped with the modifier trimer at m/z 223, and $[Arg·2B·H]^+$ m/z 249) due to steric hindrance produced by an intramolecular bridge. (d) Mass spectrum of a 100-µM solution of phenylalanine (Phe) at the same 2-butanol concentration as in (a) to (c); cluster peaks of 2-butanol were evident at m/z 149 (dimer), 223 (trimer), and 297 (tetramer), and the clusters of phenylalanine with 2-butanol occurred at m/z 240 and 314.

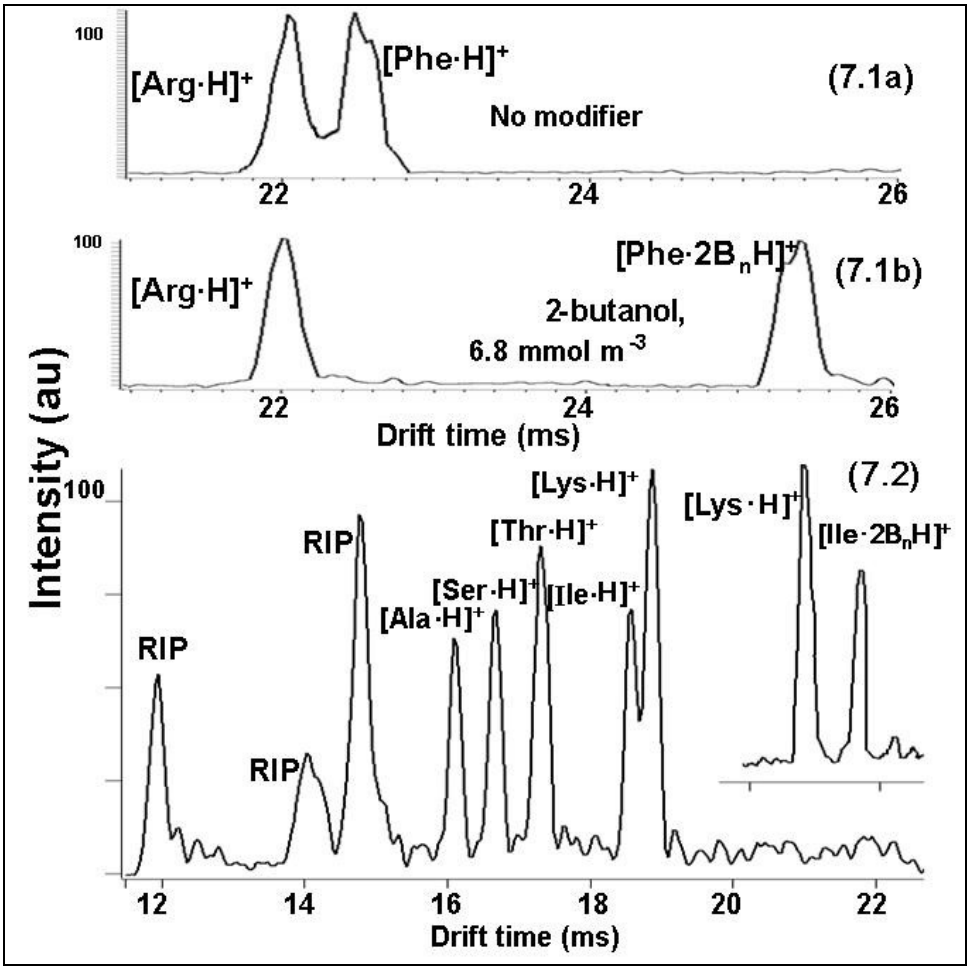

Figure 7. IMS separations by introducing 2-butanol into the buffer gas. (a) IMS spectra (1600 averages) of a 100-μM mixture of arginine (Arg) and phenylalanine (Phe) in N_2-only buffer gas and (b) when 6.8 mmol m^{-3} of 2-butanol (2B) were injected into the buffer gas. (c) IMS spectra, (1600 averages) of a 50-μM mixture of alanine (Ala), serine (Ser), threonine (Thr), isoleucine (Ile), and lysine (Lys) in N_2-only buffer gas. The inset demonstrates the separation of a mixture of lysine and isoleucine with 6.8 mmol m^{-3} of 2-butanol (2B) in the buffer gas. 2-butanol made possible the baseline resolution of these two pairs of compounds by forming $[Ile{\cdot}2B{\cdot}H]^+$ and $[Phe{\cdot}2B{\cdot}H]^+$ clusters (showed in Figure 6d for Phe), which reduced the mobilities of Ile and Phe. The steric hindrance in arginine and lysine, caused by an intramolecular bridge, deterred an extensive formation of clusters, and these amino acids' mobilities were not affected by the modifier.

Chapter Four

Chemical Standards in Ion Mobility Spectrometry

Roberto Fernández-Maestre,[1,7] Charles S. Harden,[2] Robert Ewing,[3] Christina L. Crawford,[1] and Herbert H. Hill Jr.[1,8]

[1]*Department of Chemistry, Washington State University, Pullman, WA 99164-4630, USA*

[2] *SAIC/US Army, Edgewood Chemical Biological Center Operations P.O. Box 68 Gunpowder, MD 21010-0068, USA*

[3]*Pacific Northwest National Laboratory, Richland, WA 99354, USA*

Submitted to

ANALYTICAL CHEMISTRY

May, 2009

[7] Permanent address: Programa de Quimica, Campus de Zaragocilla, Universidad de Cartagena, Cartagena, Colombia

[8] To whom correspondence should be addressed. E-mail: hhhill@wsu.edu. Fax: 509-335-8867

ABSTRACT

In ion mobility spectrometry (IMS), reduced mobility values (K0) are used as a qualitative measure of gas phase ions, and are reported in the literature as absolute values. Unfortunately, these values do not always match those collected in the field. One reason for this discrepancy is that the buffer gas may be contaminated with moisture or other volatile compounds. In this study, the effect of moisture and organic contaminants in the buffer gas on the mobility of IMS standards and analytes was investigated for the first time using IMS directly coupled to mass spectrometry. 2,4-dimethylpyridine, 2,6-di-tert-butyl pyridine (DTBP), and tetrabutylammonium, tetrapropylammonium, tetraethylammonium, and tetramethylammonium chlorides were used as chemical standards. In general, the mobility of IMS standard product ions was not affected by small amounts of contamination while the mobilities of many analytes were affected. In the presence of contaminants in the buffer gas, the mobility of analyte ions is often decreased by forming ion-molecule clusters with the contaminant. To ensure the measurement of accurate reduced mobility values, two IMS standards are required: an instrument and a mobility standard. An instrument standard is not affected by contaminants in the buffer gas, and provides an accurate measurement of the instrumental parameters, such as voltage, drift length, pressure, and temperature. The mobility standard behaves like an analyte ion in that the compound's mobility is affected by low levels of contamination in the buffer gas. Prudent use of both of these standards can lead to improved measurement of reduced mobility values.

INTRODUCTION

Ion mobility spectrometry (IMS) is an analytical technique that separates gas-phase ions according to their size to charge ratios, and is used in a growing number of applications. Initially developed in the 1970s as an inexpensive method for quantifying trace organic compounds and for estimating their mass,[1] IMS has grown into the analytical method of choice for the detection of chemical warfare agents,[2] toxic industrial chemicals,[3] drugs of abuse,[4-6] and explosives.[6-7] Ion mobility spectrometers have been coupled to mass spectrometers, and employed for separation and detection of biomolecules such as proteins,[8] peptides,[9-10] carbohydrates,[11] and lipids.[12] When coupled to mass spectrometry, ion mobility spectrometry offers value-added information of size, shape, and charge number.[13] When mass spectra are spread out along the mobility axis, noise reduction, isomer separation, and charge identification are possible.[14] In addition, mobility-mass correlation curves aid in class identification of unknowns.[15,16] For all these applications, it is critical that the ion mobilities measured are accurately and reproducibly reported.

Ion mobility spectrometry differs from mass spectrometry in that the separation of gas phase ions occurs by interaction of the ions with a buffer gas in an electric field. While there are several types of ion mobility spectrometers, the traditional drift time instrument measures the velocity of an ion in a buffer gas under the influence of a homogeneous electric field. Under ideal conditions, the velocity of these ions is proportional to the electric field strength and dependent on the ion's identity. The proportionality constant between ions' velocity and electric field strength, known as the ion mobility constant (K), becomes a qualitative measure of the ion:

$$K = \frac{v}{E} = \frac{L^2}{V.t_d} \quad (1)$$

where v is the velocity of the ion in cm s^{-1}, E the electric field in the drift region in V cm^{-1}, L the length of the drift region in cm, V the total voltage drop in volts across the drift region, and t_d the time the ion spends traveling the distance L in seconds. As early as 1892, Ernest Rutherford measured the mobility of ions formed by x-ray ionization,[17] and characterized the ions using ion mobilities.[18] Because the velocity of the ion varies with both temperature and pressure, measured mobility constants are commonly corrected to standard temperature and pressure to produce a reduced mobility constant (K_0):

$$K_0 = K\frac{P}{760}\frac{273}{T} = \frac{L^2}{V.t_d}\frac{P}{760}\frac{273}{T} \quad (2)$$

where P is the pressure in the drift region in Torr and T is the buffer gas temperature in Kelvin. [19] In 1928, Dusault and Loeb expressed the necessity of using chemical standards to calibrate the mobility values obtained in their laboratory.[20]

In theory, K_0 values are constant for a given compound in a given buffer gas, and are a qualitative indicator of the ion's identity. The primary advantage of K_0 values in IMS is that they are fundamentally related to the ion collision cross sections through the Mason Schamp Equation and to the ion's diffusion coefficient through the Einstein relation.[21] A compilation of reduced mobility values for a variety of gas phase ions was published in 1986.[22] In general, published K_0 values are considered to match one another if their uncertainties are within 2% (~0.02 $cm^2V^{-1}s^{-1}$).

In practice, however, K_0 values do not always match those reported in the literature. These variations are generally attributed to instrumental parameters, such as inhomogeneities in temperature and electric field, which are often not well characterized. In 1931, Loeb started using the term reduced mobility constant and proposed air ions as a calibration gas.[23] To calibrate instrumental parameters, Karpas suggested the use of chemical standards to correct reduced mobility values. He specifically suggested 2,4-lutidine, with a known and well characterized K_0 value of 1.95 $cm^2V^{-1}s^{-1}$, because it has a high proton affinity and produced a single peak at his experimental conditions.[24] Viidanoja et al. defined an ideal chemical standard for ESI-IMS as "a compound that produces only a single ion mobility peak, and for which the IMS spectrum and drift behavior are insensitive to solvent composition and gaseous impurities within the ion source and the drift tube".[25] Using an accepted standard, reduced mobility values can be calculated from measured mobility values by the following relation:[26]

$$\frac{K_{o\,(\text{unknown})}}{K_{o\,(\text{standard})}} = \frac{t_{d\,(\text{standard})}}{t_{d\,(\text{unknown})}} \qquad (3)$$

Berant and Karpas corrected uncertainties in the measurement of electric field strength, temperature, and pressure in IMS experiments using this method.[27] Rearden et al. used the proton-bound dimer peak of 2,4-lutidine as an external standard to calibrate the reduced mobility scale[28] because the K_0 value (1.43 $cm^2V^{-1}s^{-1}$) has been reported to be unaffected by humidity at the temperatures used in the study.[26]

Protonated dimethyl methylphosphonate $(DMMP)H^+$ and proton-bound dimer $(DMMP)_2H^+$ were investigated as chemical standards for IMS, but changes in mobility were found between -13 to 207 °C for these compounds.[29] Tabrizchi proposed the reactant ion as an

internal standard for IMS.[30] However, Eiceman et al. considered that to use the reactant ion as an internal standard was not acceptable.[26] Reactant ions are often ion clusters and their mobility values change as a function of temperature and moisture. Eiceman et al. also considered 2,4-lutidine·H^+ and (DMMP)H^+ unsuitable as chemical standards for IMS due to significant changes in their reduced mobilities between ambient temperature and 250 °C. They showed that the reduced mobilities of the proton-bound dimer of 2,4-lutidine (2,4-DMP)$_2H^+$ and (DMMP)$_2H^+$ were almost unchanged between ambient temperature and 250 °C. These proton-bound dimers, however, were not considered good standards because high concentrations of 2,4-lutidine and DMMP were required to see the dimers. The presence of high concentrations of these high-proton-affinity compounds would be detrimental to the observation of other analytes.[26] In 2006, Ewing et al. found that the reduced mobilities of (DMMP)$_2H^+$ were stable from 290 to 490 K at concentrations of 6.0, 5.0x10^2, and 2.0x10^3 ppmv of water; they also observed the reduced mobilities of (DMMP)H^+, 2,4-lutidine, and $(H_2O)_nH^+$ to increase with temperature, which they attributed to loss of water of hydration.[31]

Di tert-butyl pyridine (DTBP) was first used as a chemical standard for IMS in 2002 by Eiceman et al.[32] In 2003, they recommended the use of this compound as a chemical standard because its mobility was independent of buffer gas temperature and moisture in the buffer gas.[26] Pedersen et al. used DTBP as an internal standard to minimize the influence of temperature, pressure, and electrical field in the characterization of proton-bound acetate dimers.[33] DTBP also has been used to correct mobilities in IMS[34] and to demonstrate the performance of ion mobility spectrometers coupled to mass spectrometers.[35,36]

In 2005, Viidanoja et al. proposed tetraalkylammonium ions as chemical standards. These compounds are inherently ionic, which guarantees no charge competition, and are detected with high sensitivity in ESI-IMS. Tetraalkylammonium ions produce only a single ion mobility peak and have a low clustering tendency, which makes them insensitive to contaminants in the buffer gas. However, their reduced mobilities are not well established.[25] Jafari used tetrabutylammonium bromide as an external standard to test the performance of a new mobility spectrometer design.[37]

In the early 20th century, it was noted that K_0 values were influenced by parameters other than pressure and temperature. These were most notably contaminants in the buffer gas. In 1910, at the suggestion of J.S. Townsend, Lattey investigated the effects of moisture on the mobility of ions.[38] Lattey also reported the influence of other contaminants, such as traces of air and carbon dioxide.[39] Erikson also found in 1927 that adding CO_2 and water vapor to the buffer gas (air) decreased the mobility of ions but adding hydrogen increased it.[40] Eiceman et al. reported that the drift time of the reactant ions peaks (RIPs) in IMS increased ~4% with the increase of moisture from 0 to 2030 ppm,[41] and Ewing et al. found reductions in mobilities of 12% and 7.3% for $(DMMP)H^+$ and 2,4-lutidine, respectively, when increasing water content from 6 ppmv to $2.0x10^3$ ppmv in the mobility spectrometer. Similar effects of moisture on the mobility of ions have been reported.[42-45.]

Although standards are becoming generally accepted and useful in IMS, little work has been conducted on the influence of contaminants in the buffer gas on the mobilities of these chemical standards for IMS. In this work, the mobility behavior of chemical standards was analyzed when contaminants, such as moisture, solvents from electrospray ionization, volatiles

from out gassing of instrumental components, or trace organics were introduced into the buffer gas.

EXPERIMENTAL SECTION

Instrument. An electrospray ionization atmospheric-pressure ion mobility spectrometer (ESI-APIMS) interfaced through a 40-μm pinhole to a quadrupole mass spectrometer (Figure 1) was used in this work. Typical operating parameters used with this instrument are shown in Table 1.

The IMS instrument was built at Washington State University, and consisted of a drift tube and an electrospray ionization source. The drift tube consisted of two sections: a desolvation and a drift region separated by a Bradbury-Nielsen ion gate. The ion gate comprised 80 parallel 75-μm Alloy-46 stainless steel wires (California Fine Wire Co., Grove Beach, CA) 0.6 mm apart. Ions were gated into the drift region with a 0.1 ms pulse. When the gate was closed, ions were stopped from passing into the drift region by applying a closure potential that was 40 V higher for one set of wires (positive wires) and 40 V lower for the other set (negative wires) than the drift voltage in the position of the gate. Positive and negative wires were alternated in the gate. Both desolvation and drift regions had stainless steel rings, alternating with ceramic insulating rings, connected in series by high temperature resistors (Caddock Electronics Inc., Riverside, CA, ±1%). A fixed electric field that ranged from 200-500 V cm^{-1} was formed in the drift tube when an electrical potential was applied to the first ring.[46] An ESI target screen was made out of 2-mm stainless steel mesh with a 0.5-cm round orifice in the center. The target screen was located in the first ring of the drift tube. Preheated

N_2 buffer gas was introduced through a stainless-steel tube at the low voltage end of the drift tube at a flow rate of 0.9 L/min countercurrent to ion motion to aide in the desolvation of the ions. The buffer gas was heated by passing it through a 2-m long stainless-steel tube coiled inside a heated aluminum block (Figure 1). The mobility spectrometer was operated at ambient pressure (680-710 Torr in Pullman, WA).

The mass spectrometer was an ABB Extrel (Pittsburgh, PA) 150-QC quadrupole (m/z 0-4000). A Keithley model 427 amplifier (Keithley Instruments, Cleveland, OH) amplified the electron multiplier detector signal of the mass spectrometer and sent it to the data acquisition systems. Merlin software (ABB Extrel, Pittsburgh, PA) controlled the mass spectrometer and collected the mass spectral data. Custom LabView software (National Instruments, Austin, TX) was used to collect the IMS data and controlled the ion gate. The electronics for controlling the gate and IMS data acquisition were built at WSU.[47]

Spectra in ion mobility spectrometers coupled to quadrupole mass spectrometers can be acquired in single ion monitoring IMS (SIM-IMS), radiofrequency-only IMS (IMS), and mass spectrometry modes. In SIM-IMS mode, the mass spectrometer voltages are set so that only ions of a given mass to charge ratio or a range of ions are detected. These settings avoid the interference of other ions when analyzing a specific compound. In SIM-IMS mode, the mobility spectra of a specific ion or ions are collected. In IMS mode, ions are pulsed into the drift region and introduced into the mass spectrometer, where they are all detected without scanning; the mobility spectrum of all ions is collected in this mode. In mass spectrometry mode, all ions are detected by the mass spectrometer, and the mobility spectrometer is used as a desolvation region with the gates always open.

Materials and reagents. Methionine, phenylalanine, serine, threonine, tyrosine, tryptophan, ethanolamine, tribenzylamine, tributylamine, valinol, 2,4-dimethylpyridine (2,4-lutidine), 2,6-di-tert-butyl pyridine (DTBP), methyl 2-chloropropionate (MCP), and α-trifluoromethyl benzyl alcohol (tFMBA), and tetrabutylammonium (TBA), tetrapropylammonium (TPA), tetraethylammonium (TEA), and tetramethylammonium (TMA) chlorides were ACS reagent grade (≥98% purity), and were purchased from Sigma Aldrich Chemical Co. (Milwaukee, WI). Amino acids were selected as analytes to provide a series of compounds with different molecular weights and steric effects. Ethanolamine, tribenzylamine, and tributylamine, selected as analytes, also provided compounds with steric effects different to those of amino acids. The chemical standards selected are the most often used in IMS.[25,26] Additionally, tetraalkylammonium ions were selected as chemical standards because they are ionic compounds, and no charge competition was expected in ESI-IMS, which guaranteed a high sensitivity for these standards. Water was selected as a buffer gas contaminant because it is the most common buffer gas impurity in IMS. MCP and tFMBA, an ester and an alcohol, were selected as buffer gas contaminants to mimic contamination with organic compounds.

Contaminant introduction. Test contaminants were continuously pumped through a 10-cm-long, 50-μm ID silica capillary (Polymicro Technologies, Phoenix, AZ) in the liquid state and introduced into the buffer gas line using a Swagelok T-junction. Gas tight syringes (Hamilton, Reno, NV) were used to ensure no leaking of contaminants during injection. The temperature of the junction was increased to 150 °C using a heating tape (OMEGA Engineering, Stamford, CT) to help vaporize the contaminant. To verify that the nominal amount of water contaminant injected was effectively introduced, the water content in the

buffer gas was measured with a GE Moisture Image Series 1 instrument (Billerica, MA). Eiceman et al. studied the effect of moisture on the reduced mobilities of dimethyl methylphosphonate, 2,4-lutidine, DTBP, and the reactant ions. They found no significant effects on the mobilities of these ions by increasing the moisture content up to 161 μmol m^{-3} (2.9 mg m^{-3}).[26] In our investigation, experiments were performed at higher concentrations of water, up to $8.8x10^2$ mmol m^{-3} ($3.3x10^4$ ppmv). Other contaminants were run from the smallest flow rate that produced a measurable change in K_0 to a flow rate where a plateau was found in K_0 values.

Sample preparation and introduction. 50 μM standard solutions of the analytes were prepared in ESI solution (47.5 % methanol: 47.5 % water: 5 % acetic acid). Electrospray ionization (ESI) was used to inject 3 μl min^{-1} of liquid samples or solvent (ESI solution) using 250-μl syringes into 40-cm long, 100-μm ID capillaries. Stainless steel unions (Valco, Houston, TX) connected these capillaries to 50-μm ID capillaries. The ends of these capillaries were placed in the center of the target screen at the entrance of the mobility spectrometer. The stainless steel unions received a high voltage of 15.6 kV, with a 3.5 kV bias with respect to the target screen in the first ring, to produce positive ions.

Calibration. Calibration of the mobility spectrometer was obtained applying Equation 3 and using DTBP and tetraalkylammonium ions as chemical standards. These chemical standards allowed the calculation of reduced mobilities without introducing errors acquired when measuring instrumental parameters such as temperature, drift tube length, pressure, and drift field.

Identification of analytes. Analytes were identified by comparing the molecular weight of their protonated molecules or clusters with their m/z signal produced in the mass spectrometer. Also, reduced mobilities of protonated analyte ions were compared with those from literature.

RESULTS AND DISCUSSIONS

1. *Effect of moisture contamination in the drift region on the ion mobility of analytes*

The mobility spectra in Figure 2a illustrates how the mobility of valinol response ions was affected when water was introduced into the buffer gas of the ion mobility spectrometer. The drift time for valinol increased greater than 1 ms as moisture increased in the buffer gas from 0.03 mmol m^{-3} (10 ppmv, the average water concentration in nitrogen buffer gas in "N_2-only" conditions) to $8.8x10^2$ mmol m^{-3}. This drift time increase corresponded to a reduction in mobility of 7.1% (Table 2). The reduction in mobility with moisture was due to formation of large analyte-water clusters, as demonstrated in the mass spectrum of valinol (Figure 3) obtained under conditions used in Figure 2a. Figure 3 shows clusters of protonated valinol with one to eleven water molecules occurring at m/z 122, 140, 158, 176, 194, 212, 230, 248, 266, 284, and 302.

The mobilities of other analytes also decreased with moisture in the buffer gas; serine, tributylamine, and tribenzylamine exhibited percentage reductions in mobility ($\%\Delta K_0$) of 7.9%, 2%, and 1 %, respectively, as moisture increased in the buffer gas from 0.03 mmol m^{-3} to $8.8x10^2$ mmol m^{-3}. $\%\Delta K_0$ is defined as the percentage difference between K_0 in N_2-only buffer gas and K_0 when a contaminant is introduced into the buffer gas at a given concentration. In

general, $\%\Delta K_0$ values decreased with molecular weight of the ion when water was introduced into the buffer gas; for serine, valinol, tributylamine, and tribenzylamine, this relation was linear with a correlation coefficient of -0.92. This trend may be due to the small effect on ion size when a water molecule clusters to large ions. Table 2 summarizes the percentage reduction in mobilities ($\%\Delta K_0$) for the test compounds when contaminants were introduced into the buffer gas.

The decrease in mobility of all ions with water concentration in the buffer gas agreed with earlier reports that moisture in the buffer gas decreased ion mobility.[38-45] In those works, ions in dry air were faster than those in moist air. In other studies by Eiceman et al., moisture was not found to produce significant effects on the mobility of dimethyl methylphosphonate, 2,4-lutidine, DTBP, and reactant ions.[26] However, Eiceman et al. only explored concentrations of water up to 0.16 mmol m^{-3}, well below the levels investigated in this study.

2. Effect of organic contamination in the drift region on the ion mobility of analytes

To simulate organic contamination of the buffer gas, a volatile alcohol and an organic ester were selected: α-trifluoromethyl benzyl alcohol (tFMBA) and methyl 2-chloropropionate (MCP).

a. Effect of tFMBA contamination in the drift region on the ion mobility of analytes

Figure 2b shows that as the concentration of tFMBA increased in the buffer gas from 0 to 2.3 mmol m^{-3} (86 ppmv) at 150°C the drift time of serine response ions increased 2.3 ms (11.7%). This mobility decrease as tFMBA was introduced into the buffer gas was due to formation of large analyte-tFMBA clusters as demonstrated in the mobility and mass spectra

data of Figure 4 obtained under conditions used in Figure 2b. In Figure 4a, protonated molecules of serine and serine-tFMBA clusters appeared as a single and broad peak at 21.8 ms in the mobility spectrum, indicating fast equilibria between these species.[25] Figure 4b displays serine clusters with one and two molecules of tFMBA in the mass spectrum occurring at m/z 282 and 457.

The mobilities of other analytes also decreased when tFMBA was introduced into the buffer gas; valinol, threonine, methionine, phenylalanine, tyrosine, and tryptophan showed $\%\Delta K_0$ values of 5.1%, 8.6%, 4.6%, 7.3%, 7.0%, and 4.0%, respectively, as tFMBA concentration increased in the buffer gas from 0 mmol m^{-3} to 2.3 mmol m^{-3} (Table 2). $\%\Delta K_0$ values decreased with molecular weight of the ion; for these amino acids and valinol, this relation was linear with a correlation coefficient of -0.52.

b. Effect of methyl 2-chloropropionate contamination in the drift region on the ion mobility of analytes

When the concentration of an organic ester, methyl 2-chloropropionate (MCP), was increased in the buffer gas from 0.00 to 0.93 mmol m^{-3} (35 ppmv), the test compounds showed the following $\%\Delta K_0$ values: valinol (31%) and ethanolamine (36%) (Table 2). The mobilities of both test compounds decreased with MCP concentration in the buffer gas.

In general, all analytes investigated experienced a decrease in mobilities when organic contamination was introduced into the buffer gas. These results agreed with earlier reports that organic molecules in the buffer gas decreased the mobility of ions.[48-51.] Nevertheless, effects of

water on ion mobility were lower than the effects of organic contaminants perhaps due to the small size of water clusters.

As discussed in the introduction, 2,4-lutidine, DTBP, and tetraalkylammonium salts have been recommended as chemical standards for IMS.[25,26] These compounds were investigated with respect to the effects that contamination of the buffer gas with water or organic compounds have on ion mobility.

3. ***Effect of moisture contamination in the drift region and ion mobility of chemical standards***

In general, the mobility of chemical standards did not significantly change as a function of water concentration in the buffer gas. When water concentration was increased in the buffer gas from 0.03 mmol m^{-3} to 2.3 mmol m^{-3}, no change in mobility was observed. However, when water concentration was increased to $8.8x10^2$ mmol m^{-3} (at 150°C), changes in mobilities were observed as follows: 2,4-lutidine (3.8%), TMA ions (4.0%), TEA ions (2.9%), DTBP (2.1%), TPA ions (1.8%), and TBA ions (0.9%). The reduction in mobility of DTBP was smaller than that of 2,4-lutidine. This difference in mobility may be due to the larger size of DTBP and the steric hindrance caused by the large t-butyl substituents on DTBP, located at positions 2 and 6 on the ring, shielding the protonated pyridine nitrogen from clustering. The two smaller methyl groups of 2,4-lutidine, which were located at positions 2 and 4 on the ring, shielded the protonated nitrogen less effectively from interacting with moisture. This interaction with water molecules produced clusters of 2,4-lutidine with water. Again, as demonstrated with analytes, $\%\Delta K_0$ values decreased with molecular weight of the chemical standards; for chemical standards, this relation was linear with a correlation coefficient of -0.98.

4. ***Effect of organic contamination in the drift region on the ion mobility of chemical standards***

A. ***Effect of tFMBA contamination on the ion mobility of chemical standards***

When tFMBA concentration in the buffer gas was increased from 0.0 to 2.3 mmol m^{-3} at 150°C, the mobility of 2,4-lutidine decreased by 0.9% and that of DTBP by 1.3%; the mobility tetraalkylammonium ions did not change.

b. Effect of MCP contamination on the ion mobility of chemical standards

The mobility of the chemical standards decreased as MCP concentration was increased in the buffer gas from 0.00 to 0.93 mmol m^{-3} at 150°C as follows: 2,4-lutidine (19%), DTBP (0.9%), TMA (0.4%), TEA (0.1%), TPA (0.1%), TBA (0.1%). The reduction in mobility of DTBP was lower than that of 2,4-lutidine due to steric hindrance

Mobility and mass spectra were studied to understand the stability of tetraalkylammonium ions' mobility values in the presence of contaminants in the buffer gas. In IMS mode, single peaks were detected for each tetraalkylammonium ion with all contaminants; single peaks indicated that no fragments, adducts, or clusters of tetraalkylammonium ions occurred at the temperatures and concentrations of contaminants used, or, at least, they decomposed in the desolvation region.[25] Figure 4c shows single peaks in the IMS spectrum of tetraalkylammonium ions when $8.8x10^{2}$ mmol m^{-3} of water were introduced into the buffer gas. Mobility and mass spectra also produced single, defined peaks for each tetraalkylammonium ion when MCP and tFMBA contaminants were introduced into the buffer gas; only small cluster peaks were seen at nominal masses 149, 204, and 262 Da for TEA, TPA, and TBA ions, respectively, when high

concentrations of water contaminant ($8.8x10^2$ mmol m^{-3}) were introduced into the buffer gas (Figure 4d); a small peak for the TMA ion-water cluster may be indistinguishable from the peak at m/z 91 , $(H_2O)_5H^+$. The formation of clusters was expected for tetraalkylammonium ions due to the permanent positive charge situated at the quaternary nitrogen atom; however, the steric hindrance exerted by the four alkyl chains enclosing the nitrogen[25] kept contaminant molecules away, which hindered the formation of ion-ligand bonding.

Similarly, when other compounds, such as DTBP, were not affected by a particular contaminant, they did not cluster with that contaminant; when they were affected, analyte-contaminant clusters appeared in the mass spectra (Figures 4a and 4b) in a number and intensity proportional to the extent of change in K_0. Also, when ion mobilities were affected by introduction of buffer gas contaminants, protonated ions disappeared or their intensity decreased. The mass spectra of methionine in Figure 5 illustrates this point; this figure shows that the ratio of the intensities of methionine-tFMBA peak to methionine protonated peak ($Met.tFMBA.H^+$:$Met.H^+$) increased when tFMBA concentration in the buffer gas increased. These ratios were 0.00, 0.15, and 0.33 at tFMBA concentrations of 0.0, 1.1, and 1.7 mmol m^{-3}, respectively, demonstrating increasing clustering with tFMBA concentration.

Figure 6 plots K_0 values for test chemical standards and analytes as a function of contaminant concentration in the buffer gas. In general, when moisture contaminated the buffer gas at low concentrations, similar to those used for organic contaminants, the mobility of analyte ions did not shift significantly; however, at high moisture concentrations some mobility shifts were observed. For the standards, only 2,4-lutidine exhibited a significant mobility shift as a function of organic contamination. In the presence of water, none of the standards

exhibited a significant change in mobility until high concentrations of water were introduced into the buffer gas.

5. ***Mobility standards and instrument standards***

As demonstrated above, mobility calculations using chemical standards may produce inaccurate values when the buffer gas is contaminated with water or an organic compound. The mobility of either the standard or the analyte may shift as a function of buffer gas contamination. For example, if the chemical standard 2,4-lutidine is used to calculate the mobility of ethanolamine in the presence of MCP, the calculation may be off by 17% or more. This error is due to 2,4-lutidine's product ion mobility value changing by 19% and the mobility of ethanolamine product ion changing by 36% when MCP concentration was varied from 0.00 to 0.93 mmol m^{-3} in the buffer gas (Table 2). Calculating mobilities with DTBP or tetraalkylammonium ions would yield larger errors than calculating the mobilities with 2,4-lutidine because $\%\Delta K_0$ values for those ions were smaller than $\%\Delta K_0$ value for 2,4-lutidine when MCP was introduced into the buffer gas.

To improve mobility calculations using standards, the chemical standards used in this study were classified based on their response to contaminants in the buffer gas. Chemical standards which have mobility values sensitive to the presence of contaminants in the buffer gas were called "mobility standards," and standards for which mobility values did not change as a function of buffer gas contamination were called "instrument standards."

Properties of mobility and instrument standards. Mobility standards should be small ions without steric hindrance at the charge site to enable the ions' sensitivity to the presence of

contamination in the buffer gas; the small size of the mobility standard would allow clustering to change significantly ion size and affect its mobility, indicating that the instrument is contaminated. Other ideal properties of mobility standards should be the production of a single mobility peak and high sensitivity. On the other hand, instrument standards should have steric hindrance at the charge site and a large size. Steric hindrance would deter the attachment of contaminants to the ion charge, and the mobility of the instrument standards would be unaffected by buffer gas contamination. Large ionic size would limit the effect on mobility if some clusters were formed. Thus, a standard with these attributes would only be affected by errors in instrumental parameters, such as voltage, pressure, length, and temperature. Other ideal properties of instrument standards are the production of a single mobility peak, high sensitivity, and stability of reduced mobility values with changes in temperature, moisture, composition of the ESI solvent, and drift field.[25,26]

DTBP as an instrument standard. DTBP was ruled out as a good mobility standard because its $\%\Delta K_0$ values were small in the presence of contaminants in the buffer gas. However, the stability of DTBP's K_0 values would make it a good instrument standard. Other reasons to use DTBP as an instrument standard are high sensitivity due to its high proton affinity, production of a single mobility peak, and relative stability of reduced mobilities with temperature, moisture, and electric field.[26]

Tetraalkylammonium ions as instrument standards. K_0 values for tetraalkylammonium ions also were found to be stable in the presence of contaminants in the buffer gas (Table 2); K_0 values for TBA and TPA ions were more stable than those of DTBP. This stability makes tetraalkylammonium ions excellent instrument standards. Additional

reasons to use tetraalkylammonium ions as instrument standards are the production of a single mobility peak, high sensitivity, and stability of reduced mobilities with temperature, moisture, composition of the ESI solvent, and drift field.[25] However, although TBA and TPA ion mobilities were more stable than those of DTBP in the presence of contaminants, their reduced mobilities are not well established, and more investigations are required to determine accurate and precise mobilities of these ions to replace DTBP as the instrument standard of choice in IMS. The reduced mobility values reported for TBA ions ranged from 1.19 to 1.40 $cm^2V^{-1}s^{-1}$ with an average value of 1.30 $cm^2V^{-1}s^{-1}$ (Table 3); this variability may be due to inaccurate measurement of instrumental parameters.

Recommended method for ion mobility calibration. For accurate calibration of an ion mobility spectrometer, both an instrument and a mobility standard should be used. An instrument standard would determine the instrument constant (C_i) by rearranging Equation 2.

$$K_{0,\,standard}.t_{d,\,standard} = \frac{L^2}{V}\frac{P}{760}\frac{273}{T} = C_i \qquad (4)$$

The value of C_i should be calculated every time *L, P, T,* or *V* might have changed.

After an instrument standard is used to determine C_i, a mobility standard such as 2,4 lutidine, should be employed to determine if the spectrometer is contaminated. If the spectrometer is free of contamination, the product of the measured drift time of the mobility standard and its reduced mobility constant equals the instrument constant, which is calculated using the instrument standard, and the reduced mobility values of unknowns can be accurately measured with the following relation:

$$K_{0,\,unknown} = \frac{C_i}{t_{d\,,\,unknown}} \tag{5}$$

CONCLUSIONS

The mobilities of selected analytes and chemical standards were measured by electrospray ionization ion mobility spectrometry-quadrupole mass spectrometry (ESI-IMS-QMS). Chemical standards were classified in two classes according to their mobility response to the introduction of contamination into the buffer gas: standards to determine contamination in the ion mobility spectrometer (mobility standards) and standards to calibrate the mobility instrument (instrument standards). An instrument standard should be insensitive to contamination in the buffer gas and solvent composition. In contrast, a mobility standard should be sensitive to the presence of neutrals in the buffer gas to detect contamination in the drift tube. DTBP was corroborated as a better instrument standard than 2,4-lutidine in IMS because its K_0 value is not only independent of temperature, moisture, and electric field,[26] but was also less affected by contamination in the buffer gas. Reduced mobilities of tetraalkylammonium ions are not only independent of field, temperature, and composition of the ESI solvent,[25] but were also independent of contamination in the buffer gas. Therefore, DTBP and tetraalkylammonium ions are not good mobility standards, but they are excellent instrument standards. The mobilities of TBA and TPA ions were the most stable of the compounds tested when doping the buffer gas with polar contamination, and could be used as instrumental standards for electrospray ionization methods. However, a drawback of tetraalkylammonium ions as chemical standards for IMS is that these salts can be only used in solution, which would hinder their use with sources that require vapors, such as radioactive sources.

ACKNOWLEDGEMENTS

This work was supported by a grant from Science Applications Intl. Document number P010007799.

REFERENCES

1. Cohen, M. J.; Karasek, F. W. *J. Chromatogr. Sci.* **1970,** *8,* 330-337.

2. Asbury, G. R.; Wu, C.; Siems, W. F.; Hill, Jr. H. H. *Anal. Chim. Acta*, **2000**, *404*, 2, 273-283.

3. Bacon, A. T.; Getz, R.; Reategui, J. *Chem. Eng. Prog.* **1991**, 87, *6*, 61-64.

4. Karasek, F. W.; Hill, H. H.; Kim, S. H. *J. Chromatogr.* **1976,** *117*, 327-336.

5. Alizadeh, N.; Mohammadi, A.; Tabrizchi, M. *J. Chrom. A,* **2008,** *1183*, 21–28.

6. Asbury, G. R.; Klasmeier, J.; Hill, Jr. H. H. *Talanta*, **2000,** *50*, 6, 1291-1298.

7. Oxley, J. C.; Smith, J. L.; Kirschenbaum, L. J.; Marimganti, S.; Vadlamannati, S. *J. Forensic Sci.* **2008**, *53*, 3.

8. Myung, S.; Wiseman, J. M.; Valentine, S. J.; Takats, Z.; Cooks, R. G.; Clemmer, D. E. J. *Phys. Chem. B*. **2006**, *110*, 10, 5045-5051.

9. Wu, C.; Siems, W. F.; Hill, Jr. H. H. *Anal. Chem.* **2000**, *72*, 391-395.

10. Taraszka, J. A.; Gao, X.; Valentine, S. J.; Sowell, R. A.; Koeniger, S. L.; Arnold, R. J.; Miller, D. F.; Kaufman, T. C.; Clemmer, D. E. *J. Proteome Res.* **2005**, *4*, 1238-1247.

11. Dwivedi, P.; Bendiak, B.; Clowers, B. H.; Hill, H. H. Jr. *J. Am. Soc. Mass Spectrom.* **2007**, *18*, 1163–1175.

12. Jackson, S. N.; Ugarov, M.; Egan, T.; Post, J. D.; Langlais, D.; Schultz, J. A.; Woods, A. S. *J. Mass Spectrom.* **2007,** *42*, 8, 1093-1098.

13. Gabelica, V.; Baker, E. S.; Teulade-Fichou, M.-P.; De Pauw, E.; Bowers, M. T. *J. Am. Chem. Soc.* **2007**, *129*, 895-904.

14. Dwivedi, P.; Wu, P.; Klopsch, S. J.; Puzon, G. J; Xun, L.; Hill, Jr, H. H. *Metabolomics* **2008**, *4*, 63–80.

15. Griffin, G. W.; Dzidic, I.; Carroll, D. I.; Stillwell, R. N.; Horning, E. C. *Anal. Chem.* **1973**, *45*, 1204-1209.

16. Johnson, P. V.; Kim, H. I.; Beegle, L. W.; Kanik, I. *J. Phys. Chem. A* **2004**, *108*, 5785-5792.

17. Rutherford, E. *Phil. Mag.* **1897**, *44*, 422-440.

18. Rutherford, E. *Phil. Mag*. **1899**, *47*, 109-163.

19. Mason, E. A.; Schamp, H. W. Jr. *Annals Phys.* **1958,** *4*, 3, 233-270.

20. Dusault, L.; Loeb, L. B. *Proc. Natl. Acad. Sci. U.S.A.* **1928**, *14*, 384-393.

21. Eiceman, G. A.; Karpas, Z. **Ion mobility spectrometry**. Taylor & Francis; 2nd ed., Boca Raton, FL, USA, **2005**.

22. Shumate, C.; St. Louis, R. H.; Hill, H. H. Jr. *J. Chromatogr.* **1986,** *373*, 141-173.

23. Loeb, L. B. *Phys. Rev.* **1931**, *38*, 549-571.

24. Karpas, *Z. Anal. Chem.* **1989**, *61,* 7, 684-689.

25. Viidanoja, J.; Sysoev, A.; Adamov, A.; Kotiaho, T. *Rapid Commun. Mass Spectrom.* **2005**, *19*, 3051-3055.

26. Eiceman, G. A.; Nazarov, E. G.; Stone, J. A. *Anal. Chim. Acta* **2003**, *493*, 2, 185-194.

27. Berant, Z.; Karpas*,* Z. *J. Am. Chem. Soc.* **1989**, *111*, 11, 3819–3824.

28. Rearden, P.; Harrington, P. B. *Anal. Chim. Acta* **2005,** *545*, 1, 13–20.

29. Shoff, D. B.; Harden, C. S. In: *Proceedings of the Fourth International Conference on Ion Mobility Spectrom*. Cambridge, **1995**, pp. 6–9.

30. Tabrizchi, M. *Appl. Spectrosc.* **2001,** *55,* 12, 1653-1659.

31. Ewing, R. G.; Eiceman, G. A.; Harden, C. S.; Stone, J. A. *Int. J. Mass Spectrom.* **2006,** *255-256*, 76-85.

32. Eiceman, G. A.; Kelly, K.; Nazarov, E. G. *Int. J. Ion Mobility Spectrom.* **2002**, *5,* 1, 22-30.

33. Pedersen, C. S.; Lauritsen, F. R.; Sysoev, A.; Viitanen, A-K.; Mäkelä, J. M.; Adamov, A.; Laakia, J.; Mauriala, T.; Kotiaho, T. *J. Am. Soc. Mass Spectrom.* **2008**, *19*, 9, 1361-1366.

34. Viitanen, A. K.; Mauriala, T.; Mattila, T.; Adamov, A.; Pedersen, C. S.; Mäkelä, J. M.; Marjamäki, M.; Sysoev, A.; Keskinen, J.; Kotiaho, T. *Talanta* **2008**, *76*, 5, 1218-1223.

35. Adamov, A.; Viidanoja, J.; Karpanoja, E.; Paakkanen, H.; Ketola, R. A.; Kostiainen, R.; Sysoev, A.; Kotiaho, T. *Rev. Sci. Instrum.* **2007,** *78*, 4, 044101.

36. Sysoev, A.; Adamov, A.; Viidanoja, J.; Ketola, R. A.; Kostiainen, R.; Kotiaho, T. *Rapid Commun. Mass Spectrom.* **2004***, 18*, 3131–3139.

37. Jafari, M. T. *Talanta* **2009**, *77*, 5, 1632-1639.

38. Lattey, R. T. *Proc. Royal Soc. London (A)* **1910**, *84*, 569, 173-181.

39. Lattey, R. T.; Tizard, H. T. *Proc. Royal Soc. London (A)* **1912**, *86*, 604, 349-357.

40. Erikson, H. A. *Phys. Rev.* **1927** *30,* 339- 348.

41. Eiceman, G. A.; Nazarov, E. G.; Rodriguez, J. E.; Bergloff, J. F. *Int. J. Ion Mobility Spectrom.* **1998,** *1,* 28–37.

42. Sohn, H.; Steinhanses, J. *Int. J. Ion Mobility Spectrom.* **1998**, 1, 1-14.

43. Wang, Y. F. Effects of moisture and temperature on mobility spectra of organic chemicals, MS Thesis, New Mexico State University, Las Cruces, NM, August **1999**.

44. Erikson, H. A. *Phys. Rev.* **1929,** *33*, 403–411.

45. Nolan, J. J. *Proc. Royal Soc. London A*, **1918,** *94,* 112-136.

46. Wu, C.; Siems, W. F.; Asbury, G. R.; Hill, H. H. *Anal. Chem.* **1998**, *70*, 23, 4929-4938.

47. Wittmer, D.; Chen, Y. H.; Luckenbill, B. K.; Hill, H. H. *Anal. Chem.* **1994**, *66*, 14, 2348–2355.

48. Eiceman, G. A.; Salazar, M. R.; Rodriguez, M. R.; Limero, T. F.; Beck, S. W.; Cross, J. H.; Young, R.; James, J. T. *Anal. Chem.* **1993,** *65,*13, 1696-1702.

49. Puton, J.; Nousiainen, M.; Sillanpaa, M. *Talanta* **2008**, *76*, 978–987.

50. Bollan, H. R.; Stone, J. A.; Brokenshire, J. L.; Rodriguez, J. E.; Eiceman, G. A. *J. Am. Soc. Mass Spectrom.* **2007,** *18,* 5, 940-951.

51. Dwivedi, P.; Wu, C.; Matz, L. M.; Clowers, B. H.; Siems, W. F.; Hill, H. H. Jr. *Anal. Chem.* **2006**, *78*, 24, 8200-8206.

52. Beegle, L. W.; Kanik, I.; Matz, L.; Hill, H. H. *Anal. Chem.* **2001**, *73*, 13, 3028-3034.

53. Karasek, F. W.; Kim, S. H.; Rokushika, S. *Anal. Chem.* **1978**, *50*, 14, 2013–2016.

54. Guevremont, R.; Siu, K. W. M.; Wang, J.; Ding, L. *Anal. Chem.* **1997**, *69*, 19, 3959-3965.

55. Hallen, R. W.; Shumate, C. B.; Siems, W. F.; Tsuda, T.; Hill, H. H. *J. Chrom.* **1989**, *480,* 233-245.

56. Kim, H.; Kim, H. I.; Johnson, P. V.; Beegle, L. W.; Beauchamp, J. L.; Goddard, W. A.; Kanik, I. *Anal. Chem.* **2008**, *80*, 6, 1928-1936.

Table 1. ESI-APIMS operating conditions summary

Parameter	*Settings*
Reaction region length	7.5 cm
Drift tube length	25.0 cm
ESI voltage	15.6 kV
Voltage at first ring	12.12 kV
ESI flow	3 µl min^{-1}
Voltage at the gate	10.80 ± 0.01 kV
Gate closure potential	±40 V
Gate pulse width	0.1 ms
Scan time	35 ms
Buffer gas	Nitrogen
Buffer gas temperature	150 ± 2 °C
Buffer gas flow	930 ml min^{-1}
Contaminant flow rate	0.03 to 1250 µl hr^{-1}

Table 2. $\%\Delta K_0$ values when organic contaminants and moisture were introduced into the buffer gas. Percent reduction in mobility, $\%\Delta K_0$, for selected compounds at a concentration of 0.93 mmol m^{-3} (35 ppmv) of MCP, 2.3 mmol m^{-3} of α-trifluoromethyl benzyl alcohol (86 ppmv), or $8.8x10^2$ mmol m^{-3} ($3.3x10^4$ ppmv) of water in the buffer gas. $\%\Delta K_0$ is defined as the percentage difference between K_0 in nitrogen buffer gas and K_0 when a contaminant is introduced into the buffer gas at a given concentration. $\%\Delta K_0$ values for water at 2.3 mmol m^{-3} (86 ppmv) in the buffer gas were 0.0 indicating a smaller influence of moisture in ion mobilities than that of tFMBA or MCP.

Compound	Methyl 2-chloropropionate	α-trifluoromethyl benzyl alcohol	Water
RIP's			3.8
2,4-lutidine	19		3.8
DTBP	0.9	1.3	2.1
TBA ions	0.1	0.0	0.9
TEA ions	0.1	0.0	2.9
TMA ions	0.4	0.0	4.0
TPA ions	0.1	0.0	1.8
Methionine		4.6	
Phenylalanine		7.3	
Serine		10.6	7.9
Threonine		8.6	
Tyrosine		7.0	
Tryptophan		4.0	
Tribenzylamine			1.0
Tributylamine			2.0
Valinol	36	5.1	7.1
Ethanolamine	31		

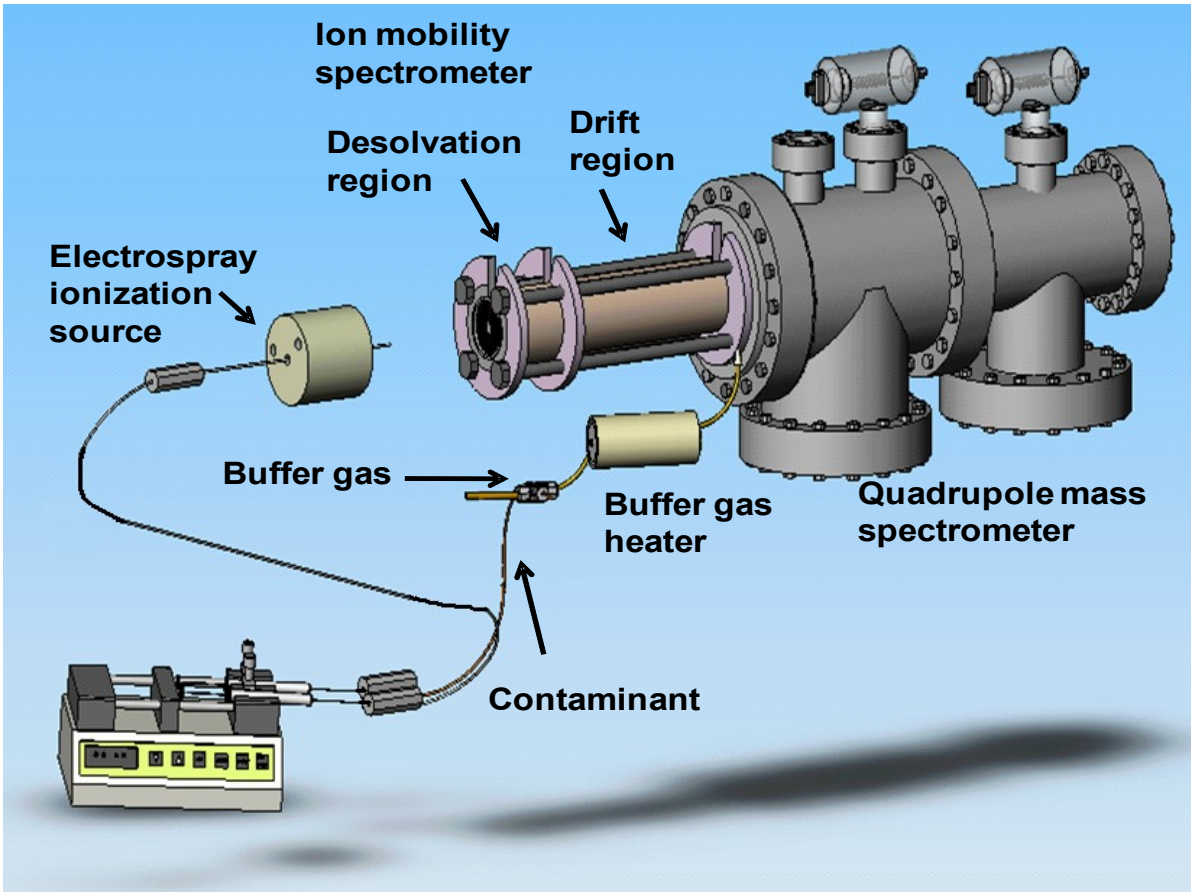

Figure 1. Instrument. Sketch of the electrospray ionization-atmospheric pressure ion mobility-mass spectrometer including setup for the injection of contaminants and heating of the buffer gas.

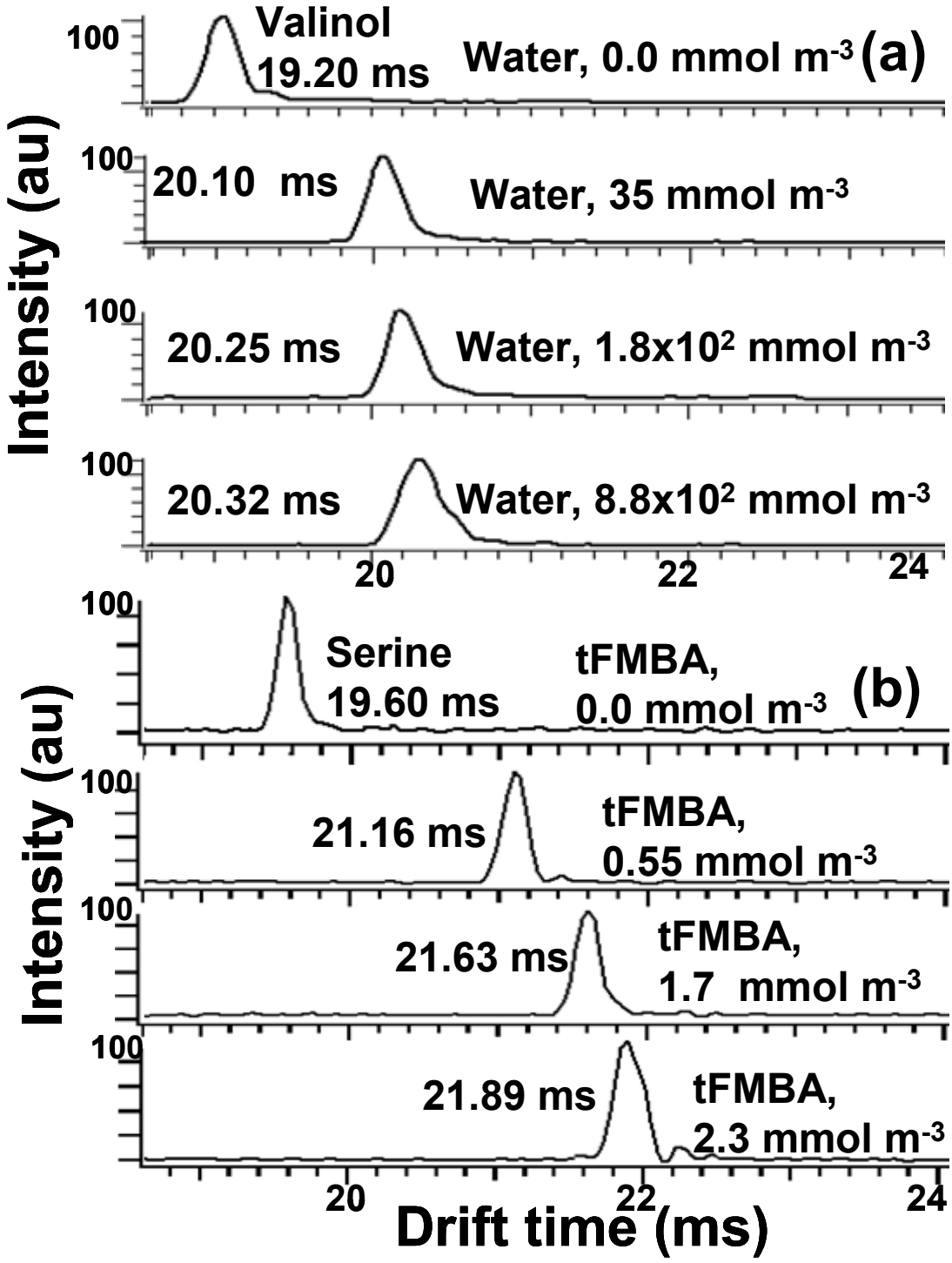

Figure 2. Changes in mobility when contaminants were introduced into the buffer gas. SIM-IMS spectra illustrating the reduction in mobility of the response ions in 100-μM solutions of analytes when contaminants were introduced into the buffer gas at 150°C. (a) Spectrum of valinol when water contaminant was introduced into the buffer gas. (b) Spectrum of serine

when tFMBA contaminant was introduced into the buffer gas.

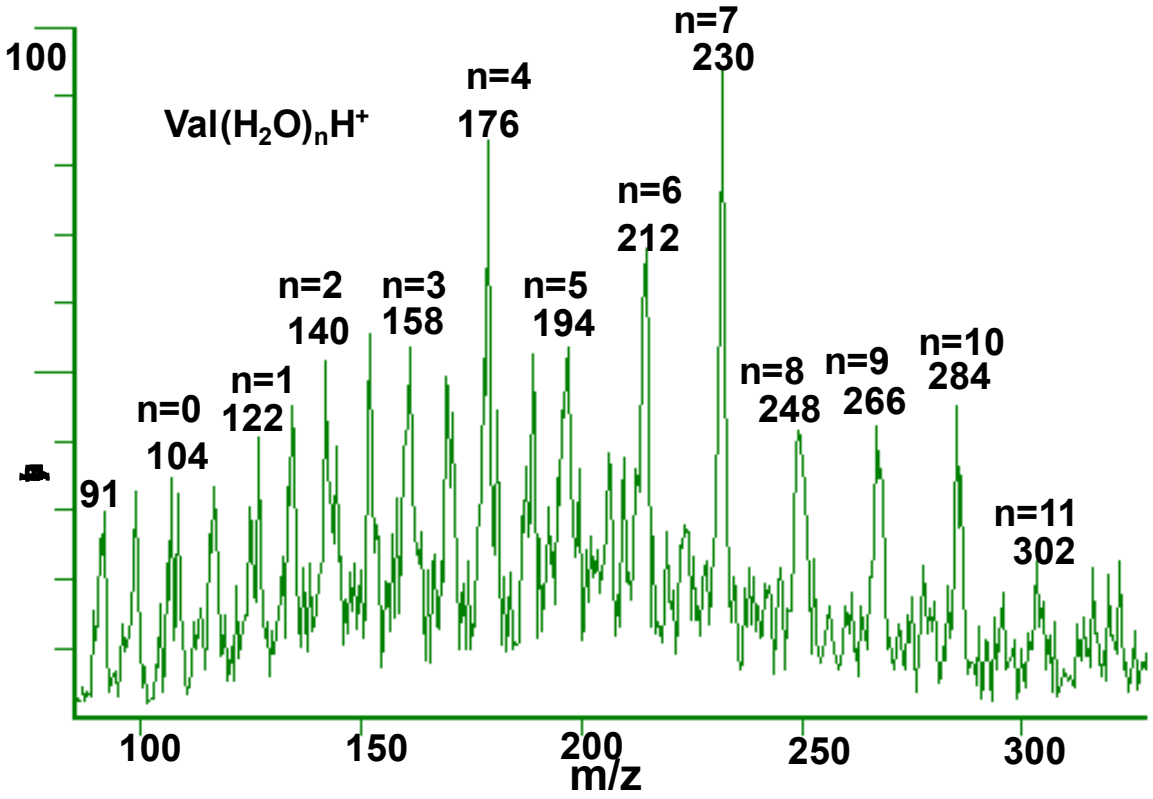

Figure 3. Valinol-water cluster formation upon introduction of water contaminant into the buffer gas. Mass spectrum of 100-μM valinol (Val) at 150°C and a water concentration of $8.8x10^2$ mmol m^{-3} in the buffer gas. The formation of valinol-water clusters with up to 11 molecules of water decreased the mobility of valinol when water was injected into the buffer gas.

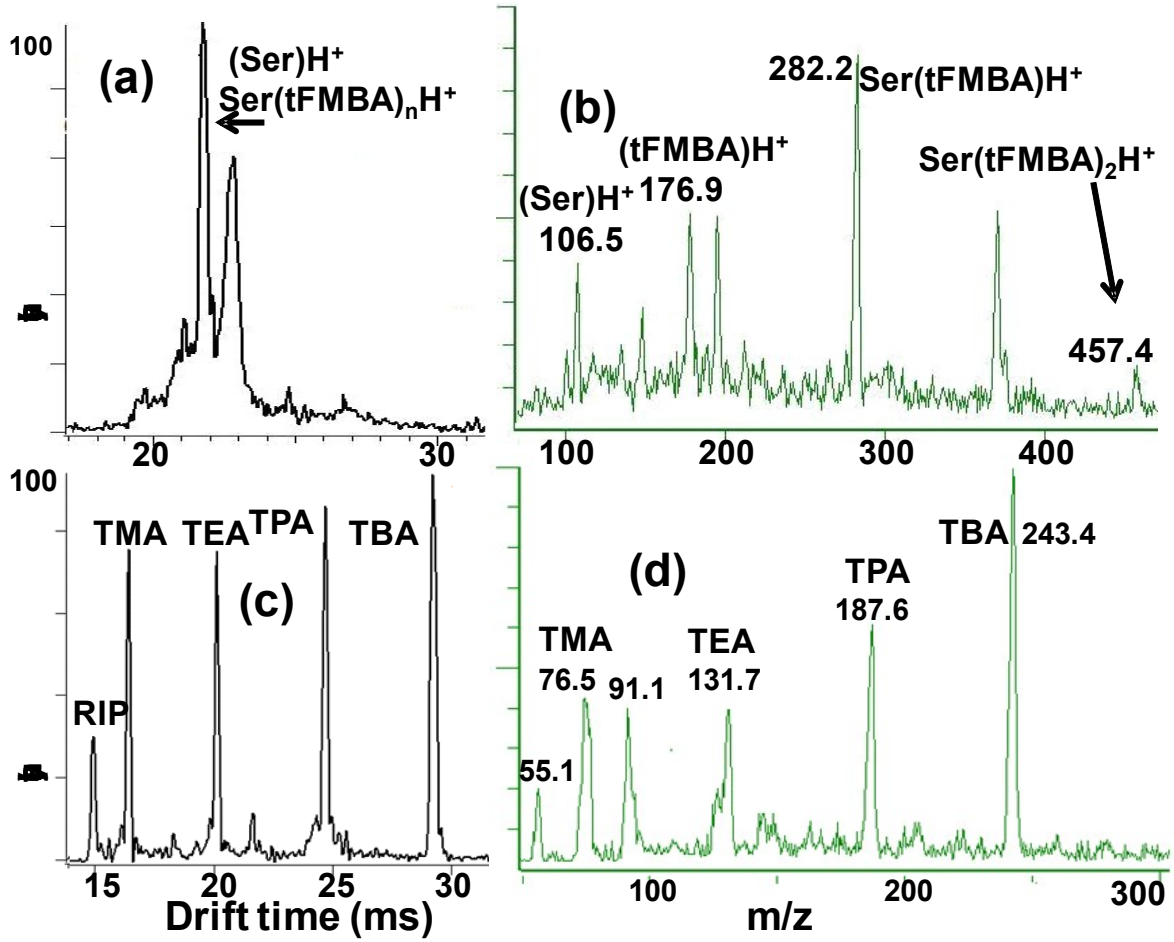

Figure 4. Clustering of tetraalkylammonium ions and serine with contaminants. Concentration was $8.8x10^2$ mmol m^{-3} for water (a and b) and 2.3 mmol m^{-3} for tFMBA (c and d) in the buffer gas. (a) (IMS spectrum) Broad peaks indicate clustering of serine with tFMBA; (b) mass spectrum showing extensive clustering of serine when tFMBA was introduced into the buffer gas; cluster formation was due to the small size and absence of steric hindrance on the amino acid structure; (c) (IMS spectrum) well-defined peaks denote the absence of fragmentation, adduction, or clustering of tetraalkylammonium ions in the drift region; (d) (mass spectrum) only small water cluster peaks were seen at m/z 149, 204, and 262 for TEA, TPA, and TBA ions, respectively, which indicates the large steric hindrance of tetraalkylammonium ions. Buffer gas temperature was 150°C.

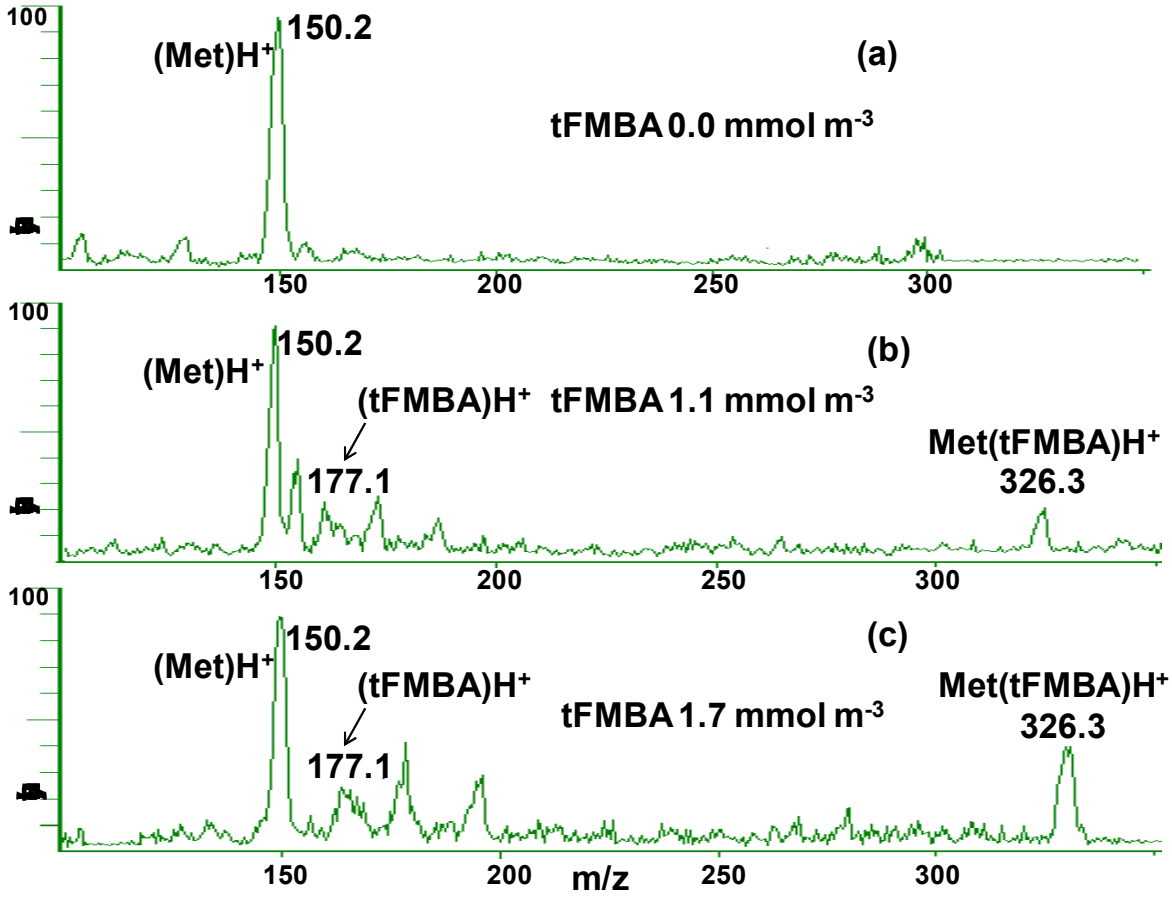

Figure 5. Methionine-tFMBA clusters. The mass spectra show that as tFMBA concentration increased from a) 0.0 to c) 1.7 mmol m^{-3} in the buffer gas, the ratio of the intensities of the analyte-contaminant peak to the protonated peak of methionine, $Met(tFMBA)H^+$:$(Met)H^+$, increased, which indicates increasing clustering of methionine with tFMBA.

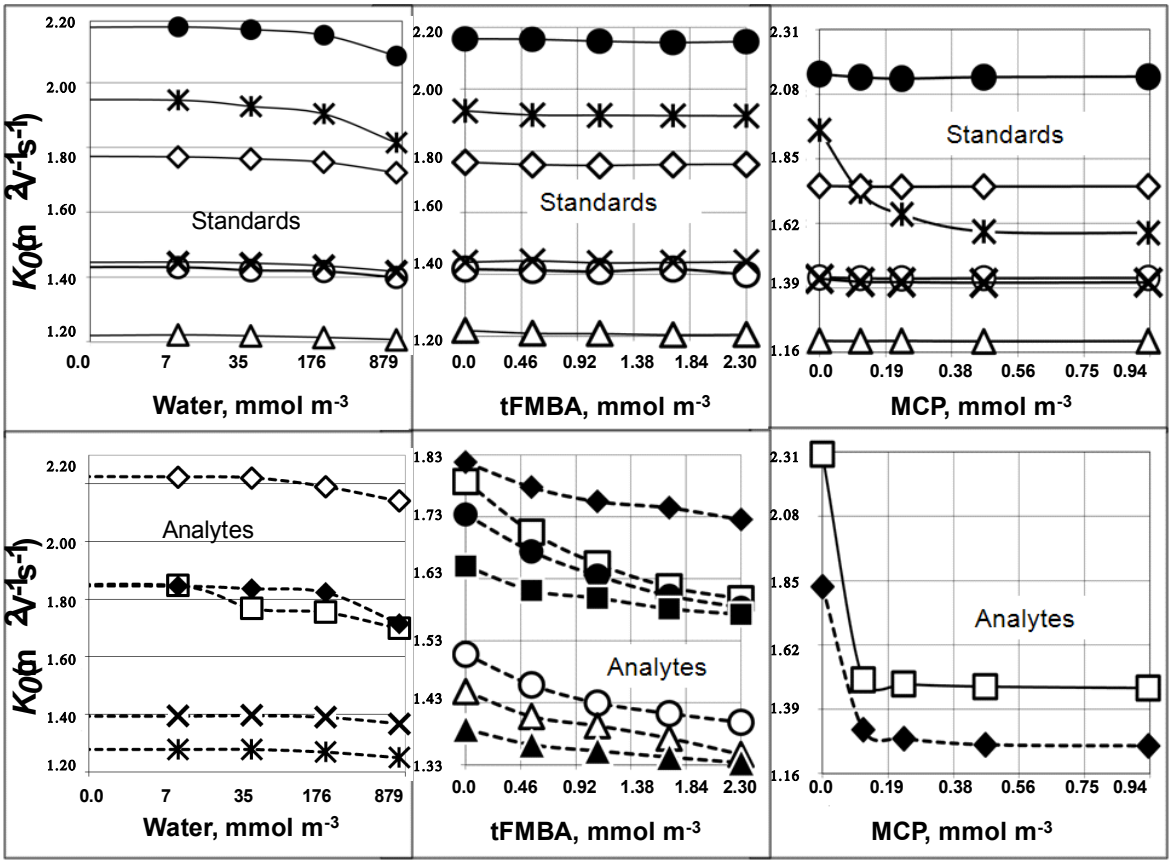

Figure 6. Change in K_0 values for test compounds upon addition of contaminants into the buffer gas. MCP: methyl 2-chloropropionate; tFMBA: α-trifluoromethyl benzyl alcohol. Standards: 2,4-lutidine (——), DTBP (–○–), TBA ions (–Δ–), TEA ions (——),TMA ions (–● –), TPA ions (–**x**–); Analytes: ethanolamine (–□–), methionine (--■--), phenylalanine (--○--), reactant ion peaks (--p--), serine (--□--), threonine (--● --), tribenzylamine (--**t** --), tributylamine (--**x**--), tryptophan (--▲--), tyrosine (--Δ--), and valinol (--♦ --).

Chapter Five

Ion mobility spectrometry for the rapid analysis of over-the-counter drugs and beverages

Roberto Fernández-Maestre[19] and Herbert H. Hill Jr.[110]

[1]*Department of Chemistry, Washington State University, Pullman, WA 99163, USA*

Submitted to

INTERNATIONAL JOURNAL OF ION MOBILITY SPECTROMETRY

May 2009

[9] Permanent address: Programa de Quimica, Campus de Zaragocilla, Universidad de Cartagena, Cartagena, Colombia

[10] To whom correspondence should be addressed. E-mail: hhhill@wsu.edu. Fax 509-335-8867

ABSTRACT

In the pharmaceutical and food industry, there are increasing requirements for analytical methods in quality assessment for the production of drugs and beverages. In this investigation, ion mobility spectrometry (IMS) was used for the rapid qualitative separation and identification of active ingredients in generic over-the-counter drugs and food additives in beverages. The active ingredients determined in drugs were acetaminophen, aspartame, bisacodyl, caffeine, dextromethorphan, diphenhydramine, famotidine, glucosamine, guaifenesin, loratadine, niacin, phenylephrine, pyridoxine, thiamin, and tetrahydrozoline. Aspartame and caffeine were determined in beverages. Fourteen over-the-counter drugs and beverages were analyzed. Analysis times below 10 seconds were obtained for IMS, and reduced mobilities were reported for the first time for 12 compounds. A quadrupole mass spectrometer coupled to a mobility spectrometer was used to assure a correct peak assignation. The combination of fast analysis, low cost, and inexpensive maintenance of IMS instruments makes IMS an attractive technique for the qualitative determination of active ingredients in over-the-counter drugs and food additives in manufacture quality control and cleaning verification for the drug and food industries.

KEYWORDS: Ion mobility spectrometry, over-the-counter drug, food additive, sweetener

INTRODUCTION

The introduction of modified foods, as well as food, drug, and cosmetic additives has been a major change in people's lives over the past three decades. Food and beverages are being altered to make them more appetizing and colorful, to retard spoilage, and to conceal spoiled products. A public increasingly interested in healthy food and aware of the health implications of these additives, together with new revelations from the scientific community on their health effects, have driven food control institutions to issue regulations on the use of these chemicals.

There is controversy on the health risks of food additives (colorings, flavorings, and preservatives). Some authors claim that artificial sweeteners, such as saccharin, cyclamate, and aspartame, do not pose carcinogenic threats (Weihrauch and Diehl 2004). However, other studies show these sweeteners as a human cancer risk (Huff and LaDou 2007; Andreatta et al. 2008). In addition, it was demonstrated that some food additives produce allergic responses (Wüthrich 1993) and may increase hyperactivity in children with behavior problems (Williamson 2008; (McCann et al. 2007).

There is a growing need in the food and pharmaceutical industries for rapid, low-cost, and sensitive analytical methods in quality assessment and cleaning verification for the quality control and production of over-the-counter drugs and food (Weihrauch and Diehl 2004). A rapid, low-cost, sensitive method is required for routine screening of batches of raw materials, the production line, and the final commercial products to avoid deterioration and changes in specifications. Rapid cleaning verification is also a challenge related to screening

pharmaceutical components on production equipment to avoid contamination of future products (Tan and DeBono 2004). The techniques currently used for quality control in the pharmaceutical industry, such as HPLC and total organic carbon (TOC), are slow and relatively inaccurate (Tan and DeBono 2004; Chiarello-Ebner 2006). TOC is fast and simple, but it can produce false positive results because it finds all organic carbon and cannot distinguish between excipients or cleaning residues and the active ingredients. These false indications are nonexistent in IMS, which gives quantitative, selective results (Tan and DeBono 2004; O'Donnell et al. 2008)

HPLC is a selective and popular analytical method for the analysis of over-the counter-drugs and beverages, but it is expensive and analysis times are between 1 and 20 minutes (Heydari 2008; Wongiel et al. 2008). In contrast, IMS can develop analysis run times of 20–45 ms, and lab-made IMS instruments can be assembled at low cost. Besides, the cost of maintenance of IMS instruments is lower than that of HPLC. With IMS, cost savings are realized in two areas: costs of consumables (solvents and column materials) needed in HPLC and savings found in the IMS's speed (Tan and DeBono 2004). Other techniques such as gas chromatography (GC) also suffer several shortcomings, namely, lengthy analysis times and use of solvents. An advantage of IMS over HPLC or GC is the absence of analysis problems associated with faulty or dirty columns. Moreover, IMS instruments are easy to use, as demonstrated by their widespread employment in military and aviation security applications.

Ion mobility spectrometry (IMS), introduced by the end of the 60's by Cohen and Karasek (1970), is an analytical technique that separates gas-phase ions at atmospheric pressure. IMS is a fast, low-cost, and sensitive method ideal for the detection of trace quantities

of volatile organic and inorganic compounds. The main applications of early IMS instruments were the detection of illegal drugs (Karasek et al. 1976), explosives (Asbury et al. 2000), and chemical warfare agents (Asbury et al. 2000b). The introduction of electrospray ionization–ion mobility spectrometry (ESI-IMS) in the late 1980's allowed the easy analyses of non-volatile and labile samples (Shumate and Hill 1989). The combination of ion mobility spectrometers with mass spectrometers permitted analysis of metabolomes (Dwivedi et al. 2008) and proteomes (Liu et al. 2007), study of protein-protein and noncovalent protein-ligand complexes (Kaddis et al. 2007), imaging of tissues (McLean et al. 2007), and separation of carbohydrate isomers (Dwivedi et al. 2007) and mixtures of peptides (Taraszka et al. 2005).

In an ion mobility spectrometer, samples are ionized at atmospheric pressure, and an electric field drives the ions through a drift tube where collisions occur between the ions and neutral buffer gas molecules. Ionization commonly occurs by a radioactive, electrospray, or corona discharge source. After ionization, the ions are focused into a drift tube composed of a desolvation and a drift region. In the desolvation region, the ions are stripped off solvent molecules with the help of a preheated counter-current of neutral gas (the buffer gas), and pulsed into the drift region by an ion gate. The ions are then accelerated through the drift region by the electric field, where they obtain a constant drift velocity. This constant velocity (v, cm s^{-1}), proportional to the electric field (E, cm^2 s^{-1}), results from the accelerating electric field and the retarding effect of random collisions with the gas (Mason and McDaniel 1988):

$$K = \frac{\mathrm{v}}{E} = \frac{L^2}{V.t_d} \qquad (1)$$

where L is the length of the drift region in cm, V the total voltage drop in volts across the drift region, and t_d the time the ion spends traveling the distance L in seconds. Ion mobilities depend on temperature and pressure. These temperature and pressure effects are normalized to standard conditions to compare values of K in different laboratories through the use of the reduced mobility constant (K_0, $cm^2V^{-1}s^{-1}$):

$$K_0 = K \frac{P}{760} \frac{273}{T} \quad (2)$$

where P is the pressure in the drift region in Torr and T the buffer gas temperature in Kelvin (Mason and Schamp 1958). K_0 values are constant for every compound in a specific buffer gas. A collection of reduced mobility values from ambient pressure ion mobility spectrometry was published in 1986 (Shumate et al. 1986).

Over-the-counter drugs have been analyzed by IMS-MS using a handheld mobility spectrometer with a radioactive source by characterizing the vapors produced through warming the pharmaceutical solids in air. Acetaminophen, brompheniramine, chlorpheniramine, pseudoephedrine, phenylpropanolamine, acetyl salicylic acid, and caffeine were determined using this method (Eiceman et al. 1990). Eckers et al. used IMS coupled to liquid chromatography/mass spectrometry to improve the separation of drug-related materials from excipients such as polyethylene glycols (PEGs) that make difficult the detection of trace level impurities in drugs (Eckers et al. 2007).

Budimir et al. analyzed pharmaceutical formulations using atmospheric pressure ion mobility spectrometry combined with liquid chromatography and nano-electrospray ionization. One beta blocker (timolol), antidepressant (paroxetine), analgesic (paracetamol), and opiate

(codeine) preparations were studied (Budimir et al. 2007). Kent et al. found IMS to be an ultra-fast alternative to HPLC for the validation of cleaning verification in the pharmaceutical industry. IMS exceeded all validation requirements for specificity, precision, linearity, LOQ/LOD, accuracy, stability, and speed. Using IMS, the sample analysis portion of the method validation was approximately 8 times faster than for HPLC to determine residual diphenhydramine on stainless steel surfaces (Payne et al. 2005). Weston et al. (2005), using IMS-time-of-flight MS coupled with DESI sample introduction, analyzed several prescription and OTC drugs including an antiseptic cream (chlorhexidine), Paracetamol (acetaminophen), Zantac (ranitidine), and a nicotine-containing skin patch, among others. A review on pharmaceutical applications of ion mobility spectrometry (O'Donnell et al. 2008) includes an ample listing of pharmaceutical compounds identified by IMS with reduced mobilities, ionic species, and methods used to identify the compounds. However, none of the over-the-counter drugs analyzed in the present work was reported in that review.

Atmospheric pressure electrospray ionization ion mobility spectrometry (ESI-IMS) may offer a detection method for the low cost, fast, and sensitive analysis of pharmaceutical formulations and foods due to its rapid monitoring and high-resolution potential. This method may be an alternative to slow and expensive methods such as chromatography or inaccurate methods such as TOC. Therefore, the specific objectives of this investigation were to establish if ESI-IMMS had the capability for the fast and sensitive qualitative determination of active ingredients and additives in complex OTC drug formulations and beverages.

EXPERIMENTAL SECTION

Instrument. An electrospray-ionization atmospheric-pressure ion mobility spectrometer coupled to a quadrupole mass spectrometer (Fig. 1) was used in this work.

The IMS instrument was built at Washington State University, and a complete description and schematics can be found in previous publications (Wu et al. 1998). The mobility spectrometer included an electrospray source and a drift tube. The drift tube consisted of a reaction (desolvation) region, an ion gate, and a drift region. Both desolvation and drift region had alternating stainless steel rings, separated by ceramic insulating rings. The metal rings were connected in series by high temperature resistors (Caddock Electronics Inc., Riverside, CA, ±1%). The resistors were 0.5 Ω for the desolvation region and 1 MΩ for the drift region. The drift and desolvation region were 25 and 7.5 cm long, respectively, with an I.D. of 50 mm. A 432 V cm^{-1} electric field was created in the drift tube when 10800 V were applied to the first ring (Hill and Simpson 1997).

The ion gate, which pulsed the ions into the drift region, was a Bradbury-Nielsen-type. It was made of two series of forty 75-µm parallel Alloy-46 stainless steel wires (California Fine Wire Co., Grove Beach, CA) 0.6 mm apart. The wires were biased to a potential, creating an orthogonal field relative to the drift field to stop the ions from passing into the drift tube. The closure potential was 40 V higher for one set of wires (positive wires) and 40 V lower for the other set (negative wires). Positive and negative wires were alternated in the gate. This closure voltage was removed for 100 µs so that a narrow pulse of ions entered the drift region. In the first ring of the desolvation region, there was an ESI target screen made out of 2-mm stainless steel mesh with a 0.5-cm round orifice in the center. To help desolvate the ions created by electrospray, hot N_2 gas was introduced as a countercurrent through a stainless-steel tube at the

end of the drift tube at a flow rate of 0.9 L/min. The buffer gas was heated by passing it through a 2-m long stainless-steel tube wound inside a heated aluminum block (Fig. 1). The mobility spectrometer was operated at atmospheric pressure (690-710 Torr in Pullman, WA).

Regular parameters used to operate the mobility spectrometer are shown ion Table 1.

The mass spectrometer used in this investigation was an ABB Extrel (Pittsburgh, PA) 150-QC quadrupole (0-4000 amu). The software, electronics, and detector of this instrument were recently upgraded. The electron multiplier detector signal of the mass spectrometer was amplified and sent to the data acquisition systems by a Keithley model 427 amplifier (Keithley Instruments, Cleveland, OH). The mass spectrometer was run by Merlin software (version 3.0, ABB Extrel, Pittsburgh, PA), which collected the mass spectral data. The IMS data was collected by custom-made LabView software (National Instruments, Austin, TX), which controlled the ion gate. The electronics for IMS data acquisition and gate control were built at WSU (Wittmer et al. 1994).

Spectra were acquired in IMS, SIM-IMS, and mass spectrometry modes. In SIM-IMS mode (single ion monitoring), the mass spectrometer voltages are set so that only ions of a given mass to charge ratio or a range of ions are detected. These settings avoid interference of other ions when determining a specific compound, and mobility spectra of a specific ion or ions are collected; in IMS mode, the mass spectrometer is operated in RF only mode so that ions are pulsed into the drift region, and enter the mass spectrometer, where they are all detected without scanning; the mobility spectrum of all ions is collected in this mode. In mass spectrometry mode, there is no pulsing of the ions; all ions continuously enter the mass spectrometer, and mass spectra are obtained; the ion mobility spectrometer is used as a

desolvation region, especially when ESI is in use.

Materials and reagents. Tetrabutylammonium (TBA) chloride, 2,4-dimethylpyridine (2,4-lutidine), and 2,6-di-tert-butyl pyridine (DTBP) (ACS reagent grade, ≥98% purity), purchased from Sigma Aldrich Chemical Co. (Milwaukee, WI), were used as chemical standards. Several over-the-counter drugs and energetic beverages were selected based on their popularity and availability. The drugs were chosen among pain relievers, antihistamines, cough suppressants, nutritional supplements, laxative and antacid medications, and eye drops. The active ingredients determined in drugs were acetaminophen, aspartame, bisacodyl, caffeine, dextromethorphan, diphenhydramine, famotidine, glucosamine, guaifenesin, loratadine, niacin, phenylephrine, pyridoxine, thiamin, and tetrahydrozoline. Aspartame and caffeine were determined in beverages. The drugs and beverages were purchased from local stores.

***Sample preparation and introduction*.** Sample preparation was simple. Liquids and creams were mixed with the ESI solution, until a homogeneous mixture was obtained, and diluted. Solid sample preparation consisted dissolving the whole pill, including the coating; solid samples were placed in a glass vial and shacked overnight in the ESI solution (4.75 H_2O: 4.75 methanol:0.5 acetic acid). Acetic acid was used to improve protonation. The clear supernatant was diluted to 0.5 mM in the case of samples with one active ingredient; in the case of samples with multiple active ingredients, the solutions were diluted until the less concentrated component reached a 10-μM concentration.

The chemical standards (TBA ions, 2,4-lutidine, and DTBP) were prepared in the ESI solvent at a concentration of 50 μM. Liquid samples or solvent (ESI solution) were injected using 250-μl syringes by electrospray ionization (ESI) at a flow rate of 3 μl min^{-1} into 40-cm

long, 100-µm ID capillaries. These capillaries were connected through stainless steel unions (Valco, Houston, TX) to 50-µm ID capillaries. The end of these capillaries was placed in the center of the target screen in the first ring of the mobility spectrometer. To produce positive ions, the metallic union received a high voltage of 15.6 kV with a 3.5 kV bias with respect to the first ring at the entrance of the mobility spectrometer.

Resolving power. Resolving power is an indication of separation efficiency and can be calculated in IMS by:

$$R = t_d / w \tag{3}$$

where t_d is the drift time of the ion of interest and w is the temporal peak width measured at half-height (Siems et al. 1994). Regardless of its resolving power, an instrument cannot separate two compounds with identical drift times. R values can be changed in IMS by operating at high electric fields, but with the undesirable effect of operating the mobility spectrometer in a region where mobility depends on voltage (where Equation 1 is no longer valid).

Calibration and identification of analytes. All analytes were detected as $M{\cdot}H^+$ ions, and were identified by mass spectrometry; their m/z ratio in mass spectrometry was compared to the molecular weight of their protonated molecules or clusters. Analytes were further identified by comparing their reduced mobilities with values reported in the literature. IMS peak identification was confirmed by SIM-IMS. The mobility scale was adjusted following the method of Eiceman et al. (2003), who recommend correcting reduced mobilities by comparing with standards:

$$\frac{K_{o\,(\text{unknown})}}{K_{o\,(\text{standard})}} = \frac{t_{d\,(\text{standard})}}{t_{d\,(\text{unknown})}} \tag{4}$$

where K_0 is the reduced mobility in $cm^2V^{-1}s^{-1}$ and t_d is the drift time in ms. This method accounts for errors in measuring instrumental parameters and eliminates the need for performing these measurements. 2,4-lutidine and DTBP are common standards to calibrate the reduced mobility scale (Eiceman et al. 2003).

RESULTS AND DISCUSSIONS

Figs. 2 to 5 show spectra of the rapid analysis of over-the-counter drugs and beverages obtained by ion mobility spectrometry. These samples were electrosprayed directly into the ambient pressure mobility spectrometer and separated and detected within 9 seconds. Mobility peaks were identified by SIM-IMS; mobility and mass spectra were averaged 250 and 500 times, respectively

1. *Single-ingredient over-the-counter drugs*

Fig. 2 shows the mass and mobility spectra of over-the-counter (OTC) drugs that comprise a single active ingredient. Fig. 2.1 displays the spectra of the sample Claritin (Claritin®, Schering, Memphis, TN). The mobility spectrum of the sample Claritin in Fig. 2.1a was generated by operating the quadrupole mass spectrometer in IMS mode. In this mode, all the ions pass through the mass spectrometer and are detected by the ion multiplier; this mode of operation yields the ion mobility spectra of all the ions in the sample, the total ion mobility spectrum. Claritin is an antihistaminic medication for treating allergies, favored over other antihistaminic formulations by its non-sedating properties (Encyclopedia Britannica). The electrosprayed solution of this sample produced a simple ion mobility spectrum with only a single peak, which occurred at a drift time of 33.5 ms. The ion species present in the mobility spectrum corresponded to the protonated peak of the pharmaceutical loratadine ($C_{22}H_{23}ClN_2O_2$), the active ingredient of Claritin. A K_0 value of 1.04 $cm^2V^{-1}s^{-1}$ was calculated for loratadine using Equation 4. Other ions from the solvent occurred in the spectrum at drift times shorter than 20 ms (not shown). 250 mobility measurements were averaged to obtain every mobility spectrum, which represents an analysis time below 9 s.

In Fig. 2.1b, the mass spectrum of the sample Claritin produced a primary peak at m/z 383.9. This is the protonated molecule of loratadine, which has a molecular weight of 382.9 g mol^{-1}. 500 scans were averaged to obtain the mass spectra presented in Fig. 2.1b. Because loratadine is an amine, it has a strong response in positive mode IMS, producing a single product ion peak through proton transfer reactions with the ions produced from the electrospray process. To ensure that the mobility peak at 33.5 ms was the peak at mass 383.9, the mass spectrometer was operated in single ion monitoring mode (SIM) in which only the m/z 383.9 peak was monitored; more specifically, a range of ± 1 Da was scanned around the MS peak (from 382.9 to 384.9). In SIM mode, the ion of interest is monitored without the interference of other ions, increasing the signal to noise ratio. When the mass spectrometer was operated in SIM mode, the ion mobility spectrum obtained looked similar to that shown in Fig. 2.1a, indicating that the ion occurring at 33.5 ms was the protonated molecule of loratadine.

Fig. 2.2 presents the spectra of a joint nutritional supplement (Spring Valley®, Schiff, Salt Lake City, UT), whose active ingredient is glucosamine. Glucosamine is an amino sugar, precursor in the biosynthesis of glycosylated proteins and lipids, commonly used as a treatment for osteoarthritis (Encyclopedia Britannica). Fig. 2.2a shows the total ion mobility spectrum of the nutritional supplement. The spectrum, produced by operating the quadrupole mass spectrometer in IMS mode, shows four peaks at 23.1, 17.0, 15.6, and 14.2 ms. The peak at 23.1 ms is the protonated peak of glucosamine ($C_6H_{13}NO_5$), for which a K_0 value of 1.54 $cm^2V^{-1}s^{-1}$was calculated. The three peaks at lower drift times correspond to reactant ions or other components of the drug. The mass spectrum of the joint nutritional supplement in Fig. 2.2b displayed peaks at m/z 198.2, 180.2, 91.1, 55.1, and 37.1. The protonated peak of glucosamine occurred at m/z 180.2 (molecular weight of glucosamine = 179.2 g mol^{-1}), and a

peak of the water cluster of glucosamine occurred at m/z 198.2. The peaks at lower masses correspond to reactant ions; m/z 55.1 and 37.1 can be assigned to $(H_3O)_3H^+$ and $(H_3O)_2H^+$, respectively. The assignment of the peak at 23.1 ms to the protonated peak of glucosamine was done by operating the mass spectrometer in SIM mode and scanning m/z 180.2 ± 1. In SIM mode, only the peak at 23.1 ms was obtained in the mobility spectrum. Also using SIM, the peak at 14.2 ms was assigned to $(H_3O)_nH^+$. The joint supplement medication contained another active ingredient, chondroitin, which is a sulfated chain of a variable number (approximately 100) of alternating glucuronic acid and N-acetylgalactosamine sugars. This component, important in the structure of cartilage, could not be detected because it comprises many chains of different lengths and molecular weights.

Fig. 2.3 includes the mobility and mass spectra of a sample of eye drops (Eyelieve®, Orallabs, Memphis, TN). The active ingredient of Eyelieve is tetrahydrozoline, which constricts the conjunctival blood vessels to relieve the redness of the eye caused by minor ocular irritants. Tetrahydrozoline (Fig. 2.3a) produced peaks in the mobility spectrum at 24.5 ms and 25.8 ms. In the mass spectrum in Fig. 2.3b, the protonated peak of tetrahydrozoline ($C_{13}H_{16}N_2$, molecular weight = 200.3 g mol^{-1}) occurred at m/z 201.3; other peak at m/z 224.3 can be assigned to the sodiated adduct of tetrahydrozoline; additional peaks at m/z 91.1, 73.1, 60.6, 37.1, and other small peaks below m/z 150 can be assigned to the reactant ions; these peaks are not shown in the mobility spectrum because they occurred at drift times below 20 ms. Operating the mass spectrometer in SIM mode by selecting the peak at m/z 201.3, the peak at 24.5 was obtained, for which this mobility peak was assigned to the protonated peak of tetrahydrozoline. A K_0 value of 1.42 $cm^2V^{-1}s^{-1}$ was calculated for this peak. The mobility peak

at 25.8 ms was assigned to the sodiated adduct of tetrahydrozoline at m/z 224.1 using SIM mode.

A generic laxative medication (Women's Laxative, Rite Aid, Harrisburg, PA) and a generic antacid medication (Acid Reducer, Rite Aid, Harrisburg, PA) were also analyzed (spectra not shown). The active ingredient of the laxative medication was bisacodyl ($C_{22}H_{19}NO_4$, molecular weight = 361.4 g mol^{-1}). The laxative medication sample yielded a protonated peak in the mass spectrum at m/z 362.4. Selecting this m/z in SIM mode, a peak at 35.4 ms was obtained for the protonated peak of bisacodyl, corresponding to a K_0 value of 0.98 $cm^2V^{-1}s^{-1}$. Famotidine ($C_8H_{15}N_7O_2S_3$, 337.4 g mol^{-1}), the active ingredient of the antacid medication, is a histamine that inhibits stomach acid production, and it is commonly used in the treatment of gastric ulcer (Encyclopedia Britannica). Famotidine produced a strong mass peak at m/z 338.4. In the IMS mode, a single peak for the antacid medication occurred at 30.7 ms; this mobility peak was identified by SIM-IMS as the protonated peak of famotidine, and a K_0 value of 1.15 $cm^2V^{-1}s^{-1}$ was calculated for it.

2. *Two-ingredient OTC drugs*

Fig. 3 shows the mass and mobility spectra of common OTC drugs composed of two-ingredients. Fig. 3.1 includes the mobility and mass spectra of a migraine medication (Excedrin®, Novartis) containing the active components caffeine and acetaminophen. Caffeine is an alkaloid that acts as a psychoactive stimulant drug and a mild diuretic; acetaminophen is a widely used over-the-counter analgesic and antipyretic used in the treatment of mild pain, such as headache and pain in joints and muscles, and to reduce fever, and is a major ingredient in numerous cold and flu remedies (Encyclopedia Britannica).

The mobility spectrum for the migraine medication produced two strong peaks at 23.3 ms and at 21.0 ms (Fig. 3.1a). SIM-IMS analysis allowed the identification of the peaks as the product ions of caffeine and acetaminophen, for which respective K_0 values of 1.66 and 1.53 $cm^2V^{-1}s^{-1}$ were calculated. The mass spectrum in Fig. 3.1b shows the protonated peaks of caffeine ($C_8H_{10}N_4O_2$, 194.2 g mol^{-1}) and acetaminophen ($C_8H_9NO_2$, 151.1 g mol^{-1}) occurring at m/z 195.2 and 152.1, respectively. Acetyl salicylic acid, another component of the drug, must be detected in the negative mode, which was not set up in our instrument at the time the experiments were performed.

The mobility and mass spectra of a cough syrup (Tussin DM Assured) are presented in Fig. 3.2. Guaifenesin and dextromethorphan were the active ingredients of the drug. Guaifenesin ($C_{10}H_{14}O_4$, 198.2 g mol^{-1}) is widely used in cough preparations to help liquefy secretions and aid expectoration; dextromethorphan ($C_{18}H_{25}NO$, 271.4 g mol^{-1}) is an antitussive drug; It acts upon the central nervous system to suppress the cough reflex (Encyclopedia Britannica). The mobility spectrum in Fig. 3.2a shows peaks at 23.8 ms (protonated peak of guaifenesin), 25.0

ms (water cluster of guaifenesin), 25.6 ms (sodium adduct of guaifenesin), and 29.3 ms (protonated peak of dextromethorphan). Guaifenesin and dextromethorphan occurred at m/z 199.2 and 272.4, respectively, in the mass spectrum (Fig. 3.2b). Two additional peaks were observed in the mass spectrum corresponding to the water cluster of guaifenesin at m/z 217.2 and its sodium adduct at m/z 221.7. K_0 values of 1.51 and 1.22 $cm^2V^{-1}s^{-1}$ were obtained for guaifenesin and dextromethorphan, respectively.

3. *Three-ingredient OTC drugs*

Fig. 4 illustrates the mobility and mass spectra of OTC drugs containing three-ingredients, demonstrating the rapid IMS separation and identification of complex over-the-counter (OTC) formulations. The spectra of a generic allergy and sinus headache medication (Benadryl®, Pfizer, Morris Plains, NJ) composed of acetaminophen, phenylephrine, and diphenhydramine is shown in Fig. 4.1. Phenylephrine, now the most common synthetic OTC decongestant in the United States, relieve swelling of the nasal mucosa accompanying such conditions as the common cold and hay fever; and diphenhydramine is a synthetic antihistamine used in the treatment of various conditions including hay fever, acute skin reactions (such as hives), contact dermatitis (such as from poison ivy), and motion sickness (Encyclopedia Britannica). The mobility peaks of the active ingredients of this drug, assigned operating the instrument in SIM-ESI mode, occurred at 21.6 ms (acetaminophen), 22.6 ms (phenylephrine), and 27.9 ms (diphenhydramine) (Fig. 4.1a). The protonated peaks of acetaminophen (151.1 g mol^{-1}), phenylephrine ($C_9H_{13}NO_2$, 167.2 g mol^{-1}), and diphenhydramine ($C_{17}H_{21}NO$, 255.4 g mol^{-1}), the strongest peaks in the mass spectrum, are shown in Fig. 4.1b; these peaks occurred at m/z 152.1, 168.2, and 256.4, respectively. K_0 values calculated for these compounds were: 1.66 (acetaminophen), 1.53 (phenylephrine), and 1.23 $cm^2V^{-1}s^{-1}$ (diphenhydramine). Benadryl® contained 16 inactive ingredients, comprising waxes, tar dyes, polymers, and carbohydrates, which gave the mobility spectrum a noisy appearance.

Fig. 4.2 illustrates the mobility and mass spectra of a generic vitamin B supplement (People's Choice, Mason Vitamins, Miami Lakes, FL). The spectra included the protonated peaks of niacin ($C_6H_5NO_2$, 123.1 g mol^{-1}), pyridoxine ($C_8H_{11}NO_3$, 169.2 g mol^{-1}), and thiamin

($C_{12}H_{17}N_4OS^+$, 265.4 g mol^{-1}). Niacin (vitamin B3 or nicotinic acid) prevents the deficiency disease pellagra; pyridoxine (vitamin B6) assists in the amino acid metabolism, as well as promoting red blood cell production; and thiamin (thiamine or vitamin B1), is necessary for carbohydrate metabolism in both plants and animal (Encyclopedia Britannica). The mobility spectrum of the vitamin supplement in Fig. 4.2a shows the protonated peaks of niacin (19.9 ms), pyridoxine (22.1 ms), and thiamin (28.3 ms). These peaks were assigned operating the instrument in SIM-ESI mode. The mass spectrum of the supplement is displayed in Fig. 4.2b, and included the protonated peaks of niacin (m/z 124.1), pyridoxine (m/z 170.2), and thiamin (m/z 266.4). Riboflavin and folic acid, other B vitamins present in the supplement, were not seen in the mass spectrum perhaps due to their low concentration. K_0 values calculated for these compounds were: 1.80 (niacin), 1.62 (pyridoxine), and 1.26 $cm^2V^{-1}s^{-1}$ (thiamin).

The mobility and mass data generated in the analysis of a generic cold medication (Rite Aid, Camp Hill, PA) is presented in Fig. 4.3. This medication contained acetaminophen, phenylephrine, and dextromethorphan. Dextromethorphan is an antitussive drug and has been used also for pain relief (Encyclopedia Britannica). The mobility spectrum of the cold medication (Fig. 4.3a) shows the protonated peaks of acetaminophen, phenylephrine, and dextromethorphan occurring at 21.0 ms, 23.1 ms, and 28.5 ms, respectively. SIM-IMS was used to identify the peaks. In the mass spectrum, the protonated peaks of the active ingredients occurred at m/z 152.1 (acetaminophen), m/z 168.2 (phenylephrine), and m/z 272.4 (dextromethorphan) in the cold medication (Fig. 4.3b). K_0 values calculated for these pharmaceuticals were: 1.66 (acetaminophen), 1.53 (phenylephrine), and 1.22 $cm^2V^{-1}s^{-1}$ (dextromethorphan).

In general, the active ingredients in OTC drugs for all the medications analyzed had one or more heteroatoms, such as nitrogen and oxygen, which imparted a large proton affinity to these ingredients. This high proton affinity allowed the active ingredients of OTC drugs to be ionized largely by proton transfer reactions with reactant ions in the electrospray process. This large ionization on the active ingredients produced clean mobility and mass spectra and sharp identifiable peaks with few exceptions. In all samples analyzed, the active ingredients and their hydrated or sodiated clusters produced the strongest peaks in the mass spectrum. All active ingredients were identified in the mobility spectra by SIM-IMS in spite of the complexity of the formulation, with few exceptions.

4. ***Analyses of energetic beverages***

The soda drink and bottled water industry in the US includes about 3,000 companies that manufacture and distribute beverages, with combined annual US revenue of $70 billion. The large production of beverages requires rapid and low-cost technologies for their chemical analysis. Fig. 5 shows the mass and mobility spectra of energetic beverages and standard solutions of caffeine and aspartame. Caffeine (194.2 g mol^{-1}) and aspartame ($C_{14}H_{18}N_2O_5$, 294.3 g mol^{-1}) were determined in Diet coke and antioxidant water. Aspartame is an artificial, non-saccharide sweetener, 180 times sweeter than sugar, without its high energy value (Encyclopedia Britannica). The IMS protonated peaks of caffeine and aspartame in Diet coke are shown in Fig. 5.1a; caffeine occurred at 23.2 ms and aspartame at 29.5 ms, as single peaks in the mobility spectrum. The peaks were assigned operating the instrument in SIM-IMS mode. Other peaks occurred at higher mobilities, probably the reactant ions peaks and peaks from other components in the beverage. The mass spectrum of Diet Coke is presented in Fig. 5.1b,

showing the protonated peaks of caffeine at m/z 195.2 and aspartame at m/z 295.3. There was an increasing baseline toward higher mobilities in the IMS spectrum and toward lower masses in the mass spectrum, probably due to the complexity of the sample, Diet Coke, which is a blend of colors, flavors, and other components.

Fig. 5.2 presents the mobility and mass spectra of a standard solution of caffeine and aspartame. The mobility spectrum in Fig. 5.2a included the protonated peaks of caffeine at 23.0 ms and aspartame at 29.4 ms in a 500-μM standard solution, identified operating the instrument in the SIM-IMS mode. Fig. 5.2b presents the mass spectrum of the standard solution showing the protonated peaks of caffeine at m/z 195.2 and aspartame at m/z 295.3. The peaks at m/z 213.2 and 313.3 were produced probably by water clusters of caffeine and aspartame. These peaks can also be seen, although less clearly, in Fig. 5.1b.

Fig. 5.3 illustrates spectroscopic data for the analysis of a sample of antioxidant water (Snapple®), which is an energetic beverage. In Fig. 5.3a, the protonated peaks of niacin (123.1 g mol^{-1}) and caffeine, identified by SIM-IMS, occurred at 19.8 ms at 23.0 ms, respectively, in the mobility spectrum of the beverage. The mass spectrum of this water in Fig. 5.3b produced the protonated peaks of niacin (123.1 g mol^{-1}) at m/z 124.1 and caffeine at m/z 195.2. Peaks of unknown ingredients occurred at m/z 219.3 and 141.1 in the mass spectrum and at 22.0, 21.5, and 21.1 ms in the mobility spectrum. K_0 values calculated in both beverages and the standards were 1.53 for caffeine and 1.16 $cm^2V^{-1}s^{-1}$ for aspartame.

These spectra revealed the capabilities of IMS for the rapid separation and identification of active ingredients in complex over-the-counter drugs and food additives in beverages. Some of

the OTC drugs and beverages contained up to 18 ingredients several of which were complex mixtures of lipids, polymers, and carbohydrates. Moreover, the concentrations of the ingredients determined were dissimilar with differences up to approximately 500-fold in some cases. However, the spectra obtained in most cases were clean, and the ingredients were identified easily. This IMS selectivity is based on the high proton affinity of active ingredients of OTC drugs and food additives due to their nitrogen and oxygen content. In the analysis of three-ingredient drugs, brompheniramine and chlorpheniramine could not be detected in the mobility spectra of two products probably due to ionization competition of other active ingredients present at higher concentrations. However, the protonated peaks of these two compounds were visible in the mass spectrum, although with a low intensity.

A common method to validate results in IMS is through comparison of reduced mobilities with literature values. Reduced mobilities of active ingredients in OTC drugs and food additives and their concentrations in the solution analyzed are presented in Table 2. Three reduced mobilities of active ingredients were found in the literature out of 15 ingredients determined: 1.67 (acetaminophen), 1.54 (caffeine), and 1.55 $cm^2V^{-1}s^{-1}$ (glucosamine). The reduced mobilities for these compounds obtained in this work were: 1.66 (acetaminophen), 1.53 (caffeine), and 1.54 $cm^2V^{-1}s^{-1}$ (glucosamine); these reduced mobilities showed only a 0.6% difference with respect to the literature values, which was within the maximum 2% of accepted variance for data obtained in different laboratories. All other active ingredients in Table 2 were first-time determined by IMS, or their reduced mobilities were not reported when they were determined. A mass-mobility correlation coefficient of -0.97 was found for the ingredients in Table 2, which indicates the increasing size, and decreasing mobility, as the molecular weight increased. The reproducibility of the values in this table was <2%, calculated as the relative

standard deviation (RSD) of the reduced mobilities of five different samples analyzed on different days. The repeatability of the values in this table was <0.5%, calculated as the RSD of the reduced mobilities of five or more consecutive analyses (250 averages each) of the sample.

5. ***Resolving power and signal to noise ratio***

A high resolving power is a desirable feature of analytical techniques intended to separate complex OTC drugs comprising several active and inactive ingredients. A high resolving power produces sharp analyte peaks that can be easily distinguished from peaks of other ingredients in the mobility spectra. Fig. 6 demonstrates the high resolving powers obtained in SIM-IMS mode when analyzing OTC drugs and beverages. Resolving powers up to 140 were obtained with an average of 100. Fig. 6 shows these high resolving powers in the mobility spectra of diphenhydramine in Benadryl® (resolving power 140), aspartame in Diet Coke® (resolving power 126), and tetrahydrozoline in Eyelieve® (resolving power 113). The high resolving powers allowed the resolution of the complex mixtures analyzed in this work. The signal to noise ratio for these analysis were 61 for diphenhydramine in Benadryl®, 41 for aspartame in Diet Coke®, and 20 for tetrahydrozoline in Eyelieve® at concentrations of 0.87, 0.12, and 0.05 mM, respectively.

6. ***Analysis time***

A short analysis time is another desirable feature of analytical techniques that increases production in the pharmaceutical and food industries due to rapid cleaning verification and quality control and lower labor requirements. A short analysis time contributes to reduce costs and increase competitiveness. The number of averages used to obtain mobility spectra in this

investigation was 250; with a scan time of 35-40 ms, instrumental analysis times below 10 seconds were obtained. The short duration of the analyses represents one of the features that translate into economy in IMS. These short analysis times were lower than those for HPLC (not including sample preparation). HPLC is a common analytical technique for the analysis of over-the counter-drugs and determination of food additives, but the analysis times are between 1 and 20 minutes, and instruments and maintenance are expensive.

CONCLUSIONS

We demonstrated the fast qualitative determination of active ingredients in over-the-counter drugs and food additives in beverages without sample pretreatment using electrospray-ion mobility spectrometry (ESI-IMS). Analysis times below 10 seconds were obtained for these samples. Clear separation and identification of the analyte peaks were obtained after a simple dissolution step in composite samples with 10-19 declared ingredients, some of which were complex mixtures of waxes, carbohydrates, polymers, dyes, and other large molecules. Complex samples with analyte concentrations down to 10 μM were analyzed with other components at higher concentrations, indicating high selectivity and sensitivity. Resolving powers up to 140, with an average of 100, made possible to obtain low-noise spectra, which allowed resolution of the complex mixtures analyzed in this work. The combination of fast detection times, selectivity, sensitivity, low cost, and easy maintenance of ESI-IMS instruments makes this technique an attractive alternative for the qualitative analysis of over-the-counter drugs and beverages.

ACKNOWLEDGEMENTS

This work was supported by NIH grant R33DK0702740351. The authors thank the Graduate professional Writing Center in WSU for proofreading the manuscript.

REFERENCES

Andreatta MM, Munoz SE, Lantieri MJ, Eynard AR, Navarro A (2008) Argentina Preventive Medicine 47: 136-139

Asbury GR, Klasmeier J, Hill HH, Jr (2000) Talanta 50: 1291–1298

Asbury GR, Wu C, Siems WF, Hill HH, Jr (2000b) Anal Chim Acta 404: 273-283

Budimir N, Weston DJ, Creaser CS (2007) Analyst (Cambridge, UK) 132: 34-40

Chen YH, Hill HH Jr, (1994) J Microcol Sep 6: 515-524

Chiarello-Ebner K (2006) Pharm Techn Pharm Technol 30: 52-64

Cohen MJ, Karasek FW (1970) J Chromatogr Sci 8: 330-337

Dwivedi P, Bendiak B, Clowers BH, Hill HH, Jr (2007) J Am Soc Mass Spectrom 18: 1163–1175

Dwivedi P, Wu P, Klopsch SJ, Puzon GJ, Xun L, Hill HH, Jr (2008) Metabolomics 4: 63–80

Eckers C, AM-F Laures AM-F, Giles K, Major H, Pringle S (2007) Rapid Commun Mass Spectrom 21, 1255–1263

Eiceman GA, Blyth DA, Shoff DB, Snyder PA (1990) Anal Chem 62: 1374-1379

Eiceman GA, Nazarov EG, Stone JA (2003) Anal Chim Acta 493: 185-194

Heydari R (2008) Anal Lett 41: 965-976

Hill HH Jr, Simpson G (1997) Field Anal Chem Technol 1: 119-134

http://Encyclopedia Britannica. Accessed on May 12, 2009

Huff J, LaDou J (2007) Int J Occup Environ Health 13: 446-448

Kaddis CS, Lomeli SH, Yin S, Berhane B, Apostol MI, Kickhoefer VA, Rome LH, Loo JA (2007) J Am Soc Mass Spectrom 18: 1206–1216

Karasek FW, Hill HH, Kim SH (1976) J Chromatogr 117: 327-336

Lee D-S, Wu C, Hill HH Jr, (1998) J Chrom A 822: 1-9

Liu X, Valentine SJ, Plasencia MD, Trimpin S, Naylor S, Clemmer DE (2007) J Am Soc Mass Spectrom 18: 1249-1264

Mason EA, McDaniel EW (1988) Transport Properties of Ions in Gases Wiley: New York

Mason EA, Schamp HW Jr (1958) Ann Phys 4: 233-270

McCann D, Barrett A, Cooper A, et al. (2007) Lancet 370: 1560–1567

McLean JA, Ridenour WB, Caprioli RM (2007) J Mass Spectrom 42: 1099–1105

McMinn DG, Kinzer JA, Shumate CB, Siems WF, Hill HH Jr, (1990) J Microcol Sep 2: 188-192

O'Donnell RM, Sun X, Harrington PB (2008) Trends Anal Chem 27: 44-53

Payne K, Fawber W, Faria J, Buaron J, DeBono R, Mahmood A (2005) Spectroscopy Magazine Online 24–27. http://www.forumsci.co.il/newsletters/IMS-for-Cleaning-Verification.doc Accessed February 12, 2009

Shumate CB, Hill HH (1989) Anal Chem 61: 601-606

Shumate C, St Louis RH, Hill HH, Jr (1986) J Chromatogr 373: 141-173

Siems WF, Wu C, Asbury GR, Tarver EE, Hill HH, Larsen PR, McMinn D (1994) Anal Chem (1994) 66: 4195-4201

Tan Y, DeBono R (2004) Today's Chemist at Work November p 15

Taraszka JA, Gao X, Valentine SJ, Sowell RA, Koeniger SL, Miller DF, Kaufman TC, Clemmer DE (2005) J Proteome Res 4: 1238

Waltman MJ, Dwivedi P, Hill HH, Jr Blanchard WC, Ewing RG (2008) Talanta 77 1: 249-255

Weihrauch MR, Diehl V (2004) Ann Oncol 15:1460-1465

Weston DJ, Bateman R, Wilson ID, Wood TR, Creaser CS (2005) Anal Chem 77: 7572-7580

Williamson CS (2008) Nutr Bull 33: 4-7

Wittmer D, Chen YH, Luckenbill BK, Hill HH (1994) Anal Chem 66: 2348–2355

Wongiel S, Hymete A, Mohammed AIM (2008) Ethiopian Pharm J 26: 39-48

Wu C, Siems WF, Asbury GR, Hill HH (1998) Anal Chem 70: 4929-4938

Wüthrich B (1993) Ann Allergy 71: 379-384

Table 1 ESI-APIMS operating conditions summary

Parameter	*Settings*
Reaction region length	7.5 cm
Drift region length	25.0 cm
ESI voltage	15.6 kV
Voltage at first ring	12.12 kV
ESI flow	180 µl hr^{-1}
Drift tube potential	10.80 ± 0.01 kV
Gate closure potential	±40 V
Gate pulse width	0.1 ms
Scan time	35 ms
Buffer gas	Nitrogen
Buffer gas temperature	150 ± 2 °C
Buffer gas flow	900 ml min^{-1}
Pressure	690-700 Torr

Table 2 Reduced mobilities of food additives and active ingredients in OTC drugs and their concentrations in the solution analyzed

	K_0, $cm^2V^{-1}s^{-1}$		
Compound	This work	Literature values	Concentration (mM)
Acetaminophen	1.66	1.67 [a]	[1] 44, [3] 4.8, [4] 33
Aspartame	1.16		[12] 0.12
Bisacodyl	0.98		[7] 0.5
Caffeine	1.53	1.54 [a] 1.54 [b]	[4] 0.067, [12] 0.067, [13] 0.05, [14] 0.05
Dextromethorphan	1.22		[3] 0.058, [5] 0.057
Diphenhydramine	1.23		[1] 0.87, [6] 0.017
Famotidine	1.15		[11] 0.50
Glucosamine	1.54	1.55 [c] 1.37 [d]	[8] 0.5
Guaifenesin	1.51		[5] 1.0
Loratadine	1.04		[9] 0.5
Niacin	1.80		[2]
Phenylephrine	1.53		[1] 0.50, [3] 0.050
Pyridoxine	1.62		[2]
Tetrahydrozoline	1.42		[10] 0.05
Thiamin	1.26		[2]

[a] (McMinn et al. 1990); [b] (Waltman et al. 2008); [c] (Chen and Hill 1994); [d] (Lee et al. 1998); [1] Allergy and sinus headache medication (Benadryl®, Pfizer, Morris Plains, NJ). [2] Vitamin B supplement (People's Choice, Mason Vitamins, Miami Lakes, FL). [3] Cold medication (Rite Aid, Camp Hill, PA). [4] Migraine medication (Excedrin®, Novartis). [5] Cough syrup (Tussin DM Assured). [6] Allergy drug (Allergy liquid, Assured, Bio-Pharm, Levittown, PA). [7] Laxative medication (Women's Laxative, Rite Aid, Harrisburg, PA). [8] Joint nutritional supplement (Spring Valley®, Schiff, Salt Lake City, UT). [9] Antihistaminic medication (Claritin®, Schering, Memphis, TN). [10] Eye drops (Eyelieve®, Orallabs, Memphis, TN). [11] Antacid medication (Acid Reducer, Rite Aid, Harrisburg, PA); [12] Diet coke. [13] Antioxidant water (Snapple®). [14] Orange Twist (Eating Right®).

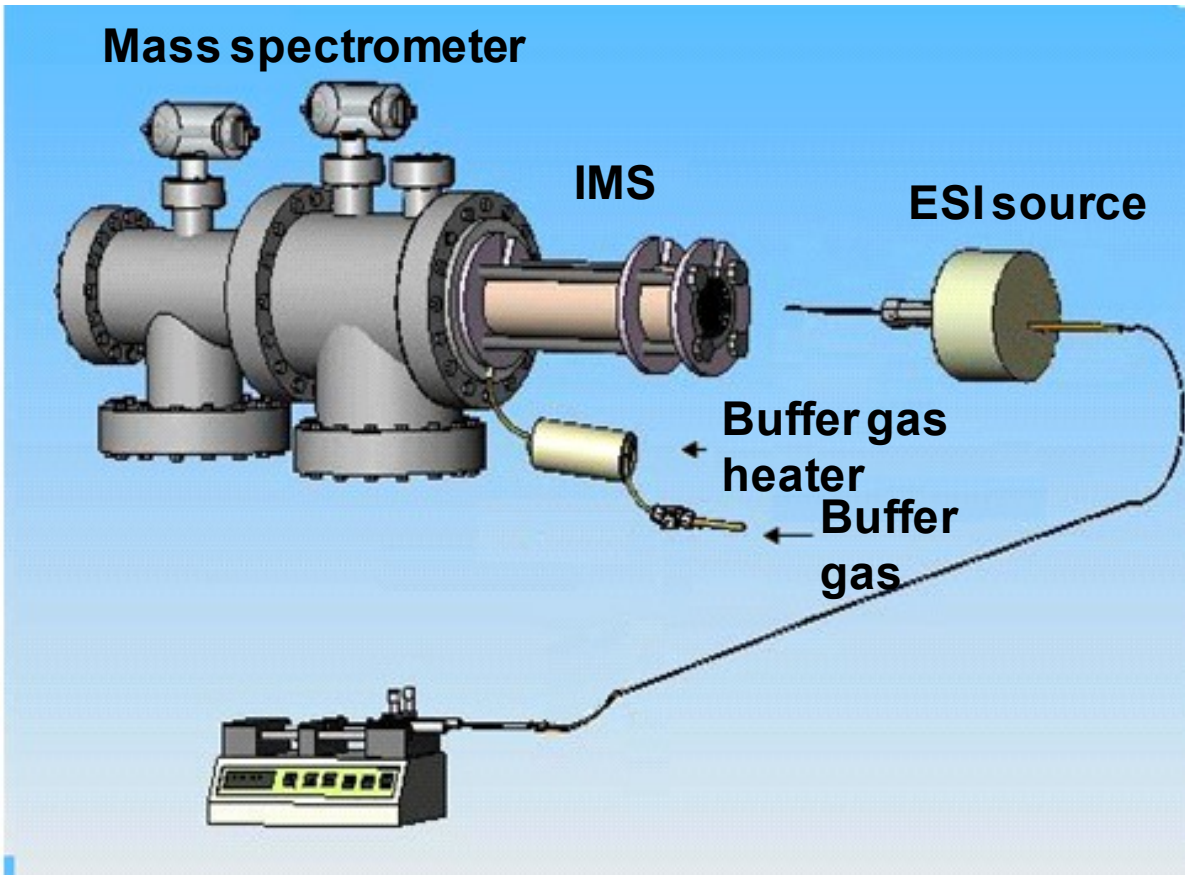

Fig. 1 Instrument. Section view of the atmospheric pressure ion mobility-quadrupole mass spectrometer

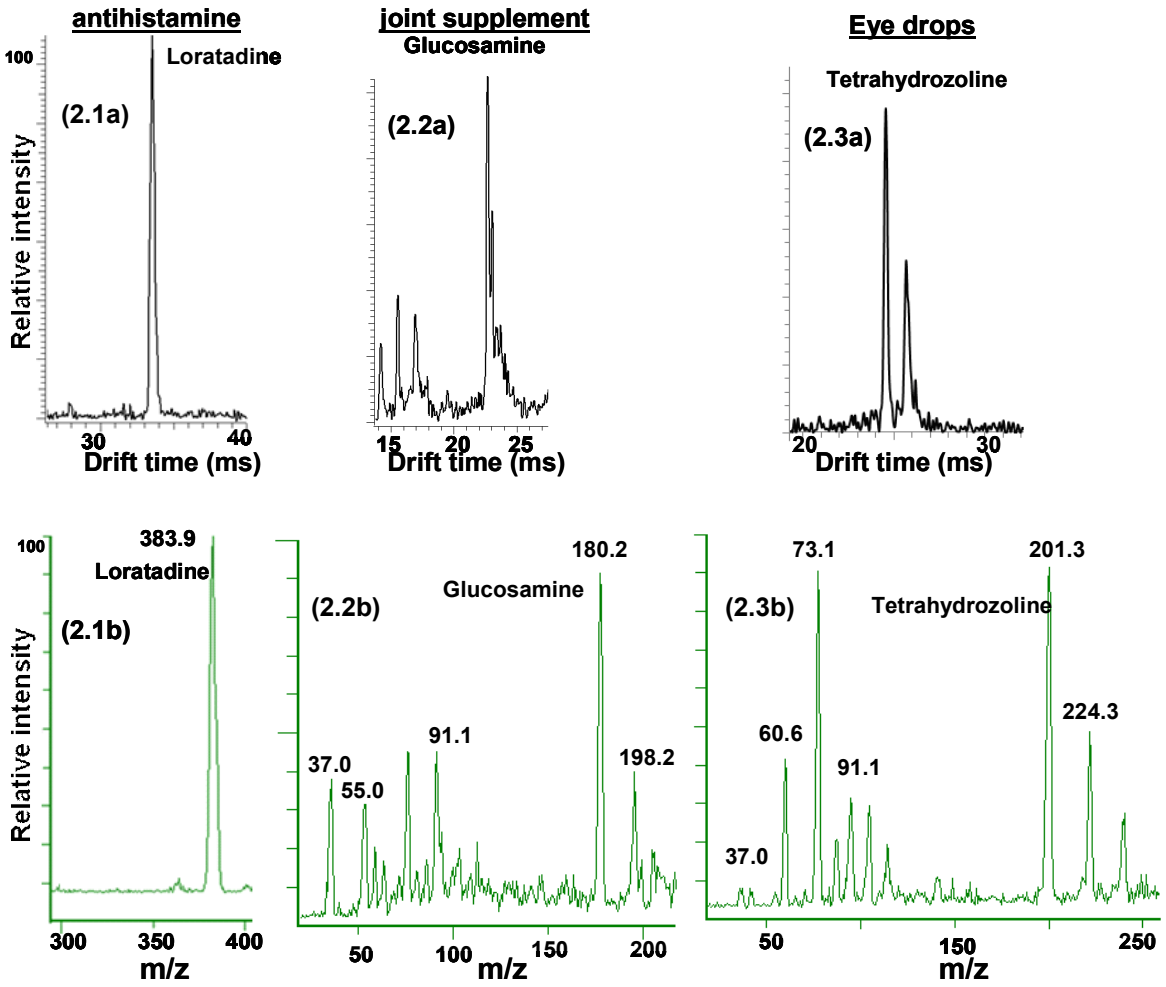

Fig. 2 Mobility (a) and mass spectra (b) of single-ingredient drugs. 2.1 Spectra of an antihistaminic medication (Claritin®, Schering, Memphis, TN) showing the protonated peaks of loratadine (382.9 g mol^{-1}) at 33.5 ms and m/z 383.9. 2.2 Spectra of a joint nutritional supplement (Spring Valley®, Schiff, Salt Lake City, UT) showing the protonated peaks of glucosamine (179.2 g mol^{-1}) at 23.1 ms and m/z 180.2. 2.3 Spectra of eye drops (Eyelieve®, Orallabs, Memphis, TN) showing the protonated peaks of tetrahydrozoline (200.3 g mol^{-1}) at 24.5 ms and m/z 201.3; the peak at m/z 224.1 and 26 ms may be the sodiated adduct of tetrahydrozoline.

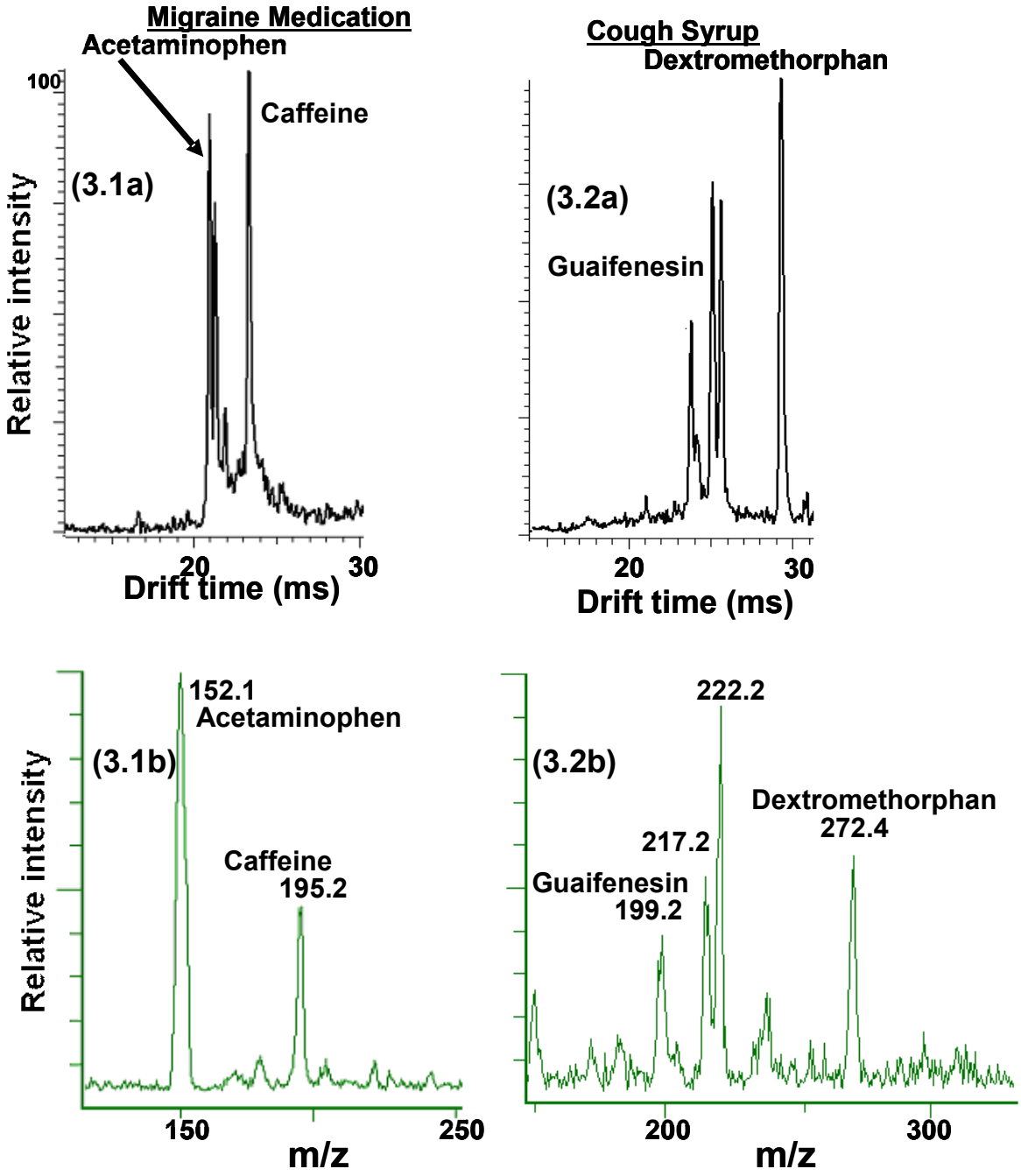

Fig. 3 Mobility (a) and mass spectra (b) of two-ingredient drugs. 3.1 Spectra of a migraine medication (Excedrin®, Novartis) showing the protonated peaks of acetaminophen (151.1 g mol^{-1}) at 21.0 ms and m/z 152.1 and caffeine (194.2 g mol^{-1}) at 23.3 ms and m/z 195.2; acetyl salicylic acid, another component of the drug, must be detected in the negative mode. 3.2 Spectra of a cough syrup (Tussin DM Assured) showing the protonated peaks of guaifenesin

(198.2 g mol^{-1}) at 23.8 ms and m/z 199.2 and dextromethorphan (271.4 g mol^{-1}) at 29.3 ms and m/z 272.4; a possible water cluster of guaifenesin is visible at 25 ms and m/z.

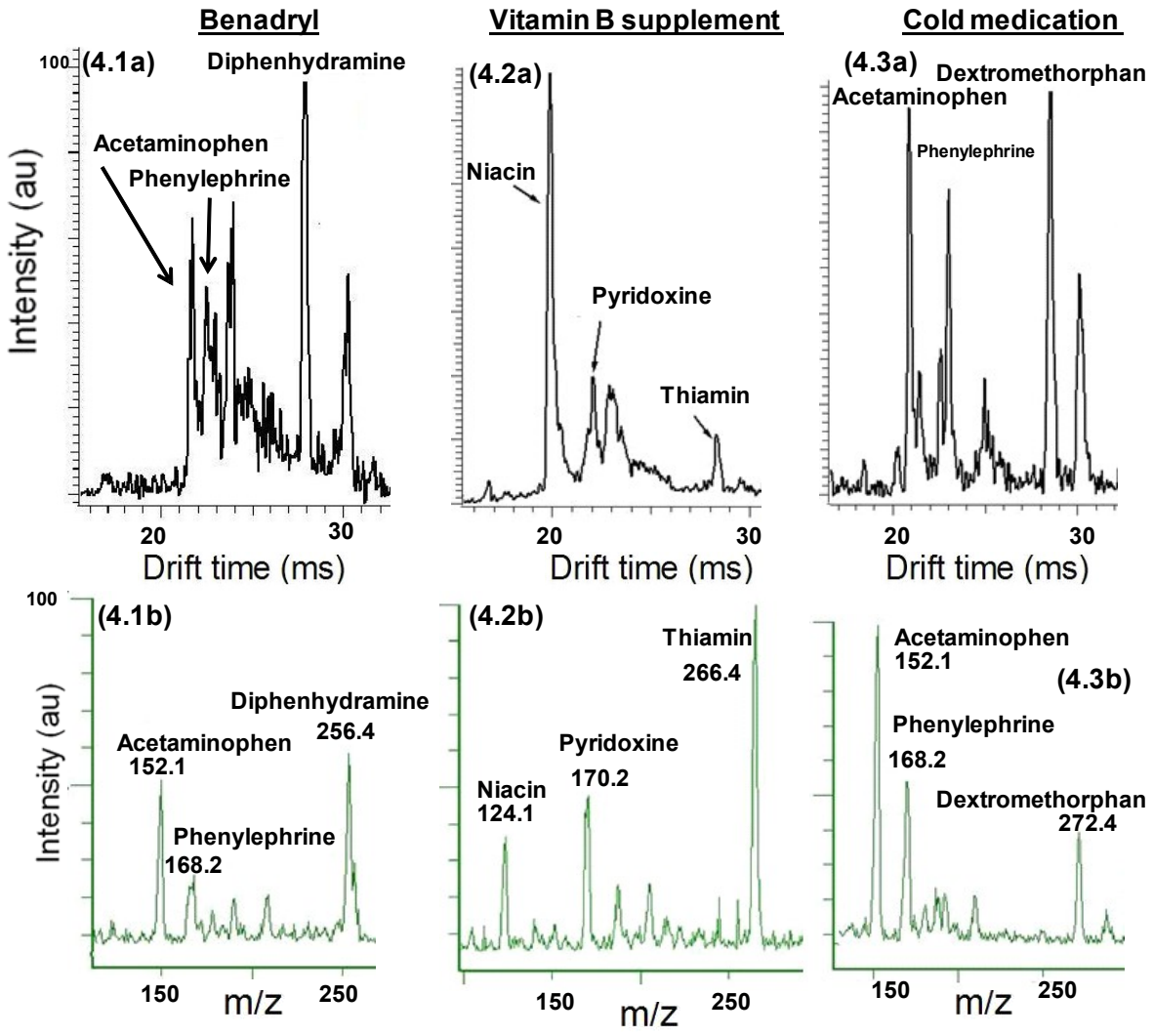

Fig. 4 Mobility (a) and mass spectra (b) of three-ingredient drugs. This figure demonstrates the rapid IMS separation and identification of complex formulations. 4.1 Spectra of an allergy and sinus headache medication (Benadryl®, Pfizer, Morris Plains, NJ) showing the protonated peaks of the drug acetaminophen (151.1 g mol^{-1}) at 21.6 ms and m/z 152.1, phenylephrine (167.2 g mol^{-1}) at 22.6 ms and m/z 168.2, and diphenhydramine (255.4 g mol^{-1}) at 27.9 ms and m/z 256.4. 4.2 Spectra of a vitamin B supplement (People's Choice, Mason Vitamins, Miami Lakes, FL) showing the protonated peaks of niacin (123.1 g mol^{-1}) at 19.9 ms and m/z 124.1, pyridoxine (169.2 g mol^{-1}) at 22.1 ms and m/z 170.2, and thiamin (265.4 g mol^{-1}) at 28.3 ms and m/z 266.4. 4.3 Spectra of a cold medication (Rite Aid, Camp Hill, PA) showing the protonated peaks of acetaminophen at 21.0 ms and m/z 152.1, phenylephrine at 23.1 ms and m/z 168.2, and dextromethorphan (271.4 g mol^{-1}) at 28.5 ms and m/z 272.4. Mobility peaks were identified by SIM-IMS.

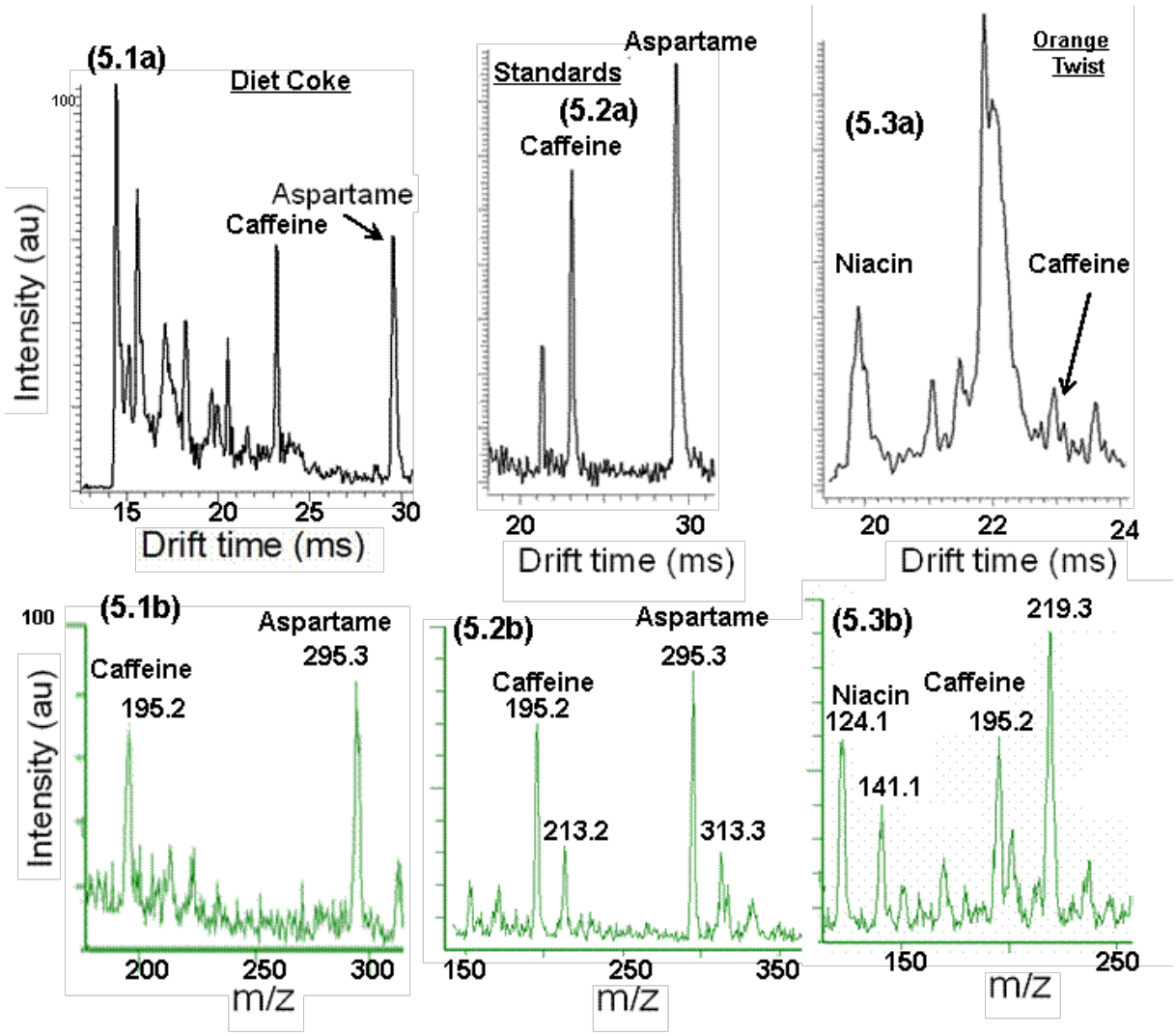

Fig. 5 Mobility (a) and mass spectra (b) of energetic beverages and standard solutions. 5.1 Spectra of Diet coke showing the protonated peaks of caffeine (194.2 g mol^{-1}) at 23.2 ms and m/z 195.2 and aspartame (294.3 g mol^{-1}) at 29.5 ms and m/z 295.3. 5.2 Standard solution of caffeine and aspartame (500µM) showing the protonated peaks of caffeine at 23.0 ms and m/z 195.2 and aspartame at 29.4 ms and m/z 295.3. The peaks at m/z 213.2 and 313.3 are most probably water clusters. 5.3 Spectra of an antioxidant water (Snapple®) showing the protonated peaks of niacin (123.1 g mol^{-1}) at 19.8 ms and 124.1 and caffeine at 23.0 ms and m/z 195.2.

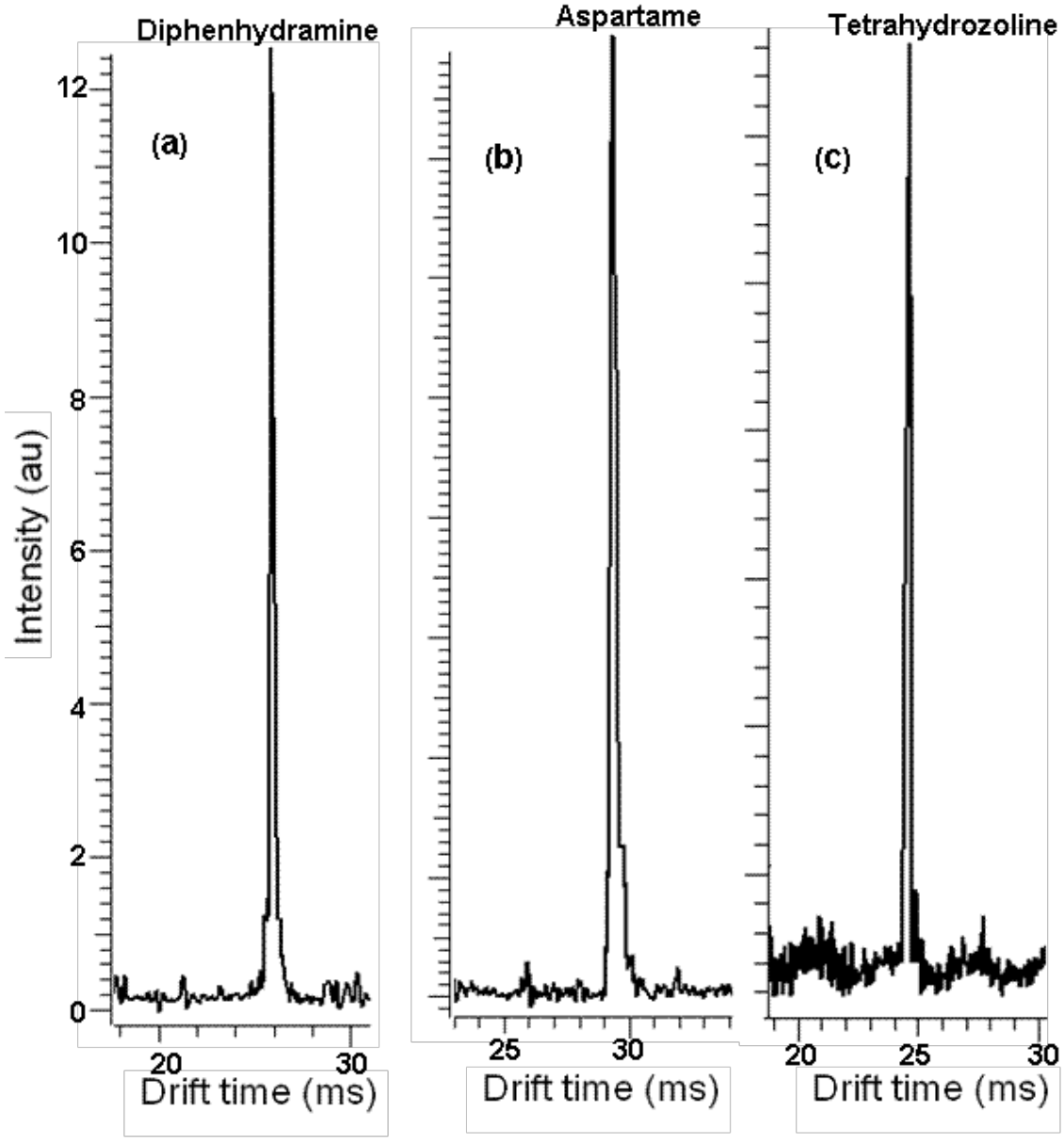

Fig. 6 Resolving power. SIM-IMS spectra of drugs and food additives showing the high resolving powers obtained by IMS. (a) Diphenhydramine (Resolving power 140) in the allergy and sinus headache medication (Benadryl®, Pfizer, Morris Plains, NJ). (b) Aspartame (Resolving power 126) in Diet Coke. (c) Tetrahydrozoline (Resolving power 113) in eye drops (Eyelieve®, Orallabs, Memphis, TN). Mobility spectra were averaged 250 times

Chapter Six

OVERALL CONCLUSIONS

i) Introduction of modifiers into the buffer gas can improve the resolution of compounds overlapping in the IMS spectra

The injection of modifiers into the buffer gas of an ion mobility spectrometer formed analyte-modifier clusters of large collision cross sections. The analyte-modifier clustering induced reductions in the mobility of the analytes, and depended on the temperature of the buffer gas and concentration and type of modifier. These reductions in mobility were different for different compounds because clustering also depended on the size and steric hindrance of the analytes; small analytes showed large reductions in mobility because the increase of the collision cross sections upon clustering is more pronounced as the size of the analytes decrease. Intramolecular bridges caused limited clustering in diamines by sterically hindering the attachment of modifier molecules to the positive charge, and delocalizing it. Other types of steric hindrance and large size of some analyte ions also produced limited clustering. These differences in clustering were applied to the separation of mixtures of compounds that overlapped in IMS by selectively changing their mobilities.

ii) Two chemical standards, an instrumental standard and a mobility standard, should be used to determine reduced mobility values.

When modifiers were introduced as contaminants into the buffer gas of an ion mobility spectrometer, the mobilities of IMS chemical standards, such as tetraalkylammonium ions

(tetramethylammonium, tetraethylammonium, tetraprophylammonium, and tetrabutylammonium ions), DTBP, and 2,4-lutidine, decreased to different extents or did not show change; the changes in mobilities depended on the molecular weight of the standards and their steric hindrance. Therefore, we classified IMS chemical standards, according to their response to contaminants, in two classes: ***instrument standards,*** used to calculate IMS instrumental parameters such as temperature and drift tube length, were sensitive to instrumental parameters and not to contamination in the buffer gas; and ***mobility standards,*** used to detect contamination in the buffer gas, clustered with contaminants and showed concomitant changes in mobility. Both standards should be used for IMS calibration; first instrument standards are used to calibrate the mobility instrument and, then, mobility standards are used to determine the presence of contamination. DTBP and tetraalkylammonium ions were better instrument standards than 2,4-lutidine, because their reduced mobilities were less affected by the presence of contamination, but they were not as good mobility standards as 2,4-lutidine. TBA and TPA ions were the best instrument standards.

iii) Ion mobility spectrometry can be a rapid alternative method to liquid chromatography for the qualitative analysis of over-the-counter drugs and beverages

Analysis times below 10 seconds were obtained in the analyses of over-the-counter drugs and beverages by ESI-IMS. Separation and identification of the analytes were obtained in complex samples after a simple dissolution step and the reduced mobilities of 15 drug and beverage ingredients are reported. The combination of fast analysis times, low cost, as well as easy and inexpensive maintenance of ESI-IMS instruments, make ion mobility spectrometry an

appealing alternative for the qualitative determination of over-the-counter drugs and food additives.

APPENDIX

Chiral Separations by Ion Mobility Spectrometry

Abstract

Chiral compounds have great economical importance, as well as varying clinical, industrial, and biological applications, and environmental impact. In this work, racemic mixtures of 20 common α-amino acids and chiral drugs were assayed for separation of enantiomers by ion mobility spectrometry-quadrupole mass spectrometry. Separations were attempted by introducing chiral selectors into the buffer gas. (R)-α-(trifluoromethyl) benzyl alcohol, (R)-tetrahydrofurane-2-carbonitrile, and L and D-enantiomers of 2-butanol and 1-phenyl ethanol were tested as chiral selectors. Experimental conditions such as buffer gas temperature, concentration, and type of chiral selectors, analyte concentration, ESI voltage, ESI solvent pH, and buffer gas flow rate were varied in the effort to resolve racemic mixtures. In several experiments, the individual enantiomers yielded different drift times for periods of several hours; these drift times were different enough (~ 0.3 ms) to partially resolve the enantiomers in a racemic mixture; however, the racemic mixtures always yielded a single mobility peak under all the conditions experimented.

INTRODUCTION

Enantiomers are molecules that are not superimposable mirror images of each other. Enantiomers were discovered by Louis Pasteur[1] in 1848 and exhibit:

- Rotation of the plane of polarization of polarized light (optical activity).
- Differences in their biological and microbial biodegradation properties.[2]
- Different properties in asymmetrical environments, i.e., the formation constants of diastereomeric complexes with chiral compounds are different for both enantiomers, which is the basis of chiral separations.

Chiral compounds are of great significance for human kind due to their economical importance, clinical and biochemical implications, industrial applications, and their environmental impact. An indication of the importance of chirality is the requirement of homochirality in all biological polymers of eukaryotes to fulfill their biological functions; racemic proteins may not fold in the specific shapes required to activate enzymes because they would have their side chains interacting randomly.[3] Therefore, the biosphere has mostly L-amino acids. D-amino acids have not been found in normal proteins though some of them are found in eukaryotic organisms but mainly in pathological states or due to aging. However, D-amino acids are essential to cell wall structure and metabolic pathways of bacteria.[4-5] Similarly, only D-sugars are present in nucleic acids and metabolic pathways.[6-9]

The post-translational modification of amino acids from L to D reveals the clinical and biochemical importance of chirality. This racemization has been well documented in small peptides, [10-16] it is functionally significant to endocrine function[17] and neurotransmission[17-26] and has been related to schizophrenia, ischemia, epilepsy, and neurodegenerative disorders,[17] aging,[27-31] cataracts,[31,32] renal disorders,[33] and Alzheimer's disease.[17,18,34-40] This amino acid racemization has found applications in food quality control,[41,42] forensic[43-48] and geological dating,[49-53] and extraterrestrial life exploration.[54-60] Chirality is also important due to the different pharmacological effects of enantiomers; (+)-ascorbic

acid, S-(-)-warfarin, S-(-)-propanolol, and (-)-epinephrine produce the expected effect of these drug (they are called eutomers) whereas their enantiomers (distomers) are inactive, far less potent, or even toxic.[61-64] The differences in aroma between some enantiomers also are explained by chirality.[65]

The economic importance of chiral compounds is growing rapidly every year. Approximately 39% of all drugs worldwide (US $152 billion) were sold as single enantiomers in 2002, and these figures are increasing at an annual rate of 7-8%. By 2008, these sales are expected to exceed US $200 billion.[66]

The environmental impact of chiral pollutants is another facet of the importance of chiral compounds and stresses the need for better chiral separations. Chiral toxic and ecotoxic compounds are produced by thousands of tons every year for agricultural, industrial, pharmaceutical, cosmetic, and other purposes.[67-76] Eutomers of pesticides, for example, have the desired effect on target species whereas distomers (or both) might have adverse effects on non-target species.[76]

The racemization of analytes could be of interest in this research given the acidic conditions of the ESI solution used as solvent. Racemization has been profusely demonstrated in compounds such amino acids.[10-16] *Acid-catalyzed racemization* occurs at a much slower rate than the base-catalyzed process. It involves protonation of the carboxyl group of the amino acid followed by the removal of the α-CH proton to form dihydroxiaminocompounds that regenerate to an equimolar mixture of D- and L-isomers.[77] Bada studied the rates of racemization of amino acids as a function of pH. For pH 2, a pH similar to that of the ESI solvent, he found that the log of the rate constant was approximately -11 at 25˚C.[78] These rates are too low to be significant in this investigation.

Interaction Models in Molecular Recognition Processes

Stereoselectivity is important in molecular recognition processes to explain the mechanisms behind chromatographic enantioresolution and rational design of drugs, chiral stationary phases, proteins, and biomimetic receptors. The most widely accepted model for stereoselectivity, the three-point interactions model, calls for three-point interactions between receptor and substrate.[76,79-80] In this model, stereochemical differences in biological activities are due to the differential binding of enantiomers to a common site on a receptor surface. To distinguish between enantiomers, the receptor must have three non-equivalent binding sites. Discrimination occurs when one isomer can simultaneously interact with all sites whereas its enantiomorph interacts only with two sites. Steric factors and other non-binding or even repulsive interactions contribute to chiral selectivity. The three-point interaction model has been extensively applied and debated.[81-92]

Current Technologies for Chiral Separation and Identification.

Enantiomers can be separated in a chiral environment by direct or indirect methods. Direct methods, such as chromatography, require the formation of selector-enantiomer complexes with different binding constants. Indirect methods are specially applied to preparative processes; indirect methods attach a chiral reagent to the enantiomers to form diastereomeric intermediates with different physical properties. To recover the pure enantiomer, the intermediates are separated by physical means, and the chiral reagent is detached.[93]

Chromatography is the method of choice for chiral separations. Chromatographic methods use a column with a chiral stationary phase which retains selectively one enantiomer. Chromatography tolerates contaminants and has low limits of detection but suffers from high capital costs and significant dilution of products. It also requires an additional unit operation to remove solvent. In addition, chiral columns need less rugged conditions than other chromatography columns.[93]

The main limitation of chromatographic separations is that most favorable conditions are compound-specific. This specificity yields a long and expensive method development for each mixture.

Enantiomers have been traditionally resolved by formation of diastereomeric derivatives that can be separated by regular techniques such as crystallization and liquid membrane extraction. In *crystallization,* the formation of two diastereomers results from temporarily attaching a chiral enantiopure reagent to the enantiomers in a racemic mixture. The diastereomers have different properties such as solubility so one can be selectively crystallized.[94] An advantage of crystallization is that it can be brought to a preparative scale. Disadvantages are the number of workers involved, duration of separation, contamination of products by organic solvents, and cost of resolution reagents.[95]

In *liquid membrane extraction* of chiral compounds, a non-polar enantiomer in a source phase is extracted into a membrane filled with a non-polar solvent (the liquid membrane phase) and finally stripped into a receiving phase. Phase transfer species added to the membrane phase facilitate the extraction of polar solutes and increase selectivity. Stripping of the polar solute from the organic phase is induced by a change in pH or salt concentration. Advantages of liquid membrane extraction are the high yield and minute quantities of chiral extractants used.[96-97] Disadvantages are swelling and leakage.[98]

Mass spectrometry has several methods to separate racemic mixtures. In one of them, a chiral mixture is introduced with a transition metal ion (M) and a chiral reference compound (ref*) into the MS cell. The analyte enantiomers (A_R or A_S) and ref* are complexed with the metal. The singly deprotonated cluster ions $[M^{II}(A_R)(ref^*)_2–H]^+$ and $[M^{II}(A_S)(ref^*)_2–H]^+$ are usually generated in the MS experiment. The intensities of the $[M^{II}(A_R/A_S)(ref^*)\text{-}H]^+$ (I_R or I_S) and $[M^{II}(ref^*)_2–H]^+$ (I_{ref*}) ions are measured. The chiral purity of the mixture can be found because there is a linear relationship between the natural logarithm of R ($R = (I_R + I_S)/I_{ref*}$) and the enantiomeric excess.[93] Unfortunately, mass

spectrometric methods for chiral separations require calibration curves and are not universal nor well established.

Sultan and Gabryelski partially separated D- and L-lactic acid by forming diastereomeric complexes with L-tryptophan in drinking water using *high-field asymmetric waveform ion mobility spectrometry* (FAIMS).[99] Enantiomer separation of amino acids by complexation with chiral reference compounds has been also obtained by high-field asymmetric waveform ion mobility spectrometry.[100] Mie et al. presented a novel method of enantioseparation using FAIMS coupled to mass spectrometry detection. Upon addition of an appropriate chiral reference compound to the analyte solution and subsequent electrospray ionization of the solution, analyte enantiomers formed diastereomeric complexes, which were separated by FAIMS.[101] Besides mass spectrometry and FAIMS, several spectroscopic techniques, such as chiroptical detection, polarimetry, circular dichroism, vibrational optical activity, and Raman optical activity, have been used in chiral analysis.[102]

Specific immunoassay with antibodies was used for chiral analysis.[9] Its main disadvantages are the requirement of one antibody for every analyte, lability and immobilization problems, potential loss of function, and production of antibodies; antibody production involves messy cell cultures and animals.[103] In *Isotope labeling*, enantiomers are labeled with stable isotopes and quantified by isotope dilution methods. Disadvantages of isotope labeling are the high cost of radioisotopes, health hazards, unavailability of labeled enantiomers, legal limitations, labeling difficulties, and chemical and biochemical instability.[104] Fluorescent semiconductor nanoparticles were made by stabilizing cadmium sulfide nanoparticles, or *quantum dots*, QD's, with penicillamine enantiomers which gave off a green–white light when excited with UV light. When a racemic mixture of the two enantiomers was used, the QD's gave off a blue–white light allowing the QD's to be used as fluorescent chirality sensors.[105] *Kinetic techniques* for chiral separations are based on the different reaction rates of enantiomers but are restricted to enzymatic reactions.[106] A new chiral separation technique is based on

the transport properties in a microfluidic flow with spatially variable vorticity.[107] Other techniques for chiral separation are thin layer chromatography,[108] biphasic recognition chiral extraction,[109] countercurrent chromatography,[110] capillary isotachophoresis,[111] and capillary electrophoresis.[112] Analytical Chemistry publishes a biannual review on chiral separations.[113]

Ion mobility spectrometry

IMS is an analytical technique that separates gas-phase ions moving under an electric field based on their size to charge ratios. In the ion mobility spectrometer, ions collide repeatedly with a buffer gas but are accelerated continuously by the field. This combination of collisions and accelerations rapidly thermalizes the ions and averages their velocities to values that depend on their collision cross sections (Equation 3).[114] These velocities can be used to calculate a property of ions drifting under the influence of an electric field, the mobility constant, *K*:

$$K = \frac{\mathrm{v}}{E} = \frac{L^2}{V.t_d} \quad (1)$$

where v is the velocity of the ion in cm s^{-1}, *E* the electric field in the drift region in V cm^{-1}, *L* the distance in cm the ion travels from the ion gate to reach the detector, *V* the total voltage drop in V in the drift region, and t_d the time the ion takes traveling the distance *L* in s. If the electric field is less than ~500 V cm^{-1} (at atmospheric pressure), v should be a linear function of *E*. In order to compare *K* values in different experimental conditions, ion mobilities must be normalized to standard conditions. This normalization yields reduced mobilities (in cm^2 V^{-1} s^{-1}) which are characteristic of every compound in a given buffer gas:

$$K_0 = K \frac{P}{760} \frac{273}{T} \quad (2)$$

where P is the pressure in Torr and T is the temperature of the buffer gas in Kelvin.[115] A compilation of reduced mobility values from ambient pressure ion mobility spectrometry was published in 1986.[116] Kinetic theory yields the Mason–Schamp equation for the reduced mobility (mobility at standard temperature and pressure conditions) of ions in an ion mobility spectrometer. This equation governs transportation of gas-phase ions:[117]

$$K_0 = \frac{3q}{16N_0}\sqrt{\frac{2\pi}{\mu kT}}\frac{1+\alpha}{\Omega}\frac{P}{760}\frac{273.16}{T} \quad (3)$$

where P is the pressure in Torr, T the temperature in ºC, q the charge of the ion, N_0 the gas number density at STP ($N_0 = P/kT$), μ the reduced mass of an ion-buffer gas pair, k the Boltzmann constant, and Ω the ion-neutral collision cross section. α is a small correction term with a magnitude of less than 0.02 when the ion mass is larger than the mass of the buffer gas molecule. The reduced mass is defined as $\mu = [mM/(m + M)]$, where m and M are the molecular mass of the analyte and the buffer gas, respectively.

Resolving power. Resolving power is an indication of separation efficiency and can be calculated in IMS by:

$$R = t_d / w \quad (4)$$

where t_d is the drift time of the ion of interest and w is the temporal peak width measured at half-height.[118] Regardless of its resolving power, an instrument cannot separate two compounds with identical drift times. A high resolving power is required for the separation of enantiomers of chiral compounds because the IMS peaks of these molecules have very similar drift times.

Polar chiral selectors introduced into the buffer gas of an ion mobility spectrometer interact selectively with the enantiomers of chiral compounds depending on the enantiomers stereochemistry. This selective interaction causes the analyte drift times to increase to different extents, which makes

possible the analyte separation. The separation factor, α, describes the degree of separation of two compounds. When this value is large, separation is easy:

$$\alpha = \frac{td_2}{td_1} \quad (5)$$

where td_1 and td_2 are the drift times of the faster and slower ions, respectively. An α value of 1 indicates that two compounds cannot be separated with the current resolution of the IMS instrument.

Chiral ion mobility spectrometry. Chiral ion mobility spectrometry separated enantiomers of sugars, drugs and amino acids using S/R-2-butanol as a chiral selector in nitrogen buffer gas. The maximum separation factor between the enantiomers was 1.004 at a flow rate of 45μL/hr (~6.1 ppmv) of (S)-2-butanol chiral selector.[119] This method enhances selective ion-molecule interaction forces by introducing a polar chiral selector into the buffer gas. The enantiomers form transient analyte-chiral selector diastereomeric complexes with different binding constants. The enantiomer having the stronger interaction with the chiral selector will drift a longer time. This difference in drift times produces the resolution of racemic mixtures. Chiral separations may be difficult to obtain in IMS due to the expected small differences in the energies of formation of the two diastereomeric complexes. Low buffer gas temperatures may increase chiral separation by increasing the stability of the diastereomeric complexes. High concentrations of chiral selector may enhance the formation of diastereomeric complexes and, therefore, increase chiral separation.

In this work, ion mobility spectrometry-quadrupole mass spectrometry was used to test mixtures of enantiomers of amino acids and chiral drugs for enantioseparation. Separation and identification of amino acids and drugs are important for clinical, biological, and pharmaceutical applications. The experiments were performed by introducing chiral selectors into the buffer gas. Several chiral liquids were used as chiral selectors and varying instrumental conditions were assayed

for chiral separation including ESI voltage, ESI solvent pH, analyte concentration, type and chiral selector concentration, and buffer gas flow rate.

EXPERIMENTAL SECTION

Instrument. Experiments were performed using an electrospray-ionization atmospheric-pressure ion mobility spectrometer (ESI-APIMS) interfaced through a 40-μm pinhole to a quadrupole mass spectrometer (Figure 2).

Table 1 shows common operating conditions used for this instrument. The IMS instrument was built at Washington State University and its full description and schematics can be found elsewhere.[120] A brief description is given here.

The ESI-APIMS instrument used was equipped with an electrospray ionization source and a drift tube. The tube consisted of two parts: a desolvation and a drift region operating in positive mode and separated by a Bradbury-Nielsen-type ion gate. Both regions had alternating 2.2”-OD, 2.0”-ID alumina insulating spacers (99.6% Al_2O_3, Advalue Tech., Tucson, AZ) and stainless steel field rings. A counterbore into each drift ring external face supplied a pocket for the neighboring ceramic insulator. Insulating spacers and steel rings were horizontally stacked in an interlocking design. All rings were kept together in a 2.5”-OD, 2.3”-ID alumina tube housed in an aluminum heating block. Field rings were connected in series by 1-MΩ (drift region) or 0.5 MΩ (desolvation region) high-temperature resistors (Caddock Electronics Inc., Riverside, CA, ±1%). When a high electrical potential was applied to the first ring, a 200-500 V cm^{-1} electric field was created throughout the drift tube.[121] An ESI target screen located at the first ring of the drift tube helped to electrospray the samples as explained later. The target screen was made out of 2-mm stainless steel mesh with a 0.5-cm diameter round orifice in the center.

The ion gate, which pulsed the ions into the drift tube, was made of approx. eighty parallel 75-μm Alloy-46 stainless steel wires (California Fine Wire Co., Grove Beach, CA) separated 0.6 mm. When the gate was open, all wires had a voltage with a value between those of the adjacent drift rings. The gate was closed when ±40 V were applied to adjacent wires so that a 320 V cm^{-1} orthogonal field stopped positive or negative ions approaching the gate. These voltages neutralized the ions on the negative or positive wires. This closure voltage was offset for 0.1 ms so that a narrow pulse of ions entered the drift region to be analyzed. A countercurrent of preheated N_2 buffer gas was introduced through a stainless-steel tube at the end of the drift tube at a flow rate of 0.9 L/min to help desolvate ions. To heat the buffer gas, it was passed through a stainless-steel tube coiled inside a heated aluminum block (Figure 2). The mobility spectrometer was operated at atmospheric pressure (680-710 Torr in Pullman, WA). Custom LabView software (National Instruments, Austin, TX) collected the IMS data and controlled the ion gate. The electronic controls for IMS gating and data acquisition were built at WSU.[122]

Modes of operation. Ion mobility spectra can be acquired in total ion monitoring (IMS) mode or by selective ion monitoring (SIM-IMS). In IMS mode, the IMS gate continually opens and closes and the mass spectrometer let all the ions reach the detector; in this mode, the ion mobility spectrum of all ions is obtained. In SIM-IMS mode, the IMS gate continually opens and closes and the DC and RF voltages are set to allow only ions with a specific mass, or a selection of specific masses, to reach the detector. SIM allows the IMS analysis of specific compounds without the interference of others of different masses. In IMS modes, the MS serves as a detector for the mobility spectrometer and no mass scan is performed. Mass spectra are obtained keeping the IMS gate open while the amplitudes of the quadrupole DC and RF voltages are ramped though keeping the RF/DC ratio constant; in this mode, all ions pass continuously through the IMS directly to the mass spectrometer where they are mass analyzed.

An ABB Extrel 150-QC (Pittsburgh, PA) quadrupole mass spectrometer (0-4000 Da) was used in this investigation. The software, electronics and detector of the mass spectrometer were upgraded in 2007. A Keithley model 427 amplifier (Keithley Instruments, Cleveland, OH) sent the output signal from the electron multiplier detector in the mass spectrometer to the data acquisition systems. The mass spectrometer was controlled with Merlin software (version 3.0 ABB Extrel, Pittsburgh, PA) and collected the mass spectral data. Igor Pro 5.0.3 (WaveMetrics, Portland, OR) was used to process the spectral data text files.

Materials and reagents. D and L forms of alanine, arginine, asparagine, aspartic acid, cysteine, glutamine, glutamic acid, histidine, isoleucine, leucine, lysine, methionine, phenylalanine, proline, serine, threonine, tryptophan, tyrosine, valine, atenolol, valinol, 2,4-dimethylpyridine (2,4-lutidine), 2,6-di-tert-butyl pyridine (DTBP), (R)-α-(trifluoromethyl) benzyl alcohol (tFMBA), (R)-Tetrahydrofuran-2-carbonitrile, and R and S enantiomers of 1-phenyl ethanol and 2-butanol, were purchased from Sigma-Aldrich (St. Louis, MO). These chemicals were ACS reagent grade and their purity was ≥98%. Water, methanol, and acetic acid were HPLC grade and were purchased from J. T. Baker (Phillipsburgh, NJ). These chemicals were selected to continue a previous study started in this laboratory.[119] They also provided a series of compounds required to test the effect of molecular weight and steric hindrance on chiral separation.

Sample preparation/introduction. All compounds were prepared at a 10 μM concentration (unless otherwise specified) in a 47.5:47.5:5 ratio of water/methanol/acetic acid. Acetic acid was used to increase the protonation of analytes. Liquid samples or blank solution (ESI solution) were infused continuously by electrospray ionization (ESI) using 250-μl syringes (Hamilton, Reno, NV) at a flow rate of ~3 μl min^{-1} into 30-cm-long, 100-μM-diameter capillary (Polymicro Technologies, Phoenix, AZ). This capillary was connected through a stainless steel union (Valco, Houston, TX) to a 50-μm inner diameter silica capillary. The end of this capillary was centered at the target screen placed at the

entrance of the mobility spectrometer. A high voltage of 15.6 kV (or 3.5 kV bias with respect to the target screen at the first ring) was applied to the stainless steel union to produce positive electrosprayed ions. To prevent cross contamination between the analytes, different syringes and capillaries were used for every compound whenever possible.

Chiral selector introduction. To introduce the chiral selectors into the buffer gas, the method used by Dwivedi et al.[119] was modified as follows. The liquid chiral selectors were injected with gas tight syringes (pumped by a KD Scientific pump, model 210) to prevent leaking. Chiral selectors were introduced through a 10-cm-long, 50-µm-inner diameter silica capillary into the buffer gas line using a T-junction, before the buffer gas heater (Figure 2). Introducing the chiral selector before the buffer gas heater provided a longer path to help obtain a homogeneous mixture of the chiral selector with the buffer gas. To help vaporize the chiral selector, the temperature of the T-junction was increased to ~150 °C using a heating tape (OMEGA Engineering, Stamford, CT). Separate capillaries and syringes were used to prevent cross contamination between the chiral selectors.

Identification of compounds. Analytes were identified by comparing their m/z signal in mass spectrometry to the molecular weight of their protonated molecules or cluster ions. Also, reduced mobilities of analytes protonated ions were compared with those from literature.

***Quantitation and calibration*.** Electrospray-ionization ion mobility spectrometry (ESI-IMS) is considered a semi-quantitative technique. The ionization process limits quantitation in ESI-IMS because analytes are ionized by charge transfer reactions with the reactant ions. When the reactant ions are depleted, analyte concentration in the electrosprayed sample cannot be derived from peak height because processes of charge competition can hinder complete ionization of the analyte. Nevertheless, this competition does not affect the measurement of enantiomeric ratios because enantiomers have the same proton affinity and ionization probability.[119] Therefore, the peak areas of the enantiomers should be proportional to their enantiomeric ratio. The reduced mobility of the

analyte ions was calculated from that of a calibrant, K_{0c}, the drift time of the calibrant at the specific conditions of the experiment, t_c, and the drift time of the analyte at the same conditions, t_d:

$$K_0 = K_{0c}(t_c/t_d) \qquad (6)$$

2,4-lutidine is commonly selected as calibrant for the mobility scale.[123] The method using Equation 6 saves the reading of barometers and eliminates the errors in measurement of the parameters in Equation 2. The length and temperature of the mobility spectrometer were calibrated using DTBP because the reduced mobility of this compound is independent of temperature.[124]

RESULTS AND DISCUSSIONS

Chiral separations of racemic mixtures of α-amino acids and chiral drugs were evaluated by introducing chiral selectors into the buffer gas of an ion mobility spectrometer-quadrupole mass spectrometer. MS spectra (500-averages) were acquired after stabilizing the chiral selector concentration for at least one hour. Mobility spectra (250-averages) were collected when the ratio of the peak of the protonated molecule to the analyte-modifier cluster ion peak was reproducible from one spectrum to the next, which indicates stable conditions in the drift tube.

1. Stability of the mobilities of valinol enantiomers with time.

Figure 4 shows the drift time of the ions of 943-μM solutions of valinol enantiomers and racemic mixtures of valinol when 0.68 mmol m^{-3} (25 ppmv) of (S)-2-butanol were introduced into the buffer gas in an 8-hr period at 150 °C. The drift times were always different for both enantiomers in this experiment. There was a minimum drift time separation of ~0.2 ms between the two enantiomers and a maximum of ~0.45 ms. This separation was large enough to resolve the enantiomers in a mixture, considering that the resolving power was high (~100). However, the racemic mixtures

yielded only one peak, with a drift time that matched that of the D-enantiomer. The standard deviations of the drift times over the 8-hr period were 0.08 ms (L-valinol) and 0.05 ms (D-valinol); this variation was caused mainly by the pressure drift. The peaks of individual solutions of the pure enantiomers of lysine, threonine, and atenolol yielded the same drift time when their enantiomers where individually analyzed using (S)-2-butanol modifier.

2. Effect of the chiral selector concentration on the mobilities of valinol enantiomers.

Figure 5a shows that the increase in chiral selector concentration from 0 to 6.8 mmol m^{-3} (254 ppmv) in the buffer gas increased the drift times of valinol enantiomers. Although there was always a drift time difference between both enantiomers (an average difference of 0.26 ms), only one peak was obtained when the racemic mixture was electrosprayed, as in the previous experiment. Figure 5a also shows that the curve at 125 °C flattened at high (S)-2-butanol concentrations; this flattened curve may indicate a ligand saturation of the sites on the analyte available for attachment of (S)-2-butanol molecules at high concentrations of (S)-2-butanol.

In other experiment with phenylalanine, (R)-1-phenyl ethanol was used as chiral selector between 0 and 10 mmol m^{-3} at 175°C. Different drift times were obtained for the pure enantiomers when (R)-1-phenyl ethanol was introduced into the buffer gas. No racemic mixtures were tested in this experiment. Results are summarized in the next table and Figure 5b.

(R)-1-phenyl ethanol, mmol m^{-3}	**L-Phenylalanine**	**D-Phenylalanine**	**Drift time difference (ms)**
0	23.63±0.02	23.64±0.02	0.01
5.0	24.83±0.02	24.7±0.025	0.08
7.5	25.12±0	25.05±0.01	0.07
10	25.37±0.04	25.28±0.02	0.09

Table 2 summarizes other experiments at different concentrations of chiral selector.

The increase in the drift time of valinol from ~20 to ~25 ms when (S)-2-butanol was

introduced into the buffer gas (Figure 5) were due to formation of a large valinol-(S)-2-butanol cluster ion; Figure 6 shows this cluster in the MS spectra of D-valinol when (S)-2-butanol was injected into the buffer gas. Figure 6 also demonstrates that, when the chiral selector concentration was increased from 2.7 to 4.1 mmol m^{-3}, the intensity of the protonated peak of D-valinol at m/z 104 decreased and that of the cluster ion peak of valinol at m/z 178 increased, as expected if the cluster was forming from protonated valinol. Figure 6 also illustrates the expected increase in intensity of the peak of the (S)-2-butanol trimer (m/z 223) and the appearance of the dimer (m/z 149) when the chiral selector concentration was increased from 2.7 to 4.1 mmol m^{-3}.

3. Effect of the analyte concentration on the resolution of its enantiomers.

The effect of valinol concentration on the mobilities of its enantiomers when (S)-2-butanol was introduced into the buffer gas was unimportant under the conditions of the experiments. Figure 7 shows the drift times of solutions of different concentrations of D- and L-valinol, and racemic mixtures of valinol enantiomers when 0.68 mmol m^{-3} (25 ppmv) of (S)-2-butanol were introduced into the buffer gas at 150 °C.

As before, the drift times of valinol enantiomers were significantly different (0.3 ms average) and the resolution was high (>100) when the individual solutions were analyzed, but a racemic mixture only produced a single peak with a drift time similar to that of the D-enantiomer. The standard deviation of the drift times over the duration of the experiment was 0.04 (L-valinol) and 0.07 ms (D-valinol); these variations were caused mainly by changes in pressure. Racemic mixtures of phenylalanine at concentrations of 10, 100 and 500 μM also were tested unsuccessfully for separation when 3.4, 5.4, and 7.5 mmol m^{-3} of (S)-2-butanol were introduced into the buffer gas at 150°C.

4. Effect of the temperature on the mobilities of valinol enantiomers.

Figure 8 shows the drift time of the response ions of 943-µM solutions of valinol enantiomers and racemic mixtures of valinol when the temperature of the buffer gas was varied from 125 to 200°C at a 0.68 mmol m^{-3} (25 ppmv) concentration of (S)-2-butanol. The drift times were always different for both enantiomers. The differences in drift times between the L and D-enantiomers of valinol were 0.41, 0.25, 0.17, and 0.08 ms at 125, 150, 175, and 200 °C, respectively. This decreasing difference indicates that the interaction valinol-(S)-2-butanol decreased probably due to the weak analyte-ligand bonds at high temperature. Again, this drift time difference was large enough to resolve the enantiomers in a mixture; however, the racemic mixtures yielded only one peak, with a drift time that also matched that of the D-enantiomer. This lack of separation was obtained in spite of the fact that the drift times of the enantiomers were sufficiently different (at 125 and 150°C) and the resolution was high enough (>80) to obtain a chiral separation.

The small interaction valinol-(S)-2-butanol at high temperature (Figure 8) agreed with data in the mass spectra in Figure 9. Figure 9a shows a large valinol-(S)-2-butanol cluster ion (m/z 168) and cluster ions of (S)-2-butanol (at m/z 149 and 223) at low temperatures (125°C), and Figure 9b shows only a small valinol-(S)-2-butanol peak along with a large protonated analyte peak that at high temperatures (≥200 °C). Additionally, the drift times of valinol remained unchanged with the increase in chiral selector concentration at 200°C (Figure 5), which indicates a weakened interaction valinol-(S)-2-butanol at high temperature. The (S)-2-butanol dimer (m/z 149) and trimer (m/z 223) did not form in Figure 9b also due to small interactions of (S)-2-butanol with (S)-2-butanol cluster ions at high temperatures.

5. Effect of the type of chiral selector on the separation of enantiomers.

(R) and (S)-1-phenyl ethanol, (R) and (S)-2-butanol, and (R)-α-(trifluoromethyl) benzyl alcohol (tFMBA) were assayed as chiral selectors. Results are summarized in Table 2. No chiral

separation was obtained analyzing racemic mixtures of the compounds recorded in Table 2 in the specific conditions used.

6. Effect of other parameters on the separation of enantiomers.

Other instrumental parameters and conditions were varied in the effort to obtain chiral separations. The following conditions were assayed but, in all cases, only single peaks were obtained for the racemic mixtures:

- Buffer gas flow rates of 3.6, 1.8, 0.9, and 0.45 l min^{-1} were used in the analysis of a 50-µM racemic mixture of valine with 6.8 mmol m^{-3} (25 ppmv) of (R)-2-butanol in the buffer gas as the chiral selector at 175°C. Low buffer gas flow rates increase the chiral selector concentration in the buffer gas.

- The ESI voltage was varied between 15.6 and 13.9 kV in the analysis of a 50-µM racemic mixture of valine with 6.8 mmol m^{-3} (25 ppmv) of (R)-2-butanol in the buffer gas as the chiral selector at 175°C; voltage differences of 3.5, 2.8, 2.4, 2.1, 1.9, and 1.8 kV with respect to the target screen were tested. The IMS signal of valine was lost when a voltage difference of 1.8 kV was reached.

- Concentrations of 5%, 1%, 0.1%, 0.03%, and 0.01% acetic acid in the ESI solution were assayed in the analysis of a 50-µM racemic mixture of valine with 6.8 mmol m^{-3} (25 ppmv) of (R)-2-butanol in the buffer gas as the chiral selector at 175°C. The IMS signal of valine was lost below 0.01% due to insufficient protonation.

- Fifty µM solutions of D and L enantiomers in 10:90, 70:30, 30:70, and 90:10 proportions (v/v) were assayed in the analysis of valine with 6.8 mmol m^{-3} (25 ppmv) of (R)-2-butanol in the buffer gas as the chiral selector at 175°C; the reason for these experiments was that the racemic mixture,

in the experiments detailed above, yielded a drift time similar to that of the D-enantiomer and different from that of the L-enantiomer; therefore, it was possible that the L-enantiomer was converting into D when they were mixed; the analyses of mixtures with different proportions of the enantiomers would show a shift from the drift time of the D-enantiomer to that of L when the concentration of L increased in the mixture, if this conversion was occurring. However, that shift was not observed and the same drift times were obtained for both enantiomers when (R)-2-butanol was introduced into the buffer gas.

- Buffer gas heater temperatures of 50, 80, 100, and 125 °C were assayed in the analysis of a 943-μM racemic mixture of valinol with 6.8 mmol m^{-3} (25 ppmv) of (S)-2-butanol in the buffer gas as the chiral selector; these temperatures were tested in order to discard the possibility of racemization of the chiral selector upon interaction with the hot metallic surface of the gas heater.

7. Reduced mobilities of compounds analyzed in this work.

Table 3 shows K_0 values for the compounds assayed in this work in nitrogen buffer gas. Values from Dwivedi et al.,[119] Beegle et al.,[125] and Asbury et al.[126] were obtained on the same instrument used in this work; the consistently higher K_0 values obtained in this investigation may be due to a better temperature control and by using Equation 3 and DTBP to establish the buffer gas temperature. This temperature was confirmed by direct measurement in the buffer gas inside the drift tube using a thermocouple. The temperature was lower than that indicated by another thermocouple in the body of the drift region aluminum heating block. The buffer gas temperature was also higher in the middle of the drift tube than at the ends. This difference in temperature between the thermocouples and between sections of the drift tube was probably due to heat transfer from the mobility spectrometer to the mass spectrometer.

The reproducibility of the reduced mobilities in Table 3 was <2%, and was calculated as the relative standard deviation (RSD) of the reduced mobilities of five different samples of the same concentration prepared independently and analyzed on different days. The repeatability of the reduced mobilities was <0.5%, and was calculated as the RSD of the reduced mobilities of five or more consecutive analyses (1600 averages each) of the sample.

CONCLUSIONS

Racemic mixtures of chiral compounds were assayed for chiral separation by introducing chiral selectors into the buffer gas of an ESI-IMS-QMS. In contrast to a previous work of our group, [119] no chiral separation was obtained; however, small differences were observed in the drift times of the enantiomers when they were analyzed individually. The lack of separation in the racemic mixtures occurred probably because we did not reproduce the precise conditions used previously. However, chiral separations seem possible as suggested by the different drift times obtained for the individual enantiomers. Several experimental conditions such as buffer gas temperature, chiral selector concentrations, drift tube voltage, pulse width, analyte concentration, ESI voltage, and buffer gas flow rate were studied for enantioseparation without success. (R)-α-(trifluoromethyl) benzyl alcohol (tFMBA), (R)-Tetrahydrofuran-2-carbonitrile, and R and S enantiomers of 1-phenyl ethanol and 2-butanol were used as chiral selectors. The lack of enantiomer separation cannot find a plausible explanation; an improper preparation of the racemic mixture cannot be argued because this mixture was prepared combining the pure enantiomeric solutions which were yielding different drift times; preferential ionization cannot be hypothesized because enantiomers have the same proton affinity and ionization probability; it was not likely that the L-enantiomer converted into D in a racemic mixture because in symmetric environments as the ESI solution both enantiomers have the same stability; finally, if this conversion would occur upon interaction with the chiral selector, a different drift time

would have been obtained when the pure L-enantiomer was analyzed. Future work must be focused to help obtain reproducible IMS parameters (such as temperature, pressure, and others that affect the mobility of the enantiomers) and to understand the chemistry underlying the singular behavior of the racemic mixture.

ACKNOWLEDGEMENTS

This work was supported by a grant from Excellims Corporation (Acton, MA) and NIH grant R33DK0702740351. The authors thank the Graduate and Professional Writing Center for proofreading the manuscript.

REFERENCES

1. Pasteur, L. *Ann. Chim. Phys.* **1848***, 24,* 442-459.

2. Kallenborn, R.; Huhnerfu, H. Springer, New York, **2001**.

3. Tverdislov, V. A.; Yakovenko, L. V. *Moscow University Physics Bulletin*, **2008**, *63*, 3, 151–163.

4. Hopkins, D. W.; O'Dowd, R. W.; Shiel, R. S. *Soil Biol. Biochem*. **1997**, *29*, 23-29.

5. Tanaka, T.; Mukahota, Y.; Yuasa, S. *Can J. Microbiol.* **1996**, *42*, 976-978. 14.

6. Frank, P.; Bonner, W. A.; Zare, R. N. **On One Hand but Not the Other: The Challenge of the Origin and Survival of Homochirality in Prebiotic Chemistry.** In *Chemistry for the 21st Century*; Keinan, E.; Schechter, I., Eds.; Wiley-VCH: Weinheim, **2001**; pp 173-208.

7. Hotchkiss, R. D. *J. Biol. Chem.* **1941,** *141*, 1, 171-185.

8. Lipmann, F.; Hotchkiss, R. D.; Dubos, R. J. *J. Biol. Chem.* **1941** *141*, 1, 163-169.

9. Beesley, T. E.; Scott, P. W. R. In *Chiral Chromatography.* Wiley, Chichester, U.K. **1998**.

10. Kreil, G. *Science* **1994**, *266*, 996-997.

11. Kreil, G. D. *Ann. Rev. Biochem.* **1997**, *66*, 337-345.

12. Shapira, R.; Chou, C. H.**.** *Biochem. Biophys. Res. Commun.* **1987**, *146*, 3, 1342-1349.

13. Shapira, R.; Wilkinson, K. D.; Shapira, G. *Prog. Clin. Biol. Res.* **1989**, *292*, 487-496.

14. Buczek, O.; Yoshikami, D.; Bulaj, G.; Jimenez, E. C.; Olivera, B. M. *J. Biol. Chem.* **2005**, *280*, 4247-4253.

15. Masters, P. M. *Calcif. Tissue Int.* **1983**, *35*, 1, 43-47.

16. McFadden, P. N.; Clarke, S. *J. Biol. Chem.* **1986**, *261*, 11503-11511.

17. Fuchs, S. A.; Berger, R.; Klomp, L. W. J.; de Koning, T. J. *Mol. Genet. Metab.* **2005**, *85*, 3, 168-180.

18. Mothet, J. P. *Pathol. Biol.* ***2001****, 49*, 8, 655-659.

19. Kartvelishvily, E.; Shleper, M.; Balan, L.; Dumin, E.; Wolosker, H. *J. Biol. Chem*. **2006**, *281*, 20, 14151-14162.

20. Shleper, M.; Kartvelishvily, E.; Wolosker, H. *J. Neurosci.* **2005**, *25*, 41, 9413-9417.

21. Mothet, J.-P.; Pollegioni, L.; Ouanounou, G.; Martineau, M.; Fossier, P.; Baux, G. *Proc. Natl. Acad. Sci. USA* **2005**, *102*, 15, 5606-5611.

22. Imai, K.; Fukushima, T.; Santa, T.; Homma, H.; Huang, Y.; Sakai, K.; Kato, M. *Enantiomer* **1997**, *2*, 143-145.

23. Schell, M. J.; Molliver, M. E.; Snyder, S. H**.** *Proc. Natl. Acad. Sci. USA* **1995,** *92*, 9, 3948-3952.

24. Tsai, G.; Yang, P.; Chung, L. C.; Lange, N.; Coyle, J. T. *Biol. Psychiatry* **1998**, *44*, 11, 1081-1089.

25. Tsai, G. E.; Yang, P.; Chang, Y. C.; Chong, M. Y. *Biol. Psychiatry*. **2006,** *59,* 3, 230-234.

26. Heresco-Levy, U.; Javitt, D. C.; Ebstein, R.; Vass, A.; Lichtenberg, P.; Bar, G.; Catinari, S.; Ermilov, M. *Biol. Psychiatry*. **2005,** *57*, 6, 577-585.

27. McFadden, P. N.; Clarke, S. *Proc. Natl. Acad. Sci. USA* **1982**, *79*, 8, 2460-2464.

28. Lindquist, J. A.; McFadden, P. N. *J. Protein Chem.* **1994**, *13*, 1, 23-30.

29. Helfman, P. M.; Bada, J. L. *Nature* **1976**, *262*, 5566, 279-281.

30. Dunlop, D. S.; Neidle, A.; McHale, D.; Dunlop, D. M.; Lajtha, A. *Biochem. Biophys. Res. Commun.* **1986**, *141*, 27-32.

31. Masters, P. M.; Bada, J. L.; Zigler, J. S., Jr. *Nature* **1977**, *268*, 71-73.

32. Masters, P. M.; Bada, J. L.; Zigler, J. S., Jr. *Proc. Natl. Acad. Sci. USA*. **1978**, *75*, 3, 1204–1208.

33. Bruckner, H.; Hausch, M. *J. Chromatogr*. **1993**, *614*, 7-17.

34. Shapira, R.; Austin, G. E.; Mirra, S. S. *J. Neurochem.* **1988**, *50*, 69-74.

35. Kubo, T.; Nishimura, S.; Kumagae, Y.; Kaneko, I. *J. Neurosc. Res.* **2002**, *70*, 474-483.

36. Takahiko, S.; Fukuda, H.; Murayama, S.; Izumiyama, N.; Shirasawa, T. *J. Neurosc. Res.* **2002**, *70*, 451-461.

37. Tomiyama, T.; Asano, S.; Furiya, Y.; Shirasawa, T.; Endo, N.; Mori, H. *J. Biol. Chem.* **1994**, *269*, 14, 10205-10208.

38. Kumashiro, S.; Hashimoto, A.; Nishikawa, T. *Brain Res.* **1995**, *681*, 1-2, 117-125.

39. Danysz, W.; Parsons, C. G. *Pharmacol. Rev.* **1998**, *50*, 597-664.

40. Fisher, G. H.; Petrucelli, L.; Gardner, C.; Emory, C.; Frey, W. H. N.; Amaducci, L.; Sorbi, S.; Sorrentino, G.; Borghi, M.; D'Aniello, A. *Mol. Chem. Neuropathol.* **1994**, *23*, 2-3, 115-124.

41. Marchelli, R.; Dossena, A.; Palla, G. *Trends Food Sci. & Technol.* **1996**, *7*, 4, 113-119.

42. Masters, P. M.; Friedman, M. *J. Agric. Food Chem.* **1979**, *27*, 3, 507-511.

43. Carolan, V. A.; Gardner, M. L. G.; Lucy, D.; Pollard, A. M. *J. Forensic Sci.* **1997**, *42,* 1, 10-16.

44. Helfman, P. M.; Bada, J. L. *Proc. Natl. Acad. Sci. USA* **1975**, *72*, 8, 2891-2894.

45. Lubec, G.; Weninger, M.; Anderson, R. *FASEB J.* **1994**, *8*, 14, 1166-1169.

46. Masters, P. M. *Forensic Sci. Int.* **1986**, *32*, 3, 179-184.

47. Ohtani, S.; Matsushima, Y.; Kobayashi, Y.; Kishi, K. *J. Forensic Sci.* **1998**, *43*, 949-953.

48. Ritz, S.; Turzynski, A.; Schuetz, H. W. *Forensic Sci. Int.* **1994**, *69*, 2, 149-159.

49. Meyer, V. R. Amino Acid Racemization. In *Chiral separation by liquid chromatography.* ACS symposium series 471, USA, Satinder Ahuja, ed. **1991.**

50. Masters, P. M.; Zimmerman, M. R. *Science* **1978**, *201*, 4358, 811-812.

51. Poinar, H. N.; Hoss, M.; Bada, J. L.; Paabo, S. *Science* **1996**, *272*, 5263, 864-866.

52. Bada, J. L.; Luyendyk, B. P.; Maynard, J. B. *Science* **1970**, *170*, 959, 730-732.

53. Bada, J. L.; Protsch, R. *Proc. Natl. Acad. Sci. USA* **1973**, *70*, 5, 1331-1334.

54. Kvenvolden, K. A.; Lawless, J. G.; Ponnamperuma, C. *Proc. Natl. Acad. Sci. USA*. **1971**, *68*, 2, 486-490.

55. McDonald, G. D.; Bada, J. L. *Geochim. Cosmochim. Acta* **1995**, *59*, 6, 1179-1184.

56. Pollock, G. E.; Cheng, C.-N.; Cronin, S. E.; Kvenvolden, K. A. *Geochim. Cosmochim. Acta* **1975**, *39*, 11, 1571-1573.

57. Kvenvolden, K.; Lawless, J; Pering, K.; Peterson, E.; Flores, J.; Ponnamperuma, C.; Kaplan, I. R. Moore, C. *Nature* **1970**,*228*, 5275, 923-926.

58. Glavin, D. P.; Bada, J. L.; Brinton, K. L. F.; McDonald, G. D. *Proc. Natl. Acad. Sci. USA* **1999**, *96*, 16, 8835-8838.

59. Bada, J. L. *Science* **1997**, *275*, 5302, 942-943.

60. Bada, J. L.; McDonald, G. D. *Icarus*. **1995**, *114,* 1, 139-43.

61. Ahuja, S. ed. **Chiral separations by liquid chromatography.** *ACS symposium series 471, American Chemical Society*, Washington D.C. **1991**.

62. Kohler, H.-P. E.; Angst, W.; Giger, W.; Kanz, C.; Müller, S.; Suter, M. J.-F. *Chimia* **1997**, *51*, 12, 947–951.

63. Ahuja, S. **Chiral Separations by Chromatography.** *Oxford*, New York, **2000**.

64. Aboul-Enein, H. Y.; Ali, I. **Chiral Separations by Liquid Chromatography and Related Technologies**. *Marcel Dekker*, New York, **2003**.

65. Russell, G. F.; Hills, J. I. *Science* **1971**, *172*, 1043-1044.

. Caner, H.; Groner, E.; Levy, L. *Drug Discovery Today*, **2004**, *9*, 105.

67. Bidleman, T. E.; Leone, A. D.; Wong, F.; van Vliet, L.; Szeto, S.; Ripley, B. D. *Environ. Toxicol. Chem*. **2006**, *25*, 6, 1448-1457.

68. Konwick, B. J.; Garrison, A. W.; Black, M. C.; Avants, J. K.; Fisk, A. T. *Environ. Sci. Technol*. **2006,** *40*, 9, 2930-2936.

69. Wong, C. S. *Anal. Bioanal. Chem*. **2006** *386*, 3, 544-558.

70. Wang, Q.; Qiu, J.; Zhu, W.; Jia, G.; Li, J.; Bi, C.; Zhou, Z. *Environ. Sci. Technol*. **2006**, *40*, 3, 721-726.

71. Konwick, B. J.; Fisk, A. T.; Garrison, A. W.; Avants, J. K.; Black, M. C. *Environ. Toxicol. Chem*. **2005**, *24*, 9, 2350-2355.

72. Kurt-Karakus, P. B.; Bidleman, T. F.; Jones, K. C. *Environ. Sci. Technol*. **2005,** *39*, 22, 8671-8677.

73. Harrad, S.; Ren, J.; Hazrati, S.; Robson, M. *Chemosphere*. **2006,** *63*, 8,1368-1376.

74. Gomara, B.; Gonzalez, M. J. *Chemosphere*. **2006,** *63*, 4, 662-669.

75. Williams, A. *Pestic. Sci*. **1996**, *46*, 3-9.

76. Garrison, A. W. *Environ. Sci. Technol.* **2006**, *40*, 1, 16-23.

77. Frank, H.; Woiwode, W.; Nicholson, G. J.; Bayer, E. *Liebigs Ann. Chem.* **1981**, 354-365. Liardon, R.; Friedman, M.; Philippossian, G. *J. Agric. Food Chem.* **1991**, *39*, 531-537.

78. Bada, J. L. *J. Am. Chem. Soc.* **1972**, *94*, 4, 1371-1373.

79. McEwen, I. *Biopolymers* **1993,** *33*, 6, 933-942.

80. Sundaresan, V.; Abrol, R. *Protein Sci.* **2002**, *11*, 1330-1339.

81. Booth, T. D.; Wahnon, D.; Wainer, I. W. *Chirality* **1997**, *9*, 96–98. Ahn, S.; Ramirez, J.; Grigorean, G.; Lebrilla, C. B. *J. Am. Soc. Mass Spectrom.* **2001**, *12*, 3, 278-287. Davankov, V. A. *Chirality* **1997,** *9*, 99–102.

82. Pirkle, W. H. *Chirality* **1997,** *9,* 103.

83. Bentley, R. *Trans. NY Acad. Sci. Ser. II* **1983,** *41,* 5–24.

84. Daniel, J. M.; Friess, S. D.; Rajagopalan, S.; Wendt, S.; Zenobi, R. *Int. J. Mass Spectrom.* **2002**, *216*, 1, 1-27.

85. Dang, T. T.; Pedersen, S. F.; Leary, J. A. *J. Am. Soc. Mass Spectrom.* **1994**, *5*, 5, 452-459.

86. Sellier, N. M.; Bouillet, C. T.; Douay, D. L.; Tabet, J-C. E. *Rapid Commun. Mass Spectrom.* **1994,** *8,* 11, 891-894.

87. Dearden, D. V.; Dejsupa, C.; Liang, Y.; Bradshaw, J. S.; Izatt, R. M. *J. Am. Chem. Soc.* **1997**, *119*, 2, 353-359.

88. Dearden, D. V.; Liang, Y.; Nicoll, J. B.; Kellersberger, K. A. *J. Mass Spectrom.* **2001**, *36*, 9, 989-997.

89. Filippi, A.; Giardini, A.; Piccirillo, S.; Speranza, M. *Int. J. Mass Spectrom.* **2000**, *198*, 3, 137-163.

90. Tao, W. A.; Zhang, D.; Nikolaev, E. N.; Cooks, R. G. *J. Am. Chem. Soc.* **2000**, *122*, 43, 10598-10609.

91. Borho, N.; Haber, T.; Suhm, M. A. *Phys. Chem. Chem. Phys.* **2001**, *3*, 11, 1945-1948.

92. Schalley, C. A.; Hoernschemeyer, J.; Li, X.; Silva, G.; Weis, P. *Int. J. Mass Spectrom.* **2003**, *228*, 2-3, 373-388.

93. Tao, W. A.; Cooks, R. G. *Anal. Chem.* **2003,** *75,* 25A-31A.

94

. Shekunov, B. Y.; York, P. *J. Crystal Growth*, **2000,** *211*, 1, 122-136.

95. Saigo, K.; Hashimoto, Y.; Kinbara, K.; Sudo, A. *Proc. Indian Acad. Sci., Chem. Sci.* **1996**, *108,* 6, 555-573.

96. Coelhoso, I. M.; Cardoso, M. M.; Viegas, R. M. C.; Crespo, J. P. S. G. *Sep. Purif. Technol.* **2000**, *19*, 3, 183-197.

97. Pickering**,** P. J.; Chaudhuri**,** J. B. *Chirality* **1997,** *9*, 3, 261 - 267

98. Scholler, C., Chaudhuri, J. B., Pyle, D. L. *Biotechnol. Bioeng*. 42:50–58, 1993.

99. Sultan, J.; Gabryelski, W. *Anal. Chem.* **2006**, *78*, 2905-2917.

100. A. Mie, M. Jörntén-Karlsson, B. Axelsson, A. Ray, C. T. Reimann *Anal. Chem.*, **2007**, *79,* 7, 2850–2858.

101. Mie, A.; Jornten-Karlsson, M.; Axelsson, B.; Ray, A.; Reimann, C. T. *Anal. Chem.* **2007,** *79*, 7, 2850-2858.

102. Busch, K. W.; Busch, M. A. eds. **Chiral Analysis**, Elsevier. Oxford, UK. 2006.

103. Mukhopadhyay, R. *Anal. Chem.* **2005,** *77*, 114A–118A.

104. Jaouen, G.; Vessières, A. *Pure & Appl. Chem*. **1985**, *57*, 12, 1865-1874.

105. Moloneyab, M. P.; Gun'ko, Y. K.; Kellya, J. M. *Chem. Commun*., **2007,** DOI: 10.1039/b704636g.

106. Ema, T.; Yoshii, M.; Korenaga, T.; Sakai, T. *Tetrahedron: Asymmetry **2002**, 13,*11*,* 1223-1229.

107. Kostur, M.; Schindler, M.; Talkner, P.; Hanggi, P. *Phys. Rev. Lett.* **2006**, *96*, 014502, 1-4.

108. Bhushan, R., Tanwar, S. *Biomedical Chromatography* **2008** *22,* 9, 1028-1034.

109. Tang K, Yi J, Huang K, Zhang G. *Chirality*. **2009**, *21*, 3, 390-5.

110. Delgado, B.; Pérez, E.; Santano, M. C.; Minguillón, C *J. Chrom. A* **2005**, *1092*, 1, 36-42.

111. Kubacak, P.; Mikus, P.; Valaskova, I.; Havrnek, E. *Drug Development and Industrial Pharmacy*, *33*, 11, **2007**, 1199 – 1204.

112. Gübitz G, Schmid MG. *Electrophoresis* **2007**, *28,* 1-2, 114-26.

113. Ward, T. J.; Baker, B. A. *Anal. Chem.*, **2008**, *80*, 12, 4363-4372.

114. Eiceman, G. A.; Karpas, Z. Ion Mobility Spectrometry. Taylor & Francis eds.; 2nd ed., Boca Raton, FL, USA, **2005**.

115. Revercomb, H. E.; Mason, E. A. *Anal. Chem.* **1975,** *47*, 7, 970-983.

116. C. Shumate, R. H. St. Louis, H. H. Hill, Jr. *J. Chromatogr.* **1986,** *373*, 141-173.

117. Mason, E. A. In *Plasma Chromatography* Carr, T. W. Ed. Plenum Press, New York. 1984; pp 43-93.

118. Siems, W. F.; Wu, C.; Asbury, G. R.; Tarver, E. E.; Hill, H. H. Larsen, P. R.; McMinn, D. *Anal. Chem.* **1994**, *66*, 4195-4201.

119. Dwivedi, P.; Wu, C.; Matz, L. M.; Clowers, B. H.; Siems, W. F.; Hill, H. H. Jr. *Anal. Chem.* **2006**, *78*, 24, 8200-8206.

120. Wu, C.; Siems, W. F.; Asbury, G. R.; Hill, H. H. *Anal. Chem.* **1998**, *70*, 4929-4938.

121. Hill, H.H. Jr.; Simpson, G. *J. Field Anal. Chem. Technol.* **1997,** *1*, 3, 119-134.

122. Wittmer, D.; Chen, Y. H.; Luckenbill, B. K.; Hill, H. H., Jr. *Anal. Chem.* **1994**, *66*, 2348-2355.

123. Karpas, Z. *Int. J. Mass Spectrom. and ion Process* **1991**, *107*, 435-440.

124. Eiceman, G. A.; Nazarov, E. G.; Stone, J. A. *Anal. Chim. Acta* **2003**, *493*, 2, 185-194.

125. Beegle, L. W.; Kanik, I.; Matz, L.; Hill, H. H. *Anal. Chem.* **2001**, *73*, 13, 3028-3034.

126. Asbury, G.R.; Hill, H.H., Jr. *Anal. Chem*. **2000**, *72,* 3, 580 -584.

Table 1. ESI-APIMS operating conditions summary

Parameter	Settings
Reaction region length	7.5 cm
Drift tube length	25.0 cm
ESI voltage	16.5 kV
ESI flow	3 μl min^{-1}
Voltage at first ring	12.12 kV
Voltage at the gate	10.8 kV
Gate pulse frequency	29 Hz
Gate pulse width	0.1 ms
Scan time	35 ms
Buffer gas	Nitrogen
Drift tube pressure	695 ± 15 Torr
Buffer gas flow	1000 ml min^{-1}
Buffer gas temperature	100 to 200 ± 2 $^{\circ}C$
Chiral selector flow rate	0 to 200 μl hr^{-1}

Table 2. Summary of experiments with different chiral selectors

Chiral selector	Analyte [Concentrations of chiral selector in mmol m^{-3}]
(R)-1-phenyl ethanol	Serine, threonine, asparagine [5] [2, 4, 6], histidine, lysine, methionine [5] [2, 4, 6], phenylalanine [5] [2, 4, 6], tyrosine, tryptophan, atenolol, valinol
(S)-1-phenyl ethanol	Phenylalanine, atenolol
(R)-2-butanol	Atenolol [13.5], serine [6.1][a], tyrosine [6.1], valinol, valine (4 experiments)
(S)-2-butanol	Atenolol [13.5] [b], serine [6.1, 12, 16][c] [2.7, 5.4] [2.7, 5.4, 8.1, 10.8,13.5, 27][d], methionine [3.4, 5.4, 7.5][e] [3.4, 6.1, 8.8][f] [0.7, 1.3, 2.7, 4.1, 5.4, 6.8, 8.1][e], phenylalanine [0.27, 0.54, 0.81, 1.3, 1.7, 2.7, 4.1, 5.4, 6.8] [3.4, 5.4, 7.5][g]
tFMBA [h]	Serine, threonine, methionine, phenylalanine, tyrosine, tryptophan, atenolol, valinol

In these experiments racemic mixtures were analyzed. The concentrations of chiral selector in the buffer gas were 5.0 mmol m^{-3} (187 ppmv) for (R) and (S)-1-phenyl ethanol and 6.8 mmol m^{-3} (254 ppmv) for (R) and (S)-2-butanol, unless otherwise specified; the concentrations of tFMBA used were 0.3, 0.55, 1.1, 1.7, and 2.3 mmol m^{-3}; the analyte concentration was 500 μM and the buffer gas temperature was 175°C, unless otherwise specified. [a] At 110, 140, 170 and 200°C. [b] 4 experiments in two days. [c] 250 μM. [d] 125 μM. [e] Two experiments in two days. [f] 138°C. [g] 10, 100 and 500 μM at 150°C [h]. 150°C.

Table 3. Reduced mobility values (K_0) in $cm^2V^{-1}s^{-1}$ for this work and literature values.

	K_0	This work		
Analytes	**Beegle, 2001[125] [Dwivedi, 2006][119] {Asbury, 2000}[126]**	K_0	**RSD**	ΔK_0
Alanine	1.82 {1.81}	1.92	0.4	5.1 {5.7}
Serine	1.73[1.73]{1.82 }	1.87	0.3	7.2 [7.5] {2.7}
Threonine	1.68[1.69]{1.76}	1.81	0.2	6.9 [6.6] {2.8}
Isoleucine	1.58{1.63}	1.68	0.4	5.8 {3.0}
Arginine	1.45 {1.50}	1.57	0.1	7.6 {4.5}
Histidine	1.54 {1.61}	1.67	0.1	7.8 {3.6}
Lysine	1.53{1.60}	1.67	0.1	8.2 {4.2}
Methionine	1.55[1.56]{1.60}	1.67	0.1	7.4 [6.6] {4.2}
Phenylalanine	1.45[1.45]{1.50}	1.55	0.1	6.7 [6.6] {3.2}
Tyrosine	1.37{1.44}	1.48	0.3	8.0 {2.7}
Tryptophan	1.31[1.32]{1.35}	1.40	0.2	7.1 [6.3] {3.6}
Atenolol	[1.18]	1.28	0.1	[7.9]
Valinol	[1.74]	1.85	0.1	[6.0]

RSD: Relative standard deviation (repeatability). Data were obtained in the SIM-IMS mode. ΔK_0: % difference in K_o to Beegle, 2001[125] to [Dwivedi, 2006],[119] or to {Asbury, 2000}.[126]

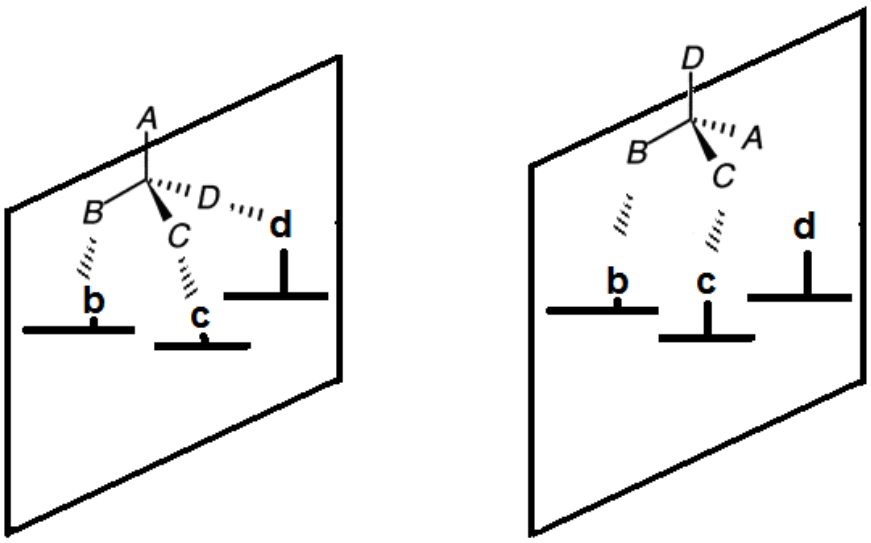

Figure 1. The three-point attachment model. Enantiorecognition occurs because one isomer (left) can simultaneously interact with all sites whereas its enantiomorph (right) interacts only with two sites.

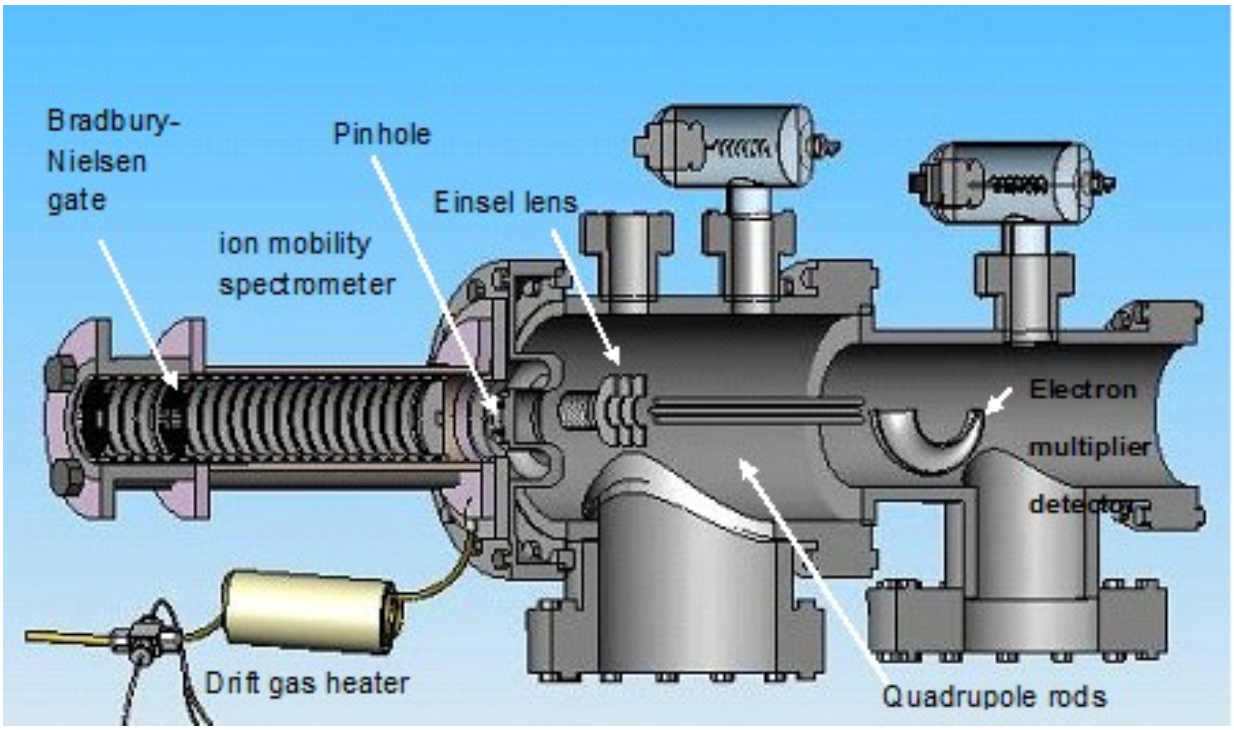

Figure 2. Instrument. Section view of the atmospheric pressure ion mobility-quadrupole mass spectrometer.

Analytes

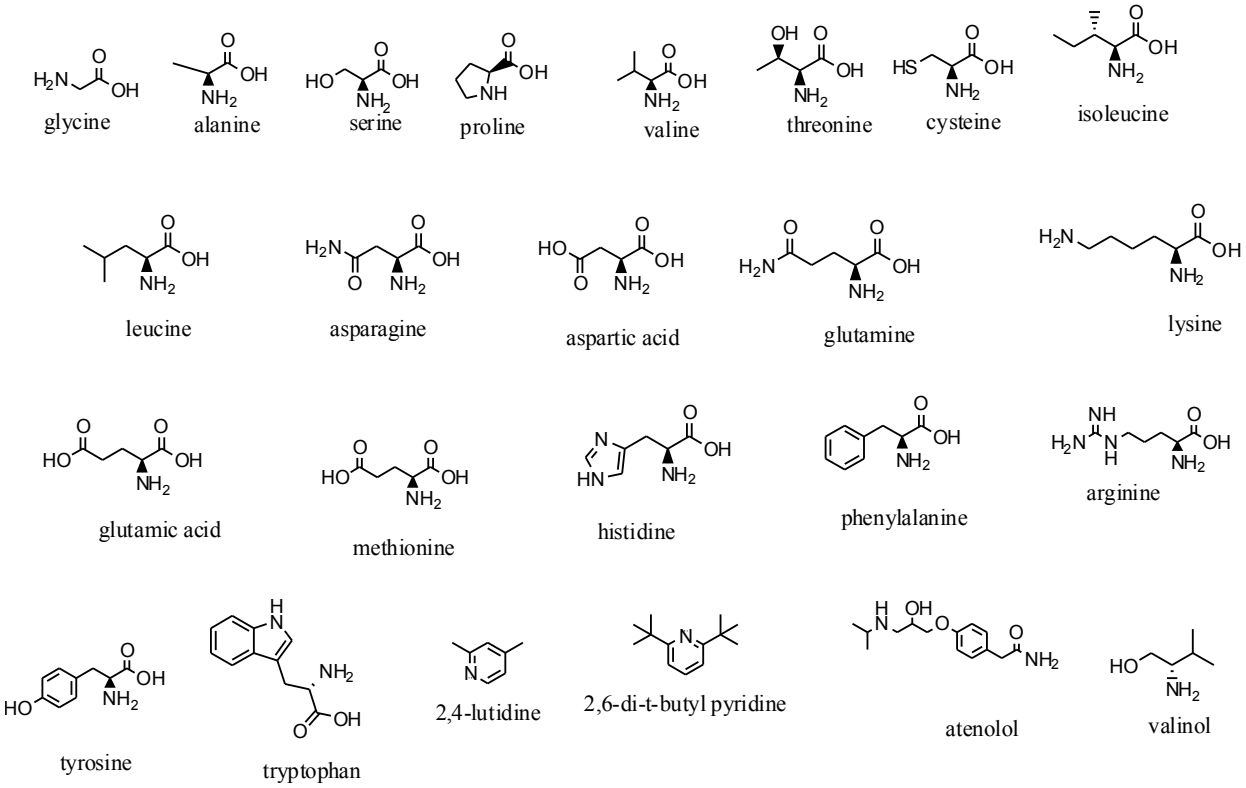

Modifiers

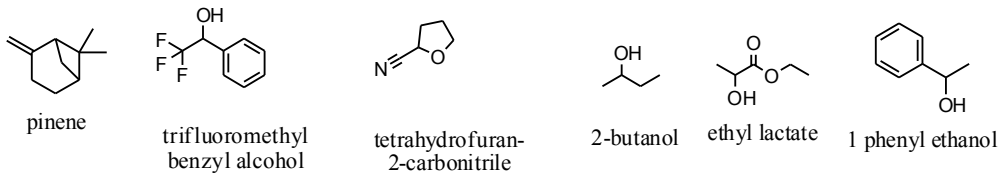

Figure 3. Compounds used in the chiral investigation.

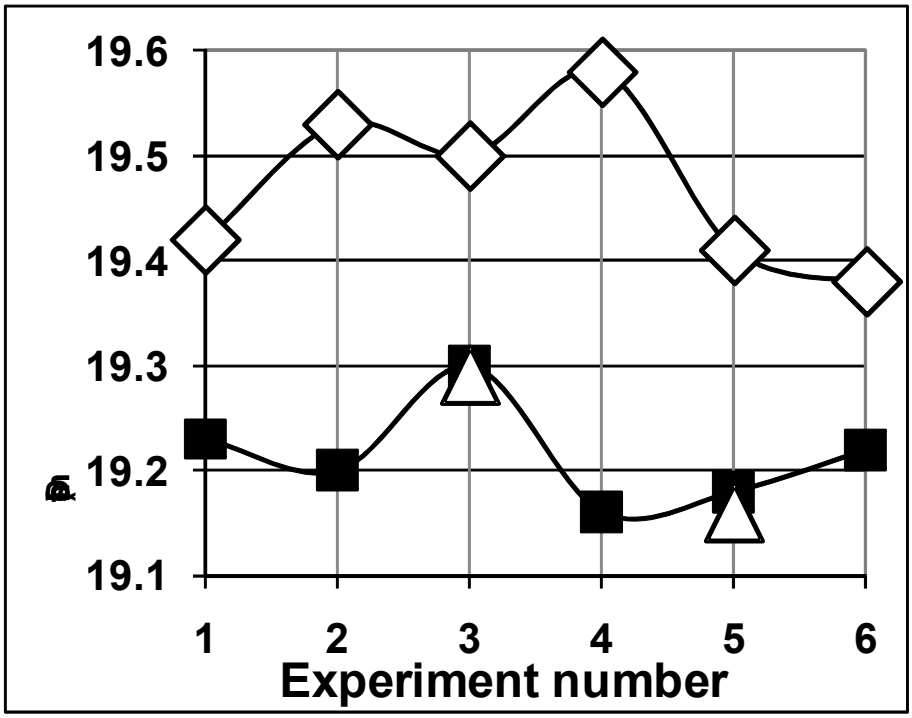

Figure 4. Drift times of valinol enantiomers in an 8-hr period using (S)-2-butanol chiral selector. Solutions of D-valinol (■), L-valinol (◊) and racemic mixtures of valinol (Δ) at a 943-μM concentration were analyzed when 0.68 mmol m^{-3} of (S)-2-butanol were introduced into the buffer gas (25 ppmv) and a buffer gas temperature of 150 °C. For both racemic data points in this experiment, the racemic mixtures were prepared from the enantiomer solutions used to obtain the data for this figure. Data were obtained in the SIM-IMS mode selecting the mass of protonated valinol. (S)-2-butanol concentration was at least one hour before collecting data.

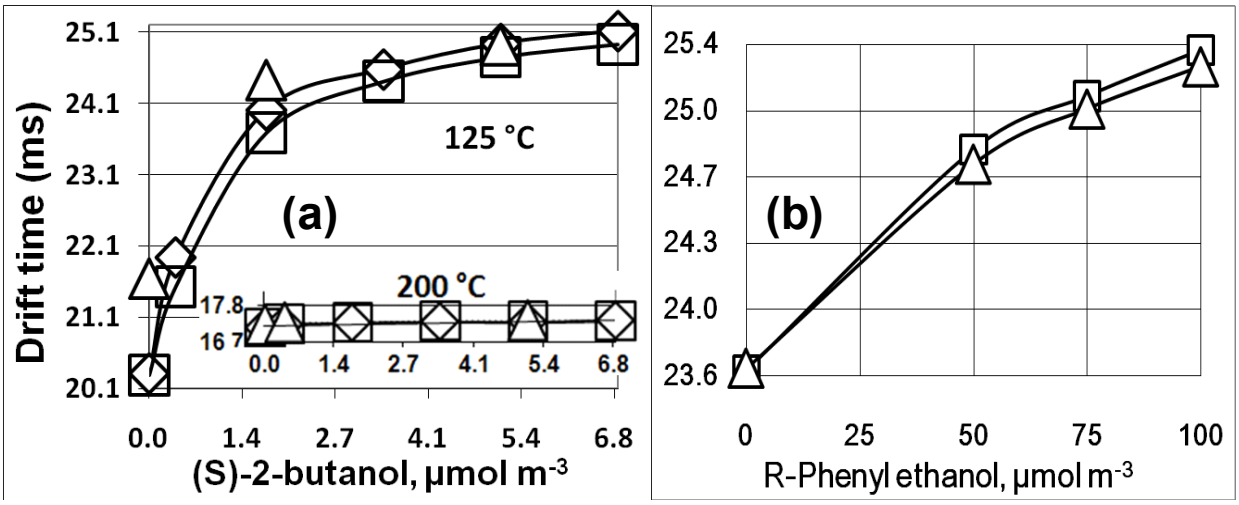

Figure 5. **Effect of chiral selector concentration on the mobilities of valinol enantiomers.** (a) 943-µM solutions of D-valinol (□), L-valinol (◊) and racemic mixtures (Δ) of valinol were analyzed at a buffer gas temperature of 125 °C and 200 °C (inset). b) 500-µM solutions of D and L-phenylalanine were analyzed using (R)-1-phenyl ethanol as chiral selector at 175°C. The x axes show the chiral selector concentration in the buffer gas. Other experimental conditions were as in Figure 4.

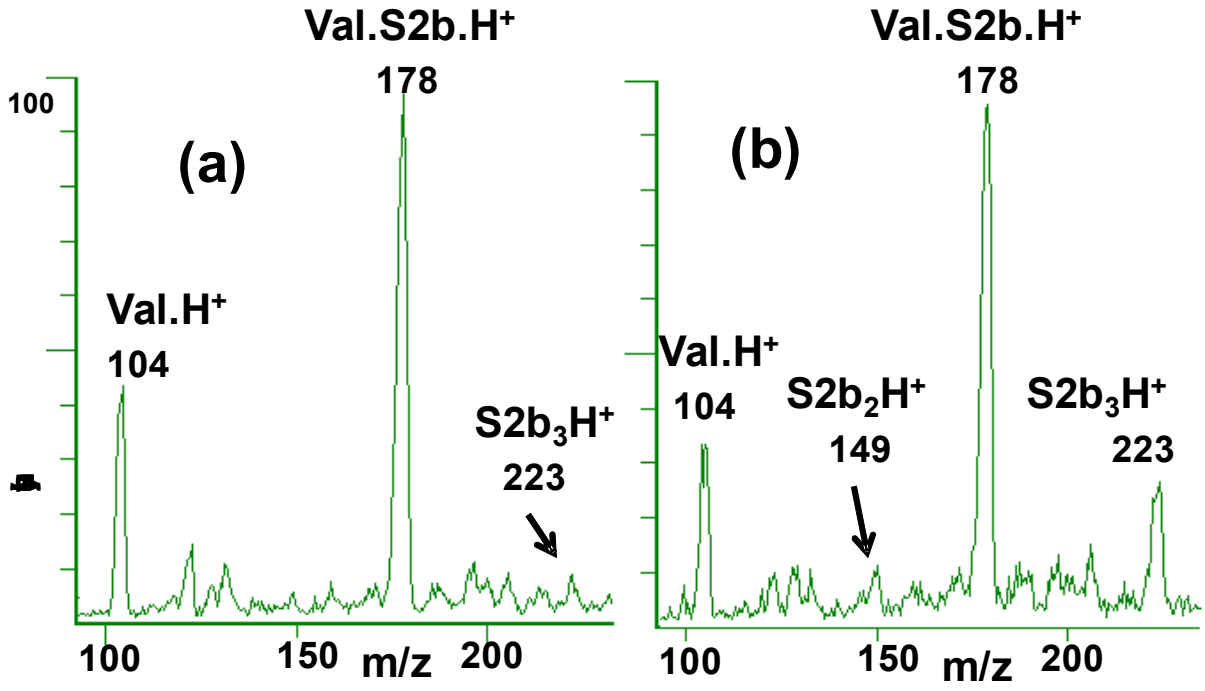

Figure 6. Increasing formation of cluster ions at high (S)-2-butanol concentrations. MS spectra of a 943-µM solution of D-valinol (Val) at 150 °C when the concentrations of (S)-2-butanol (S2b) in the buffer gas increased from (a) 2.7 mmol m^{-3} (102 ppmv) to (b) 4.1 mmol m^{-3} (152 ppmv). The unknown peaks at m/z 133 and 137 appeared when 2-butanol was used as chiral selector.

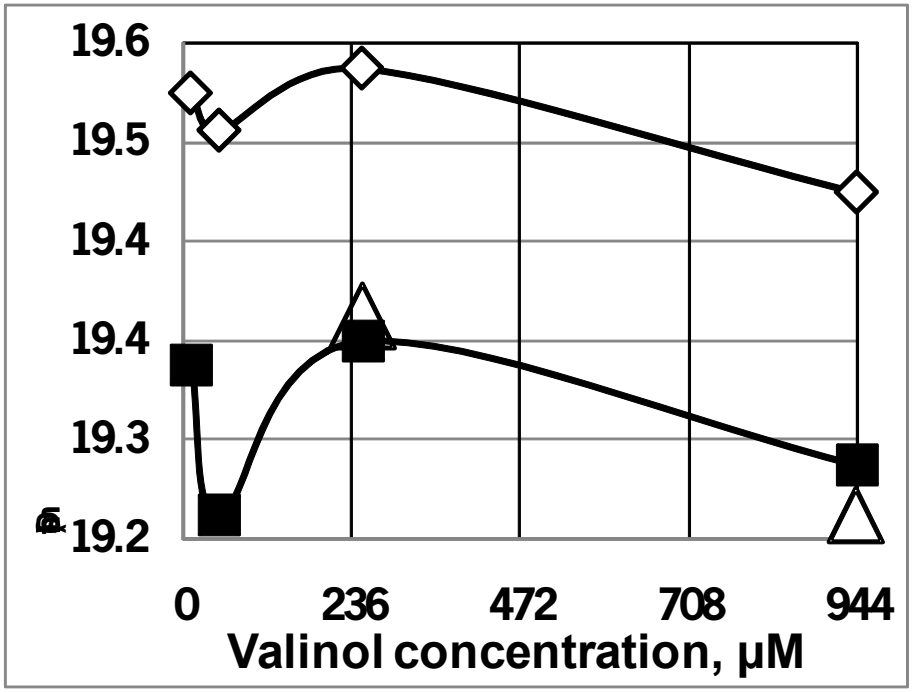

Figure 7. **Effect of valinol concentration on the mobilities of its enantiomers.** Solutions of D-valinol (■), L-valinol (◊), and racemic mixtures (Δ) of valinol at concentrations of 10, 50, 250, and 943-µM were analyzed when 0.68 mmol m^{-3} (25 ppmv) of (S)-2-butanol were introduced into the buffer gas and a buffer gas temperature of 150 °C. Other experimental conditions were as in Figure 4.

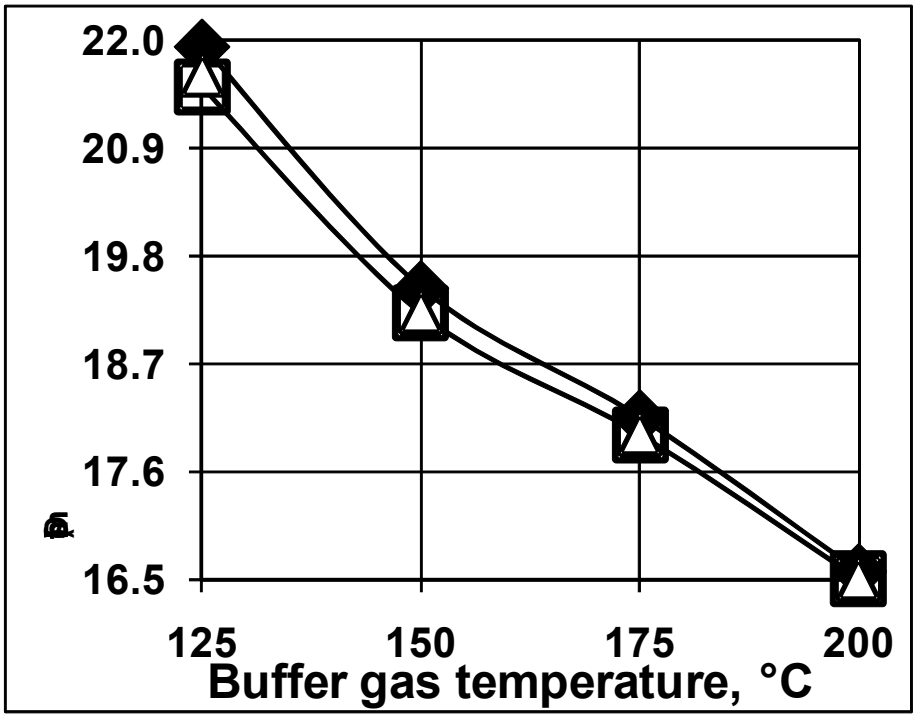

Figure 8. Effect of temperature on the mobilities of valinol enantiomers. Solutions of D-valinol (( ), L-valinol (♦), and racemic mixtures (Δ) of valinol at concentrations of 943-μM were analyzed when 0.68 mmol m^{-3} (25 ppmv) of (S)-2-butanol were introduced into the buffer gas at four different temperatures. There was a waiting time of at least one hour to stabilize every (S)-2-butanol concentration and buffer gas temperature before collecting data. Other experimental conditions were as in Figure 4.

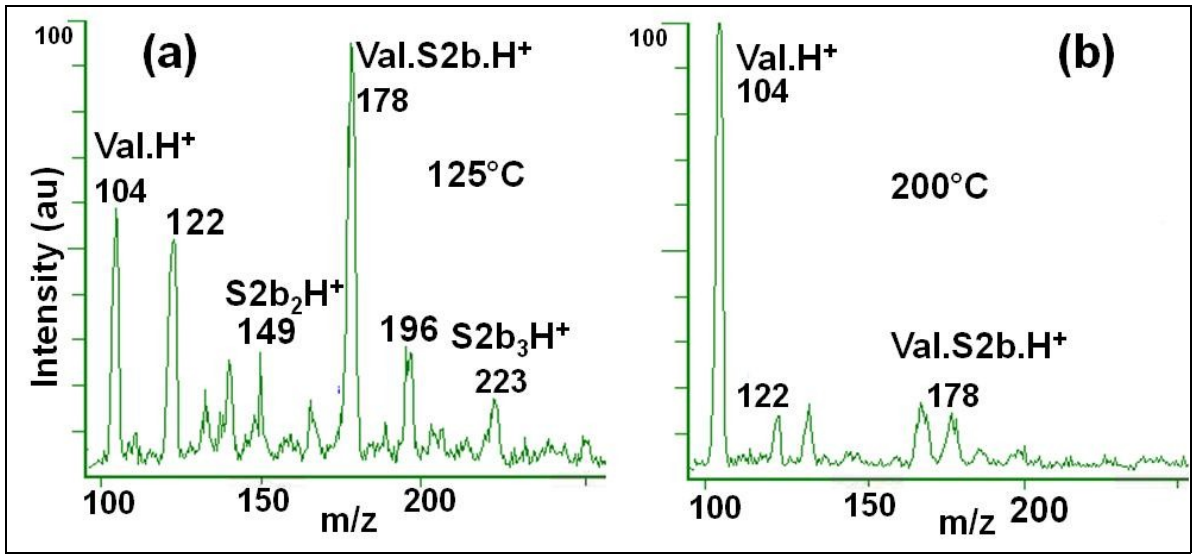

Figure 9. Extensive formation of cluster ions at low temperatures. (a) MS spectrum of valinol (Val) at 125 °C; (b) MS spectrum of valinol at 200 °C. The concentration of (S)-2-butanol (S2b) in the buffer gas was 0.27 mmol m^{-3} (10 ppmv) and valinol concentration was 943 μM, in both spectra.